REQUIREMENT OF A HIGH-FLUX METABOLIC STATE FOR MOUSE EMBRYONIC STEM CELL SELF-RENEWAL

APPROVED BY SUPERVISORY COMMITTEE

Steve McKnight, Ph.D.

Joseph Ready, Ph.D.

Qinghua Liu, Ph.D.

Masashi Yanagisawa, Ph.D.

DEDICATION

To Krista

REQUIREMENT OF A HIGH-FLUX METABOLIC STATE FOR MOUSE EMBRYONIC STEM CELL SELF-RENEWAL

By

PETER BARTON ALEXANDER

DISSERTATION

Presented to the Faculty of the Graduate School of Biomedical Sciences

The University of Texas Southwestern Medical Center at Dallas

In Partial Fulfillment of the Requirements

For the Degree of

DOCTOR OF PHILOSOPHY

The University of Texas Southwestern Medical Center at Dallas

Dallas, Texas

June, 2010

Acknowledgements

I would like to thank my advisory committee, Qinghua Liu, Joseph Ready, Masashi Yanagisawa, and Steve McKnight for their guidance and advice. I need to especially thank Steve for his enthusiasm and scientific perspective. Whenever I got discouraged from negative results he always had new experimental approaches and hypotheses to test, for which I am very grateful.

I sincerely thank all the past and present members of the McKnight lab for their encouragement and helpful discussions. I am particularly indebted to Jian Wang, who initiated the experiments on ES cell metabolism that led to this project. The metabolite analysis would not have been possible without the aid of Ben Tu. Leeju Wu was also involved in many experiments during the early stages of this study.

Next, I need to thank everyone in the high-throughput screening core facility for their help with the TDH inhibitor screen. I am especially grateful to Shuguang Wei, who was actively involved in all aspects of the screen from assay development to secondary screening. I also thank Bruce Posner and Chun Hui Bu for their help with the analysis of the screening results.

Finally, I need to thank everyone who helped with the generation of the TDH knockout mice. Bob Hammer provided advice and reagents for targeting vector construction, and also performed the in vitro blastocyst development experiments. The transgenic core facility, especially Robin Nguyen, helped with the electroporation, selection, and injection of targeted ES cells. I also thank Latisha McDaniel and Sandi Jo Estill for their efforts to breed and characterize the TDH knockout mice.

REQUIREMENT OF A HIGH-FLUX METABOLIC STATE FOR MOUSE EMBRYONIC STEM CELL SELF-RENEWAL

Publication No. _____

Peter Barton Alexander, Ph.D.

The University of Texas Southwestern Medical Center at Dallas, 2010

Supervising Professor: Steven L. McKnight, Ph.D.

Abstract: Unbiased profiling of global metabolite levels has revealed that cultured mouse embryonic stem (ES) cells exist in a unique metabolic state. Metabolites fluctuating dramatically in response to ES cell differentiation include purine nucleotides, acetyl-CoA, the amino acid threonine, and folic acid derivatives. These altered metabolic pathways, collectively known as the high-flux backbone (HFB) of metabolism, are surmised to be responsible for the rapid proliferation of this cell type. In particular, the amino acid threonine is shown here to be critical for mouse ES cell self-renewal.

Gene and protein expression analysis has revealed that the enzyme threonine dehydrogenase (TDH) has the potential to play a major role in the establishment of HFB metabolism. TDH breaks down threonine into glycine and acetyl-CoA, molecules which are used to drive purine biosynthesis and ATP production, respectively. Using multiple approaches, we show here that TDH is strongly expressed both in ES cells and in the inner cell mass of the mouse blastocyst.

Identification of potent and specific small molecule inhibitors has made possible the targeted elimination of the TDH enzyme in mouse ES cells. Using these compounds, we have determined that metabolic flux through this pathway is essential for ES cell self-renewal. TDH inhibition is shown to cause an alteration in the cell's metabolic state that results in increased autophagic activity and cell death. This study also reports on the generation of TDH conditional knockout mice, which will enable further elucidation of the role of HFB metabolism in adult and developing animals.

TABLE OF CONTENTS

PRIOR PUBLICATIONS

Wang J, **Alexander P**, Wu L, Hammer R, Cleaver O and McKnight SL. (2009). Dependence of Mouse Embryonic Stem Cells on Threonine Catabolism. **Science**. 325, 435-439.

Alexander P and McKnight SL. (2010). Requirement of a High-Flux Metabolic State for Mouse Embryonic Stem Cell Self-Renewal. Manuscript in preparation.

LIST OF FIGURES

LIST OF DEFINITIONS

AICAR – 5-Aminoimidazolecarboxamide-R

AMP – Adenosine Monophosphate

ATP – Adenosine Triphosphate

βME – Beta-mercaptoethanol

BMP – Bone Morphogenetic Protein

cDNA – Complimentary DNA

C. elegans – *Caenorhabditis elegans*

ceTDH – *Caenorhabditis elegans* Threonine Dehydrogenase

CoA – Coenzyme A

Cys – Cysteine

DIC – Differential Interference Contrast

DMSO – Dimethyl Sulfoxide

DNA – Deoxyribonucleic Acid

DTA – Diphtheria Toxin A

DTT – Dithiothreitol

EB – Embryoid Body

EC_{50} – Half Maximal Effective Concentration

E. coli – *Escherichia Coli*

EDTA – Ethylenediaminetetracetic Acid

EpiS – Epiblast-Derived Stem

ES – Embryonic Stem

FBS – Fetal Bovine Serum

FGF – Fibroblast Growth Factor

GAPDH – Glyceraldehyde-3-Phosphate Dehydrogenase

Gcat – Glycine *C*-acetyltransferase

Gly – Glycine

GMEM – Glasgow Minimum Essential Medium

GMP – Guanosine Monophosphate

GSK3 – Glycogen Synthase Kinase-3

GST – Glutathione S-Transferase

HBSS – Hank's Buffered Salt Solution

LC-MS/MS – Liquid Chromatography-Mass Spectrometry

HEK 293T – Human Embryonic Kidney 293 Cells Containing the SV40 Large T-antigen

HeLa – Human Cancerous Cervical Cell Line

HFB – High-Flux Backbone

HNV – Hydroxynorvaline

HRP – Horseradish Peroxidase

HSDH – Hydroxysteroid Dehydrogenase

IC_{50} – Half Maximal Inhibitory Concentration

ICM – Inner Cell Mass

IMP – Inosine Monophosphate

IPS – Induced Pluripotent Stem

k_{cat} – Turnover Number

kB – Kilobase

kD – Kilodalton

KLH – Keyhole Limpet Hemocyanin

K_m – Michaelis Constant

LC3 – Light Chain 3

LIF – Leukaemia Inhibitory Factor

MEF – Mouse Embryonic Fibroblast

mRNA – Messenger RNA

MSS – Mitochondrial Signal Sequence

mTHF – Methyl-tetrahydrofolate

NaCl – Sodium Chloride

NAD^+ - Nicotinamide Adenine Dinucleotide

NADH – Reduced Nicotinamide Adenine Dinucleotide

ORF – Open Reading Frame

PAGE – Polyacrylamide Gel Electrophoresis

PBS – Phosphate Buffered Saline

PCR – Polymerase Chain Reaction

PFA – Paraformaldehyde

PRPP – 5-Phosphoribosyl-1-Pyrophosphate

Qc – Quinazoline Carboxamide

qPCR – Quantitative Polymerase Chain Reaction

RNA – Ribonucleic Acid

RNAi – RNA Interference

SAR – Structure-Activity Relationship

SDS- Sodium Dodecyl Sulfate

T. brucei – *Trypanosoma brucei*

TBS – Tris-Buffered Saline

TBST – Tris-Buffered Saline with 0.5% Tween-20

tbTDH – *Trypanosoma brucei* Threonine Dehydrogenase

TCA – Tricarboxylic Acid

TDH – Threonine Dehydrogenase

TEM – Transmission Electron Microscopy

Tfase – Transformylase

Thf – Tetrahydrofolate

Thr – Threonine

TGF-β - Transforming Growth Factor Beta

TkTDH – Threonine Dehydrogenase from *Thermococcus kodakaraensis*

UV – Ultraviolet

V_{max} – Maximal Velocity

CHAPTER ONE
Introduction I

BIOLOGY OF EMBRYONIC STEM CELLS

Embryonic stem (ES) cells are immortal cell lines derived from the inner cell mass (ICM) of the preimplantation blastocyst. These cells have contributed much to our knowledge of mammalian biology, both as a model for cellular differentiation processes and as a tool that enables exquisite manipulation of the mouse genome. The ability to inactivate a single gene in the mouse through targeted mutation, made possible by the culture of ES cells, provides valuable information about that gene's biological function in the normal animal, and has allowed scientists to assign functions to scores of genes whose roles were previously obscure.

ES cells were initially derived by culturing mouse blastocysts on a bed of mitotically inactivated mouse fibroblast cells in medium containing fetal calf serum (Evans and Kaufman, 1981; Martin, 1981). Subsequently, many refinements have been made to the culture conditions for mouse ES cells. For example, the pluripotency factors provided by the feeder and serum components have been identified, such that ES cells can now be cultured in fully defined media (Ying et al., 2003). This has significantly advanced our understanding of stem cell biology, especially of the signaling pathways and transcription factors that regulate an ES cell's decision to self-renew or differentiate. In addition, the elucidation of signaling pathways regulating ES cell self-renewal has enabled the establishment of the first germline-competent ES cell lines derived from rats (Buehr et al., 2008, Li et al., 2008). Pluripotent stem cell lines from primates, including

humans, have also been derived (Thomson et al., 1995, 1996, 1998). These cells, while useful, are quite different from mouse ES cells in several important ways.

This chapter introduces the broad field of ES cell biology. First, the key properties distinguishing authentic ES cells from other cell lines will be discussed. Next, a historical perspective will be presented on the derivation and culture of mouse ES cells, including the conditions that have been used to culture ES cells and what these culture conditions have revealed about normal ES cell biology. Finally, ES cell lines from rats and primates, and their relationship to mouse ES cells, will be considered.

DEFINING PROPERTIES OF ES CELLS

Pluripotency

Mouse ES cells originate from the ICM of the cavitated blastocyst, a structure formed 4 days after the fertilization of the egg (Figure 1-1). The blastocyst is derived from the morula (Latin for "mulberry"), a solid ball containing 16 cells. In addition to the ICM, which will form the embryo, the blastocyst contains an outer layer of cells, the trophoblast, and a fluid-filled cavity called the blastocoele. The trophoblast cells are specialized for mediating the attachment of the blastocyst to the uterus, and will later form the placenta (Gardner, 1998). In mice, at 5.5 days after fertilization, the blastocyst implants in the uterine wall and differentiates into what is called an epiblast.

Pluripotency is defined as the ability of a cell to differentiate into multiple cell types representative of the three primary germ layers of the embryo. These germ layers are endoderm (gastrointestinal tract, liver, lungs), mesoderm (muscle, blood, bone,

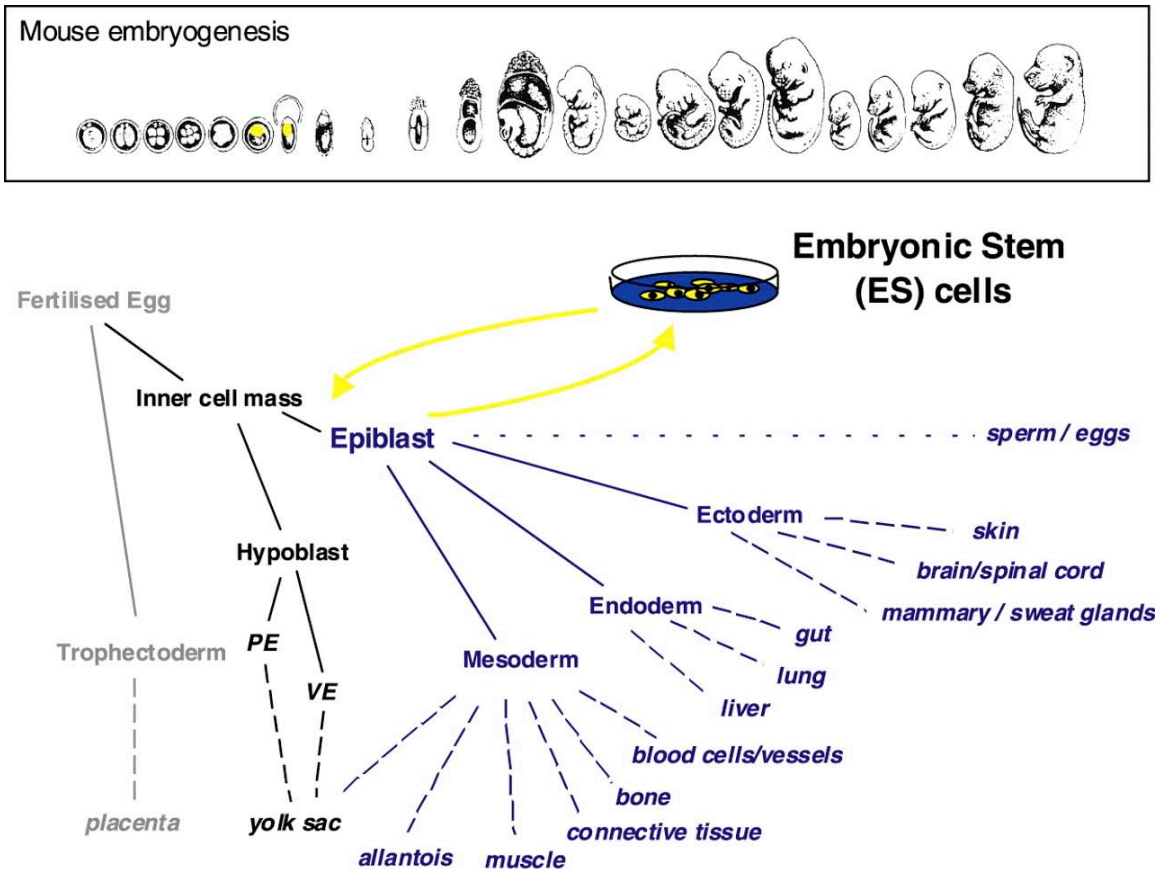

Figure 1-1 Pluripotency of mouse embryonic stem cells
The top panel depicts the stages of mouse embryogenesis. ES cells are derived from the inner cell mass of the blastocyst, which is present 4 days after fertilization (E4). At E5.5 the blastocyst implants in the uterine wall and differentiates into epiblast. The bottom schematic depicts in blue the cell lineages that can be derived from ES cells. ES cells are termed pluripotent because they can give rise to ectoderm, endoderm and mesoderm both in vivo and in vitro. However, ES cells are not totipotent because the trophectoderm lineage is restricted. Figure taken from (Smith, 2001).

urogenital), and ectoderm (skin and nervous system). When injected into animals, ES cells form teratomas with tissue components resembling normal derivatives of all three germ layers. Since blastocyst injection experiments are not possible in humans, teratoma formation in animal models is often used to demonstrate the pluripotency of human ES cells. ES cells have also been extensively differentiated in vitro into many cell lineages using appropriate culture conditions (Smith, 2001).

ES cells are sometimes referred to as totipotent. However, ES cells rarely differentiate into extraembryonic endodermal tissue (like yolk sac) in vivo, and never differentiate into trophectoderm, which gives rise to placenta (Figure 1-1). Thus, pluripotent stem cells can give rise to any fetal or adult cell type, but can not develop into a fetal or adult animal because they lack the potential to contribute to extraembryonic tissue such as the placenta and yolk sac. Totipotent stem cells include the fertilized egg and the cells that comprise the morula.

Self-renewal

Through the process of self-renewal, ES cells maintain their pluripotency while expanding in culture. ES cells can self-renew indefinitely, and are thus considered to be immortal. Theoretically, the first ES cell line derived by Evans in 1981 could still be maintained today with no change in its differentiation capacity. In reality, random mutational events can occur during prolonged culture, so it is advisable to use low-passage number ES cells when generating chimeric mice.

ES cells are the only non-transformed mammalian cells that are immortal.

Whereas cancer cells are immortal as a result of genetic transformation, ES cells are derived without transformation or immortalization. Another distinction between ES cells and cancer cells is that, through the process of self-renewal, ES cells maintain a stable diploid karyotype, whereas cancer cell division often results in aneuploidy. This maintenance of diploidy is critical because ES cells capable of contributing to the mouse germline must contain a balanced chromosome number in order to undergo meiosis.

Cultured mouse ES cells also possess an extraordinary amplification capacity. These cells measure only several micrometers in diameter, as compared to the 10- to 30-μm range typical of cultured somatic cells (Alberts et al., 2002). This small size dictates that ES cells are composed almost entirely of nucleus and contain little cytoplasm. Mouse ES cells divide at an astonishing rate. The feeder-independent ES cells grown in our lab have a cell division cycle of only five hours. This doubling time is shorter than that of even the most rapidly dividing cancer cells and approaches that of single-celled microbial organisms. One factor contributing to this rapid cell division is the lack of either G1 or G2 checkpoints; an ES cell spends most of its lifespan in S phase of the cell cycle replicating its DNA (Smith, 2001). Together, these properties have led some researchers to suggest that mouse ES cells might be more akin to rapidly growing yeast than they are to other mammalian cell types (Silva and Smith, 2008).

The ability to contribute to chimeric blastocysts

Clonogenic mouse ES cells that are grown in culture for long periods of time can, upon return to a host embryo, differentiate normally and give rise to chimeric (mosaic)

animals. Chimeric mice are typically generated by introducing ES cells into blastocysts, and then implanting the chimeric blastocysts into pseudopregnant recipient mice. Once injected into the blastocoele, ES cells become trapped and must either participate in development or die (Gardner, 1998). If the injected ES cells colonize the germline then the effects of specific genetic manipulations performed in ES cell cultures can be studied in the context of the whole animal. The ability to form germline-competent chimeras is the most definitive proof of authentic ES cells. When it is not possible to test whether a cell line can give rise to chimeric animals, as in the case of human ES cells, the most rigorous test available is teratoma formation.

Molecular hallmarks of pluripotent stem cells

In the past two decades much progress has been made in identifying the molecules responsible for the maintenance of ES cell self-renewal. Oct4 and Nanog are two transcription factors that are specifically associated with the generation and maintenance of pluripotency. Oct4 is a POU domain transcription factor that is expressed in epiblast and hypoblast cells (Palmieri et al., 1994). Oct4 expression is essential both for development of the ICM (Nichols et al., 1998) and for the self-renewal of cultured ES cells (Niwa et al., 2000). In contrast to Oct4, Nanog expression is confined to the epiblast. Nanog is not absolutely required for ES cell maintenance, but its absence reduces the threshold for differentiation (Chambers et al., 2007), and forced expression of Nanog alleviates the requirement for the cytokine leukemia inhibitory factor (LIF) in ES cell cultures (Chambers et al., 2003).

Because of their roles in ES cell self-renewal, the expression levels of Oct4 and Nanog are commonly measured to assess the quality of ES cells. In addition, since the promoters of both of these genes are demethylated in pluripotent stem cells, methylation analysis can be performed to evaluate new lines. Other transcription factors that play important roles in ES cell pluripotency include Sox2 and Klf4, and genome-wide studies are now being carried out to map transcriptional interaction networks among these factors that regulate pluripotency in mouse ES cells (Kim et al., 2008; Lu et al., 2009).

DERIVATION AND MAINTENANCE OF MOUSE ES CELLS

Embryonal carcinoma cells

The study of pluripotent stem cells began in the 1960s with the observation that embryonal carcinoma (EC) cells were capable of both unlimited self-renewal and multilineage differentiation (Kleinsmith and Pierce, 1964). EC cells are derived from teratocarcinomas, which are germ cell tumors that are mixtures of differentiated teratomas and undifferentiated EC cells. Beginning in the 1970s, EC cell lines were established that could be stably propagated in vitro (Kahan and Ephrussi, 1970). Although some EC cell lines could participate in embryogenesis when injected into mouse blastocysts (Brinster, 1974), most had limited differentiation potential and contributed poorly to chimeric mice, likely due to aneuploidy and other genetic changes. Nevertheless, the similar developmental properties of EC cells and early embryonic cells led to a search for pluripotent cells that were present during the course of normal mammalian development.

Original derivation of mouse ES cells

The first ES cell lines were derived from the ICM of mouse blastocysts using fibroblast feeder layers and serum, conditions previously used for the culture of mouse EC cells (Evans and Kaufman, 1981; Martin, 1981). ES cell cultures established in this way could differentiate into a wide variety of cell types in vitro and form teratomas when injected into mice. It was observed that, upon death of the feeder cells, the ES cells differentiated into embryonic endoderm, indicating that the feeders were supplying some factor required to maintain ES cell self-renewal (Figure 1-2). In addition, when ES cells

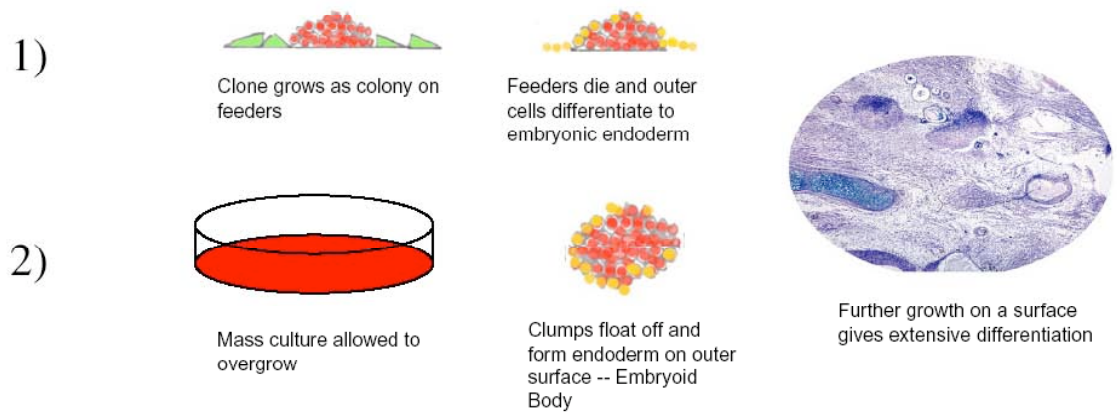

Figure 1-2 Original derivation of embryonic stem cells
Mouse ES cells were initially derived by plating blastocysts on a bed of mitotically inactivated mouse fibroblast (feeder) cells. If the feeders died then the ES cells differentiated into embryonic endoderm, suggesting the feeder cells were supplying some factor critical for self-renewal. When the cells were allowed to overgrow on low adherence dishes, clumps of cells would detach from the dish and form spherical structures called embryoid bodies that contained all three primary germ layers. ES cells could also be differentiated extensively in attachment culture. Figure taken from (Evans, 2007).

were overgrown on low adherence tissue culture dishes, clumps of cells detached from the plate and formed embryoid bodies containing all three primary germ layers (Evans and Kaufman, 1981). Unlike EC cells, ES cells contained a normal karyotype, a feature which made possible the generation of germ-line chimeras and provided a method to introduce modifications into the mouse genome (Bradley et al., 1984).

The first ES cells derived by Evans and Martin, and indeed most new ES cell lines derived today, come from the 129/Sv strain of mice (Kawase et al., 1994). While germline-competent ES cell lines have been established from the C57BL/6 strain, their derivation is inefficient and requires modified culture conditions (Ledermann and Burki, 1991). BALB/c, BXSB/MpJ-Yaa and MRL/Mp-lpr/lpr mouse strains are also non-permissive to the generation of ES cell cultures (Kawase et al, 1994). Thus, it was perhaps fortuitous that the initial efforts to derive ES cells made use of mice from the inbred 129 strain. The underlying factors that cause one strain to be permissive for ES cell derivation while another strain is refractory are currently unknown.

Role of LIF in maintenance of pluripotency

The initial derivation of ES cells depended on the presence of both mouse embryonic fibroblast cells and fetal calf serum, and removal of either of these components resulted in extensive cellular differentiation (Evans and Kaufman, 1981). However, the molecular identities of the factors that originated from these sources and were responsible for supporting ES cell self-renewal were unknown. Thus, the conditions required for maintenance of pluripotency in culture were poorly understood.

In 1988, two groups independently purified the feeder-derived factor responsible for inhibiting ES cell differentiation using fractionation of conditioned medium (Smith et al., 1988; Williams et al., 1988). This factor was identified as the cytokine leukemia inhibitory factor (LIF), and purified recombinant LIF was able to substitute for the feeder layer in the maintenance of pluripotent ES cell lines (Figure 1-3). This important discovery enabled the culture of pure populations of ES cells, that, when injected into mouse blastocysts, retained the capacity for germline transmission (Nichols et al., 1990). It was subsequently shown that LIF maintains self-renewal by binding the gp130 receptor to activate the transcription factor STAT3. STAT3 activity appeared to be a key switch regulating stem cell fate, because expressing a dominant negative form of STAT3 in ES cells abrogated self-renewal and promoted differentiation (Niwa et al., 1998), whereas expressing an active form of STAT3 maintained pluripotency in the absence of LIF (Matsuda et al., 1999). Today, LIF is routinely added to culture media to prevent unwanted ES cell differentiation. However, even after the discovery of LIF, ES cell culture conditions were incompletely understood, because the contribution of the fetal calf serum media component had not been identified.

Culture of ES cells in fully defined media

In the absence of LIF and serum, mouse ES cells differentiate into neural precursor cells. This neural differentiation pathway requires autocrine fibroblast growth factor (FGF) signaling through the Ras-ERK pathway (Ma et al., 1992). Fgf4 in particular plays a major role in this process because Fgf4-null ES cells are deficient in

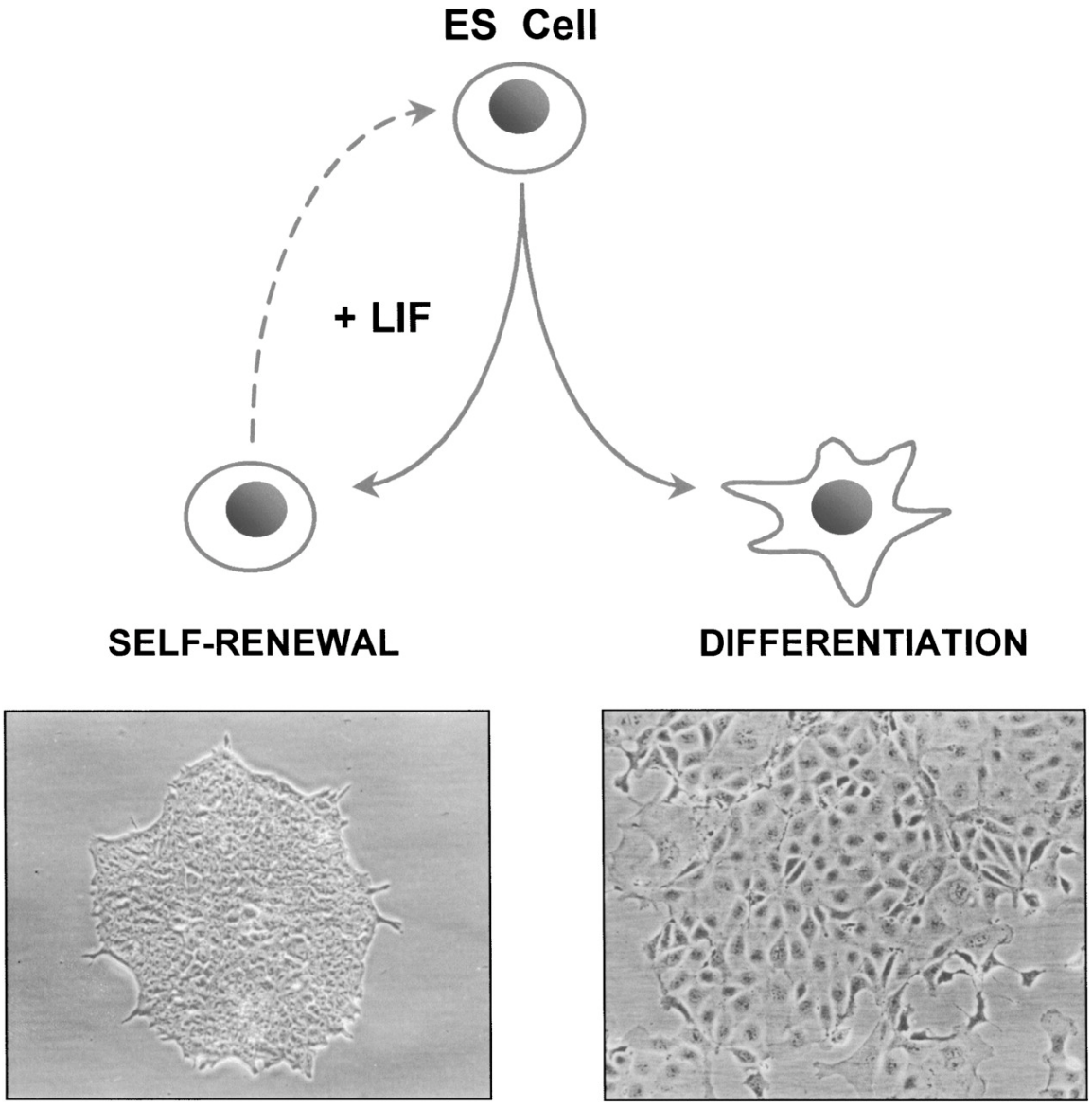

Figure 1-3 Promotion of mouse ES cell self-renewal by leukemia inhibitory factor Diagram depicts two possible fates for a dividing ES cell. Under conditions favoring self-renewal, ES cells form dense colonies of small, rapidly dividing cells. The cytokine leukemia inhibitory factor (LIF) promotes self-renewal by activating the JAK/STAT signaling cascade. In the absence of LIF and serum, ES cells produce autocrine Fgf4 that drives them toward the neuroectoderm lineage. Differentiating ES cells change shape, expand in size, and slow their growth rates. Figure taken from (Smith, 2001).

neural induction and remain pluripotent for prolonged periods of time even in the absence of LIF and serum (Kunath et al., 2007). Erk2-null cells also fail to undergo differentiation in adherent culture and retain the expression of pluripotency markers such as Oct4 and Nanog (Kunath et al., 2007). Thus, Fgf-mediated activation of Erk is an autoinductive stimulus that triggers the transition of ES cells from self-renewal to lineage commitment.

Bone morphogenetic proteins (BMPs), which are members of the TGF-β superfamily of secreted growth factors, are known anti-neural factors in mammalian embryogenesis (Wilson and Hemmati-Brivanlou, 1995). Knowing that ES cells differentiate into neural precursors in serum-free media, Smith hypothesized that BMPs might be important for suppressing the differentiation of cultured ES cells. Whereas BMPs alone induced ES cell differentiation into epithelial cells, the addition of both LIF and BMP4 to the culture medium sustained ES cell self-renewal in the absence of serum (Ying et al., 2003). Mechanistically, BMPs were found to act by inducing expression of Id genes via the Smad pathway, because forced expression of Id liberated ES cells from BMP or serum dependence and allowed self-renewal in LIF alone (Ying et al., 2003). In sum, the use of BMPs to activate the Smad/Id pathway alleviated the requirement for serum during the derivation and culture of mouse ES cells.

Maintenance of pluripotency by signal inhibition

The identification of LIF and BMPs as regulators of ES cell pluripotency enabled the culture of ES cells in fully defined media and shed light on signaling pathways

involved in self-renewal. One question that remained was whether these extrinsic factors were absolutely required for ES cell pluripotency. Alternatively, it was possible that LIF and BMPs acted by counteracting intrinsic differentiation pathways, such that when shielded from this tendency to differentiate the basal ES cell state was self-renewal. An elegant series of studies by Smith and coworkers addressed this very issue.

Armed with the knowledge that FGF signaling through ERK is important for the differentiation of ES cells into neural precursor cells, these researchers used small molecule inhibitors to block the function of FGF receptor tyrosine kinases and the ERK cascade (Ying et al., 2008). Culture of ES cells in the presence of these inhibitors enabled the expansion of undifferentiated ES cells, but cell growth and viability was compromised due to high levels of apoptosis. However, the addition of a third inhibitor specific to GSK3, a compound that had been previously reported to enhance ES cell propagation (Sato et al., 2004), resulted in the efficient expansion of ES cells in media completely lacking growth factors and cytokines. Furthermore, use of media containing all three pharmacological inhibitors (3i media) allowed the establishment of germline-competent ES cells from CBA strain mice, which are refractory to ES cell production under standard culture conditions (Buehr and Smith, 2003).

Importantly, ES cell propagation in 3i media does not involve activation of the STAT3 transcription factor, because STAT3-null ES cells cultured in 3i were indistinguishable from wild-type (Ying et al., 2008). Since ES cells can be derived and maintained without growth factors or cytokines, it appears that cultured ES cells exist in a basal cell state that is intrinsically self-maintaining if shielded from inductive

differentiation stimuli (autocrine FGF, see Figure 1-4 for summary).

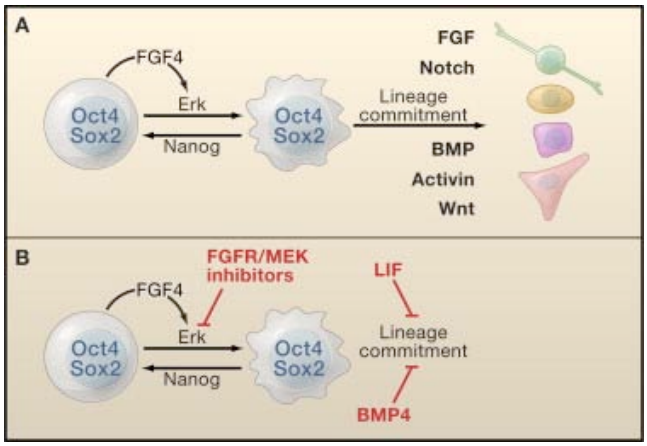

Figure 1-4 Maintenance of mouse ES cell pluripotency in culture
Factors important for ES cell pluripotency are shown. Oct4, Sox2 and Nanog are transcription factors that maintain the undifferentiated state through gene expression programs. Under basal conditions, ES cells produce autocrine FGF4 that signals through the Erk pathway and poises the cells for differentiation. Inhibition of this pathway using small molecule FGFR and MEK inhibitors promotes ES cell self-renewal. Lineage commitment can also be blocked further downstream using LIF and BMP4. Figure taken from (Silva and Smith, 2008).

PLURIPOTENT STEM CELLS FROM OTHER SPECIES

Rats

Using small molecule inhibitors of the ERK and GSK3 pathways to shield the pluripotent ground state from inductive differentiation stimuli, authentic ES cells capable of germline transmission have been recently derived from rats (Buehr et al., 2008, Li et

al., 2008). These ES cells pass all of the criteria required of mouse ES cells, and are the first germline-competent ES cell line established from a species other than mouse. These rat ES cells should allow researchers to genetically manipulate the rat genome in an manner analogous to mice, and create new models for the study of human disease. However, the use of these cells to generate knockout rats has yet to be reported. It is possible that there is a technical hurdle to overcome at another step in the gene targeting procedure. For example, homologous recombination might be more difficult in rat cells than in mice. Nevertheless, it is anticipated that reports of the production of knockout rats using rat ES cells will be forthcoming.

Primates

The first pluripotent cell lines from primates were established in the mid-1990s from rhesus monkey and common marmoset blastocysts (Thomson et al., 1995, 1996). While their ability to contribute to chimeric blastocysts has not been tested, these cells do form teratomas when injected into mice and appear to self-renew indefinitely in culture. Study of these cells from nonhuman primates facilitated the derivation of the first human pluripotent cell lines (Thomson et al., 1998).

Although they are typically called ES cells, human pluripotent stem cells are not equivalent to mouse ES cells. First, human ES cells grow at a far slower rate than mouse ES cells, with doubling times of up to 35 hours, compared to the 5 hour cell cycle seen in mouse ES cells (Amit et al., 2000). In addition, the growth factor requirements for human ES cells are substantially different than those for mouse ES cells. For example,

LIF can not take the place of feeder cells in human ES cell maintenance, and STAT3 activity appears to have little effect on human ES cell self-renewal (Daheron et al., 2004). More strikingly, the roles of BMPs and FGFs appear to be reversed in human ES cells compared to mouse. Whereas in mouse ES cell cultures BMPs are added to the medium to counteract FGF signaling and maintain pluripotency, human ES cell self-renewal requires FGF activity to suppress BMP signaling (Xu et al., 2005).

A new cell line derived from mouse post-implantation epiblast may help to explain this apparent paradox. While remaining pluripotent, epiblast stem cells (EpiSCs) have different properties than ES cells, including altered growth rates, gene expression patterns, and media requirements, and these cells are not competent to contribute to blastocyst chimeras (Tesar et al., 2007). EpiSCs can also be produced from ES cells in culture via differentiation (Guo et al., 2009). Interestingly, human ES cell lines share many of the properties of EpiSCs, prompting researchers to suggest that human ES cells might be more similar to EpiSCs than they are to mouse ES cells (Nichols and Smith, 2009). Whereas ES cells are believed to exist in a ground state of self-renewal, EpiSCs are thought to be in a state poised for differentiation (Silva et al., 2009). In spite of their apparent differences, both mouse and human ES cells remain valuable tools for the study of differentiation pathways in mice and humans.

CHAPTER TWO
Introduction II

METABOLIC PATHWAYS ALTERED IN MOUSE ES CELLS

Intermediary metabolism is the set of chemical reactions that converts substrates into end products through many specific chemical intermediates. These processes allow cells to grow and divide, maintain their structures, and respond to changes in their environments. Their unusually fast rates of cell division suggest that proliferating mouse ES cells might contain unique metabolic features not normally seen in other mammalian cell types.

Previous work by our laboratory has shown that ES cells exist in a unique metabolic state that facilitates rapid growth (Wang et al., 2009). To survey the levels of numerous common metabolites, mouse ES cells (line E14) grown without feeder cells were exposed to organic solvents that allow soluble extracts to be subjected to liquid chromatography-mass spectrometry (LC-MS/MS), This method (described in Tu et al., 2007) enables multiple reaction monitoring of scores of metabolites. Parameters necessary for the detection of the two most abundant daughter ions for each metabolite upon collision-induced fragmentation were optimized so that metabolite identity could be simultaneously assessed.

The relative amounts of individual metabolites prepared from ES cells were compared with those of embryoid body cells deprived of LIF for 3, 5, or 7 days (Figure 2-1). Using this method, we identified three primary metabolic pathways that change dramatically as a function of ES cell differentiation. These were the purine biosynthetic

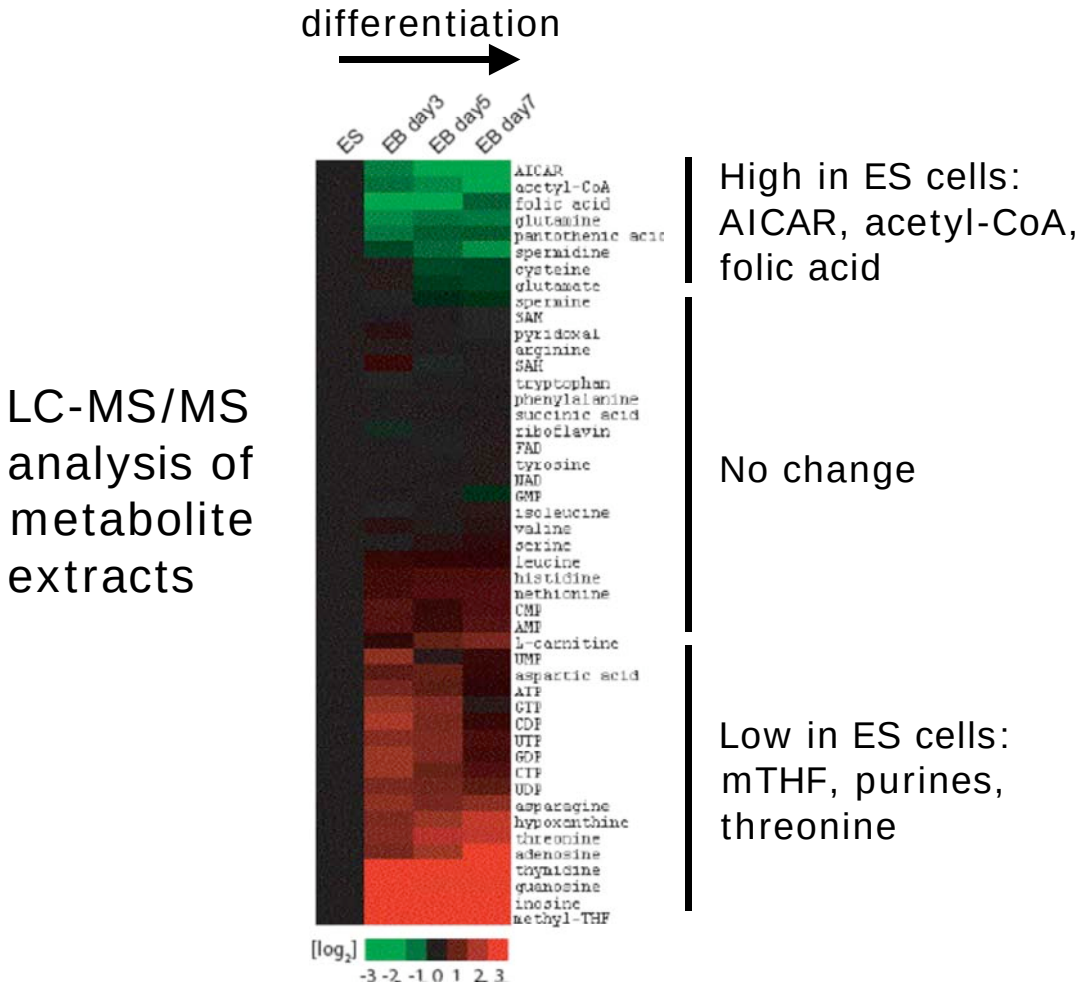

Figure 2-1 Metabolic profile of ES cells as a function of differentiation
Feederless mouse ES cells (E14 strain) were differentiated into embryoid bodies using LIF withdrawal. Organic metabolites were extracted in cold 50% aqueous methanol, dried on a vacuum concentrator, and reconstituted in 0.1% formic acid or 5 mM ammonium acetate. Metabolite levels were analyzed by LC-MS/MS analysis (Tu et al., 2007). Green indicates metabolites that decreased during the course of embryoid body differentiation, and red indicates metabolites that increased. Assays were performed in triplicate. Figure from (Wang et al., 2009).

pathway, one-carbon folate metabolism, and catabolism of the amino acid threonine into glycine and acetyl-CoA. All three of these pathways are contained within the network of reactions called the high-flux backbone (HFB) of metabolism, which is used by microbial organisms to sustain cell division rates under growth-liming conditions (Almaas et al., 2004; Hartman, 2007). These observations raised the possibility that ES cells might exist in a HFB metabolic state comparable to that of rapidly growing bacterial cells.

PURINE BIOSYNTHESIS

The first class of metabolites that changed significantly during the course of ES cell differentiation was purine nucleosides. Purines and pyrimidines are the building blocks of nucleic acids. Pyrimidines are six-membered heterocyclic aromatic rings containing two nitrogen atoms. A purine is the combination of a pyrimidine joined to a five-membered imidazole ring. Purines and pyrimidines are not typically catabolized to generate energy, but instead utilized in the processes of DNA replication and DNA-RNA transcription. Rapidly proliferating cells synthesizing large amounts of DNA have an increased demand for nucleic acid synthesis, and must increase their production of purines and pyrimidines to maintain growth rates. For this reason, many anti-microbial and anti-cancer drugs work by inhibiting these metabolic pathways (Garrett and Grisham, 1999).

In our studies, the purines adenosine, guanosine, and inosine all increased by approximately ten fold as a result of ES cell differentiation into embryoid bodies (Figure 2-2 C-E). Thus, there appears to be a rapid consumption of purines in undifferentiated

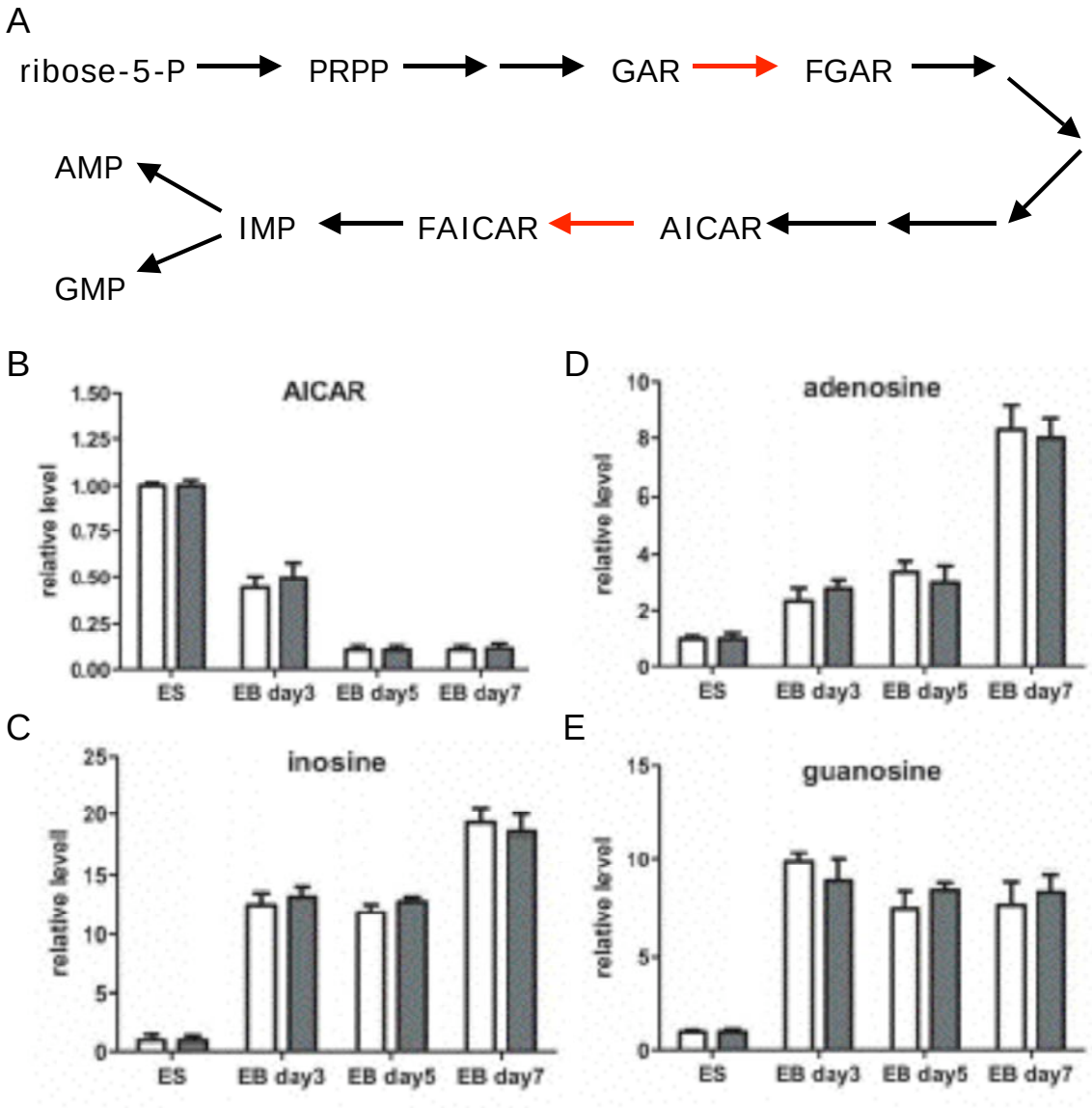

Figure 2-2 The purine biosynthetic pathway
A. 5-Phosphoribosyl-1-pyrophosphate (PRPP), the first molecule specific to *de novo* purine biosynthesis, is made from ribose-5-phosphate by the enzyme PRPP synthetase. Purine nucleotides are generated by successive additions to the purine ring to form inosine 5'-monophosphate (IMP). IMP is the common precursor to adenosine 5'-monophosphate (AMP) and guanosine 5'-monophosphate (GMP). The two steps requiring formyl-THF as a one-carbon donor, catalyzed by the transformylase enzymes GAR Tfase and AICAR Tfase (Benkovic, 1984), are highlighted in red. B-D. Levels of the purines AICAR, inosine, adenosine, and guanosine as a function of ES cell differentiation. Figures from (Wang et al., 2009).

ES cells. ES cells have an unusual cell cycle, with a very short G1 phase and a high proportion of cells in S phase. As ES cells differentiate, their growth rates slow down and their cell division cycle becomes more similar to that of other mammalian cell types (Smith, 2001). It makes intuitive sense therefore to hypothesize that ES cells might have a high demand for purines in order to maintain their high rates of cell division.

The *de novo* purine biosynthetic pathway is energetically expensive, requiring the hydrolysis of six ATP molecules per molecule of inosine monophosphate (IMP) produced (Devlin, 2002). The pathway is initiated when the sugar ribose-5-phosphate is activated by the transfer of a pyrophosphate group to yield phosphoribosyl pyrophosphate (PRPP, see simplified scheme in Figure 2-2A). PRPP is the first molecule specific to purine biosynthesis. In the second enzymatic reaction, PRPP reacts with glutamine to produce phosphoribosylamine (PRA). Production of PRA is thought to be the most highly regulated step in de novo purine biosynthesis, with no known regulatory mechanisms operating between PRA and IMP (Wyngaarden, 1976; Watts, 1983). Next, glycinamide ribonucleotide (GAR) is synthesized from PRA, glycine, and ATP by GAR synthetase. In the first of two transformylation reactions requiring tetrahydrofolate (THF), GAR transformylase transfers the N^{10}-formyl group of formyl-THF to the free amino group of GAR to yield formyl-GAR (FGAR). The requirement for folic acid compounds has been demonstrated for both of the transformylase reactions in the purine biosynthetic pathway (Warren and Buchanan, 1957). A series of five reactions requiring the hydrolysis of four moles of ATP results in the production of the metabolite aminoimidazole carboxamide ribonucleotide (AICAR).

In contrast to purine nucleosides, the purine intermediate AICAR was highly abundant in ES cells, decreasing by about ten fold during embryoid body formation (Figure 2-2B). This finding suggests that metabolic flux might be limited by the next step in the pathway. In step ten of the de novo purine biosynthetic pathway, AICAR transformylase adds the formyl carbon of formyl-THF to generate formyl-AICAR (FAICAR). This carbon is the final atom necessary for the formation of the purine nucleus. The IMP synthase enzyme appears to form a functional complex with AICAR transformylase, resulting in the sequential formylation and ring closure of AICAR to yield IMP (Benkovic, 1984). IMP is the precursor to both adenosine monophosphate (AMP) and guanosine monophosphate (GMP). The high level of AICAR indicates that in mouse ES cells the formylation of AICAR might be a rate-limiting step for purine biosynthesis. Therefore, we turned our attention to the one-carbon metabolic pathways required for this reaction to occur.

ONE-CARBON FOLATE METABOLISM

Folic acid derivatives (folates) are acceptors and donors of one-carbon units for all oxidation states of carbon except that of carbon dioxide, which is typically carried by biotin (Garrett and Grisham, 1999). Folic acid itself, also known as vitamin B_9, is not biologically active, but is activated by two successive reductions performed by the enzyme dihydrofolate reductase. This results in the formation of the active derivative tetrahydrofolate (THF), a coenzyme that is important for the metabolism of amino acids and nucleotides, where it acts as a one-carbon donor.

THF is charged to produce methyl-THF and formyl-THF by reactions utilizing carbon units from the amino acids glycine, serine, and histidine. The biosynthetic pathways for purine nucleotides and the pyrimidine thymine require incorporation of one-carbon units from folate derivatives (Figure 2-3A). For this reason, synthetic folate analogs (also called antifolates) such as methotrexate are sometimes used to disrupt DNA synthesis in human cancer cells (Devlin, 2002).

We observed dramatic changes in folate levels resulting from mouse ES cell differentiation (Figure 2-3 B and C). The amount of methyl-THF in particular was almost twenty fold higher in embryoid bodies than in pluripotent ES cells. This depletion of methyl-THF in ES cells is likely to be the basis for the accumulation of AICAR, which must be formylated to generate the purines IMP, AMP and GMP. Since high levels of charged folates are necessary to sustain rapid cell division cycles, the demand for these one-carbon donors appears to be unusually high in pluripotent ES cells.

THREONINE CATABOLISM

The catabolism of the amino acid threonine was also observed to be substantially altered in rapidly growing mouse ES cells. The mitochondrial enzyme threonine dehydrogenase (TDH) is responsible for catabolizing threonine into acetyl-CoA and glycine. The relative levels of threonine and acetyl-CoA changed in opposite directions as a consequence of ES cell differentiation. Whereas threonine levels were low in ES cells and increased during differentiation, the level of acetyl-CoA was initially high but declined during embryoid body formation (Figure 2-1). These features suggest that flux

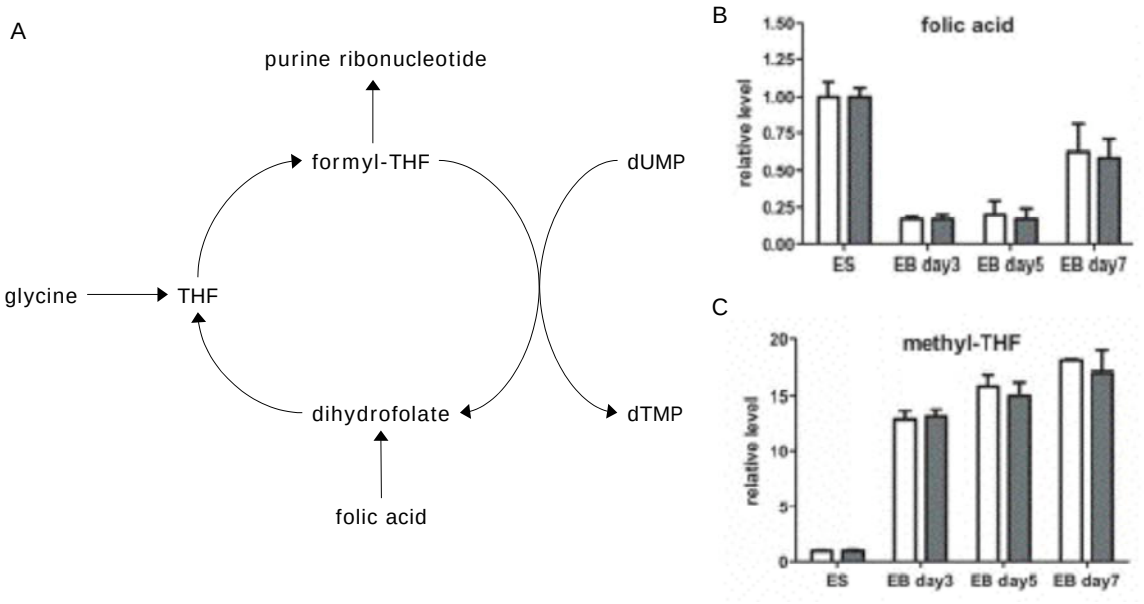

Figure 2-3 One-carbon folate metabolism
A. Sources of one-carbon units for incorporation into THF include glycine, serine, histidine and formate. The biosynthetic pathways for purines, methione, and the pyrimidine thymine all rely on the incorporation of one-carbon units from THF derivatives. Figure adapted from (Devlin, 2002). B-C. Levels of folic acid and mTHF as a function of ES cell differentiation. Figures from (Wang et al., 2009).

through the TDH pathway might be high in pluripotent stem cells. Indeed, this enzyme is robustly expressed in ES cells but is absent in differentiated cells (discussed in chapter 3). Importantly, glycine generated in the mitochondria by this pathway is used to charge THF via the glycine cleavage system (Dale, 1978). Thus, it appears we have uncovered a metabolic network operative in ES cells where one-carbon units originally derived from threonine pass through folate intermediates to drive high rates of purine biosynthesis.

In the mitochondria, TDH forms a stable complex with its partner enzyme glycine *C*-acetyltransferase (Gcat, also called 2-amino-3-ketobutyrate-CoA ligase). NAD^+-dependent oxidation of threonine by TDH produces the short-lived intermediate 2-amino-3-ketobutyrate, which in the absence of Gcat is spontaneously decarboxylated to produce aminoacetone. However, in a process referred to as channeling, TDH is able to pass this molecule directly to the Gcat enzyme, which catabolizes it into glycine and acetyl-CoA (Figure 2-4; Dale, 1978; Srere, 1987). Whereas in mice TDH appears to be exclusively expressed in ES cells, Gcat expression is ubiquitous. Recently solved X-ray structures of microbial TDH enzymes suggest a binding surface for Gcat (Ishikawa et al., 2007; Bowyer et al., 2009). The overall structure of TDH consists of a Rossman fold motif and is similar to that of alcohol dehydrogenase enzymes (Figure 2-5).

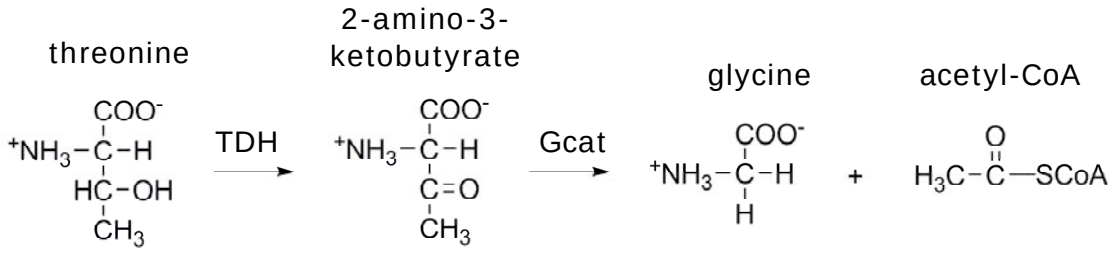

Figure 2-4 Catabolism of threonine into glycine and acetyl-CoA
In mitochondria, threonine is catabolyzed by TDH to yield the short-lived intermediate 2-amino-3-ketobutyrate. In the absence of Gcat, 2-amino-3-ketobutyrate is spontaneously decarboxylated to produce aminoacetone. However, Gcat, which is expressed ubiquitously in mice, forms a complex with TDH in mitochondria, resulting in a sequential reaction that produces glycine and acetyl-CoA from threonine (Dale 1978, Srere 1987).

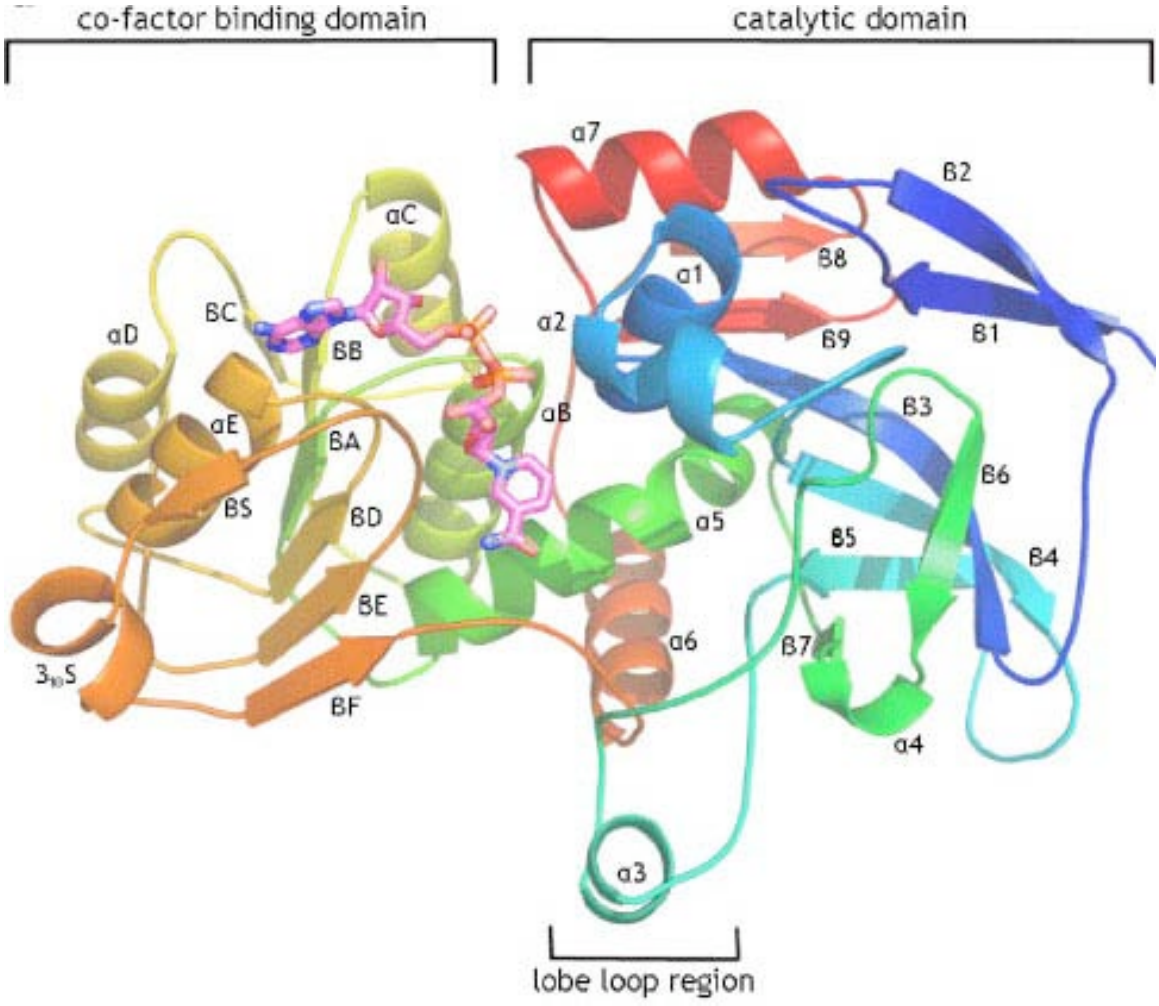

Figure 2-5 Structure of threonine dehydrogenase from *Thermococcus kodakaraensis* Ribbon diagram of a TkTDH monomer with the NAD^+ cofactor shown in pink. The X-ray structure was determined at 2.4 Å resolution. The NAD^+-binding domain adopts a Rossman fold characteristic of di-nucleotide binding domains. Despite low sequence homology, the overall structure is similar to alcohol dehydrogenases from lower organisms. Figure taken from (Bowyer et al., 2009).

HIGH-FLUX BACKBONE METABOLISM

Elegant studies of metabolic flux in bacteria have defined reaction pathways that flow at rates more than three to four orders of magnitude higher than those of other pathways of intermediary metabolism (Almaas et al., 2004). Under conditions facilitating rapid growth rates, the overall cellular metabolism is dominated by this high-flux backbone (HFB) of metabolism, which is embedded in a network of mostly lower-flux reactions. Upon perturbation of bacterial growth conditions, only the reactions constituting the HFB of metabolism undergo noticeable changes in flux, whereas the low-flux reactions remain virtually unaltered, suggesting the high-flux pathways play a decisive role in dictating rates of cell division.

The core circuitry of the HFB of metabolism includes the TCA cycle and the purine biosynthetic pathway, as well as the TDH enzyme (Figure 2-6). Indeed, TDH occupies an important position in the HFB metabolic network. This is because the two products of the TDH reaction, acetyl-CoA and glycine, are needed to fuel the high-flux reactions of the TCA cycle and purine biosynthesis, respectively. Under growth conditions that permit HFB metabolism, most of the twenty naturally occurring amino acids are processed into biomass via protein synthesis. Strikingly, rapidly growing bacteria convert the majority of threonine present in the cell into glycine and acetyl-CoA using the TDH enzyme (Almaas et al., 2004).

Evidence for the existence of the HFB of metabolism in eukaryotes comes from experiments performed using yeast grown in the presence of hydroxyurea, an inhibitor of nucleotide biosynthesis (Hartman, 2007). Under these conditions yeast cells upregulate

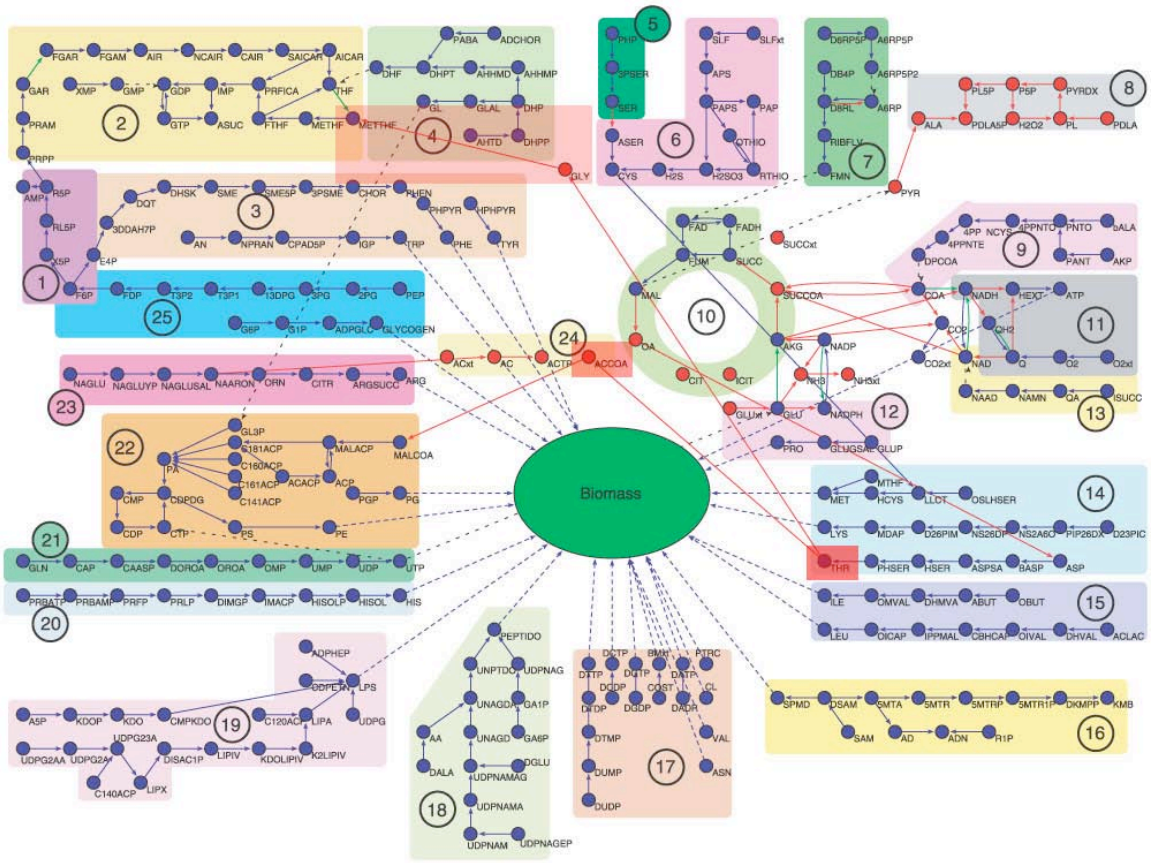

Figure 2-6 The high-flux backbone of metabolism in *E. coli*
In rapidly growing bacteria, metabolic activity is dominated by several reactions with very high fluxes (shown in red). This high-flux backbone (HFB) of metabolism includes the TCA cycle and the purine biosynthetic pathway, as well as the TDH enzyme. Whereas most of the twenty naturally occurring amino acids are processed into biomass via protein synthesis, threonine is catabolized by TDH to provide glycine and acetyl-CoA to satisfy the demands of purine biosynthesis and the TCA cycle, respectively. Figure taken from (Almaas et al., 2004).

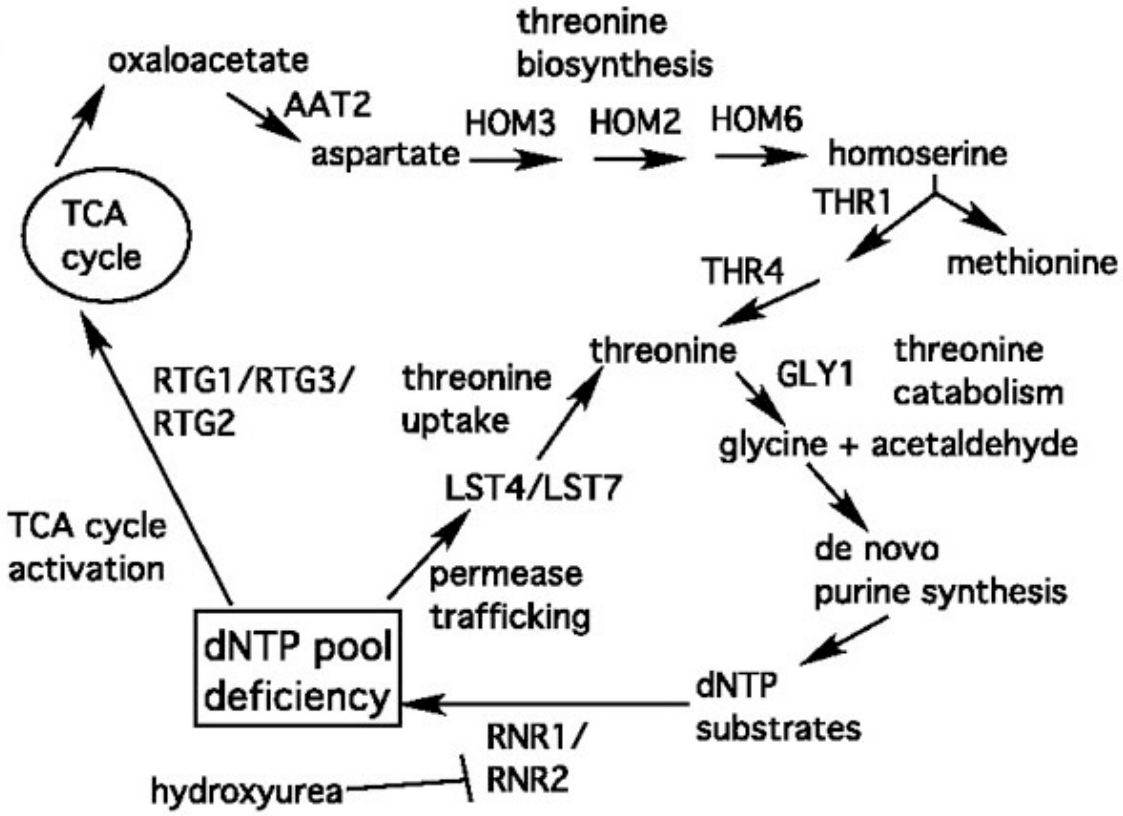

Figure 2-7 Threonine catabolism buffers purine depletion in budding yeast
De novo synthesis in yeast provides sufficient threonine to satisfy the demands of both protein synthesis and purine synthesis under nutrient-limiting conditions. As a result, cellular growth rates can be maintained by using the HFB of metabolism to increase rates of threonine synthesis and breakdown to buffer depletion of purine pools. Extracellular uptake and catabolism of threonine can be used for purine biosynthesis in mammalian cells. Figure taken from (Hartman, 2007).

their synthesis of threonine, which is catabolized to glycine and acetyl-CoA. This process is used to buffer depleted purine pools and maintain high rates of cell division (Figure 2-7). Since mammalian cells cannot synthesize threonine de novo, extracellular uptake of threonine is required to satisfy the demands of both translation and purine biosynthesis during conditions where HFB metabolism is operative.

DEPENDENCE OF MOUSE EMBRYONIC STEM CELLS ON THREONINE

To test whether ES cells might deploy the TDH enzyme to adopt a metabolic state comparable to the HFB of bacterial cells, we prepared culture media that were individually deprived of each of the 20 amino acids. ES cells of the E14 line were plated and exposed to each of the single amino acid "drop-out" culture media. After 36 hours of exposure, normal ES cell colonies were observed to grow in all culture media except that deprived of threonine (Figure 2-8). Colonies grown from either control media, or media individually lacking each amino acid except threonine, stained positively with the alkaline phosphatase marker indicative of undifferentiated ES cells. Light microscopic inspection of ES cell colonies showed little or no difference in colony morphology, cell size, or cell number as a function of media type. All of the media samples tested contained 10% fetal bovine serum. The serum component provides cells with residual amounts of amino acids, as well as with serum proteins that can be hydrolyzed by cells to salvage amino acids for protein synthesis and other metabolic needs. These residual amounts of amino acids appear to be sufficient for the growth of ES cells in all cases except threonine deprivation.

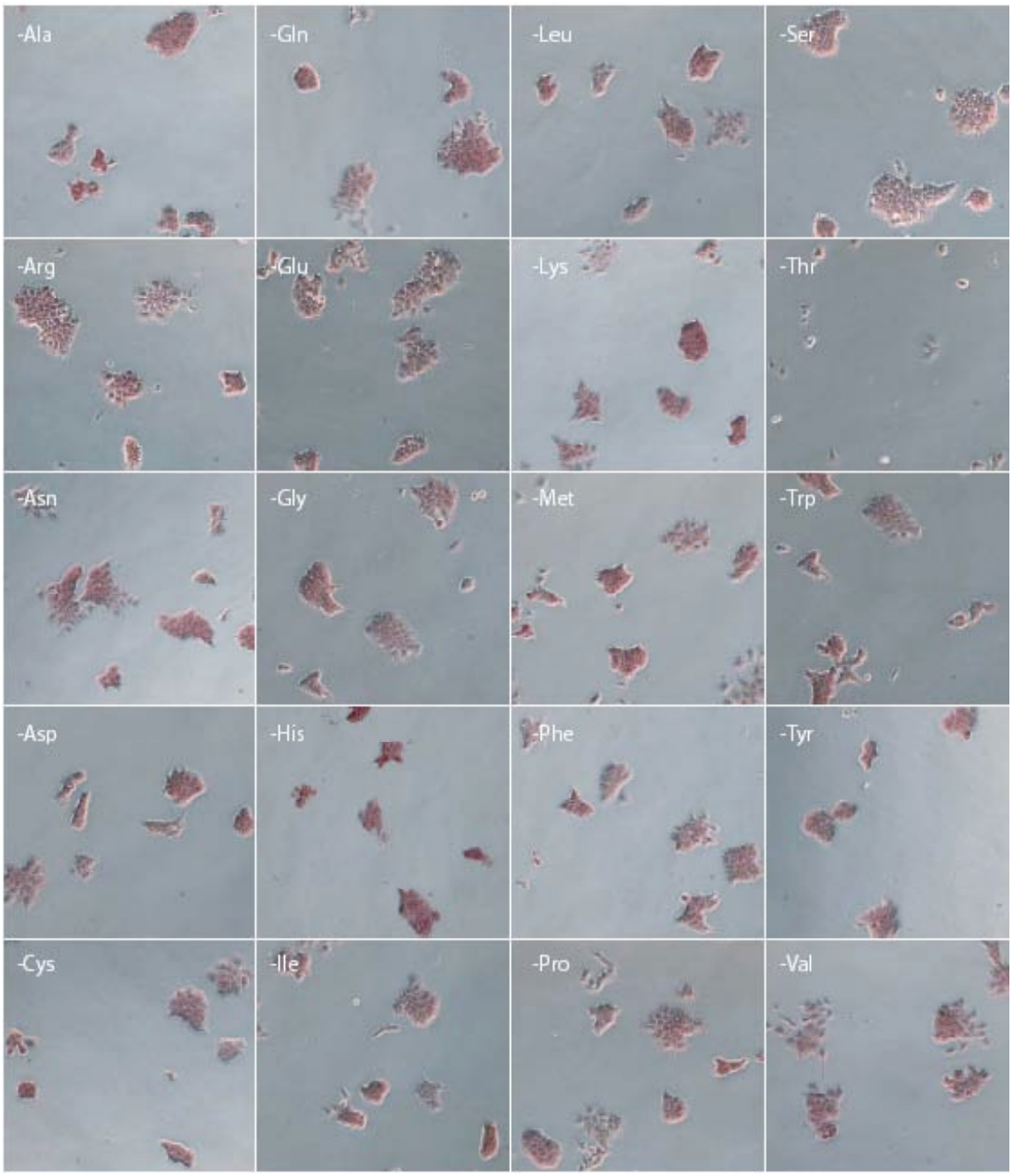

Figure 2-8 Mouse ES cell proliferation is critically dependent on threonine
CCE line ES cells were plated at single cell density and grown for 6 hours before exposure to culture medium prepared to be missing a single amino acid. After 36 hours, colonies were stained with an alkaline phosphatase detection kit (Chemicon) and photographed under a Zeiss AxioObserver microscope using bright field optics. Figure from (Wang et al., 2009).

If TDH-mediated threonine breakdown in ES cells indeed supplies glycine to fuel one-carbon metabolism for enhanced purine biosynthesis, one might anticipate that deprivation of threonine would impede DNA synthesis. To test this hypothesis, we cultured ES cells in the presence of varying levels of threonine and exposed the cells to brief labeling with [^{3}H]thymidine. The incorporation of [^{3}H]thymidine into DNA was substantially reduced as a function of threonine concentration in the culture medium (Figure 2-9C). Reduction of threonine supplementation to 30 μM partially inhibited [^{3}H]thymidine incorporation into DNA. When threonine concentrations were reduced to 10 μM, DNA synthesis was impeded to a level similar to that observed by complete elimination of threonine from culture medium (except for residual amounts present in serum). By contrast, when HeLa cells were grown in culture medium supplemented with varying concentrations of threonine, DNA synthesis was unimpeded even under conditions of complete threonine deprivation (Figure 2-9C).

The growth of fibroblast cell lines was not selectively sensitive to threonine deprivation. Unlike the threonine dependence of ES cells, it was instead observed that both MEF and 3T3 cells failed to grow in cysteine-deprived medium. Thus, threonine-high:cysteine-low (ThCl) culture media could rationally be predicted to selectively support ES cell growth relative to that of differentiating or differentiated cells of the early mouse embryo. As an initial test of this hypothesis, small numbers of ES cells were mixed and cultured with a vast excess of either MEF or 3T3 cells and exposed to culture media supplemented with varying amounts of cysteine. As expected, deprivation of cysteine favored the growth of ES cells relative to either MEF or 3T3 cells (Figure 2-10).

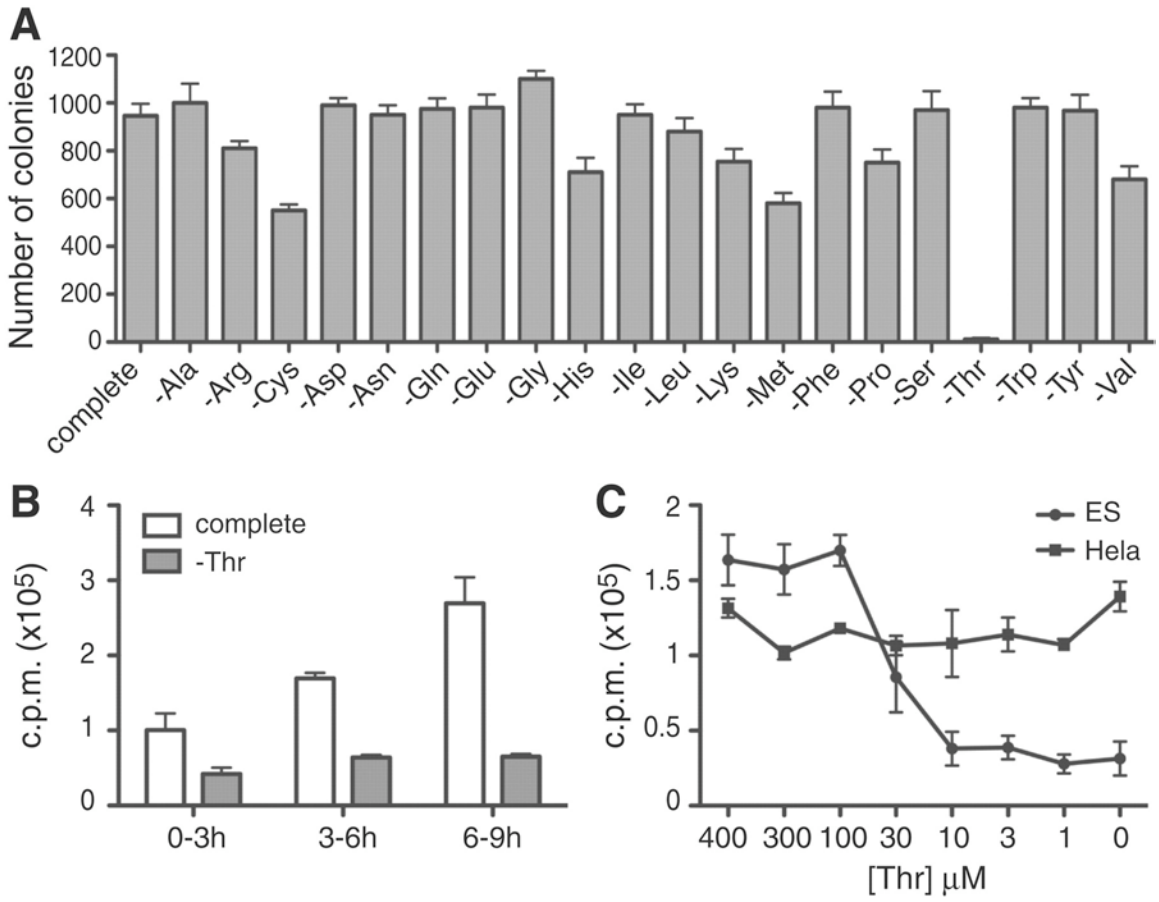

Figure 2-9 Inhibition of DNA synthesis in ES cells deprived of threonine
A. Quantification of colony number from Figure 2-6. Threonine supplementation to the culture media is critical for ES cell colony formation. B. Mouse ES cells were exposed to complete or threonine-deprived medium for 3, 6, or 9 hours, and then metabolically labeled with 2 μCi of [^{3}H]thymidine for 3 hours. Following three washes with PBS, DNA was precipitated with 5% trichloroacetic acid, and then suspended in 0.5 M NaOH/0.5% SDS for liquid scintillation counting. C. ES or HeLa cells were exposed to culture medium containing the indicated amounts of threonine for 3 hours and then metabolically labeled for 3 hours with [^{3}H]thymidine. Purified DNA was assayed for radioactivity using scintillation counting. Figure from (Wang et al., 2009).

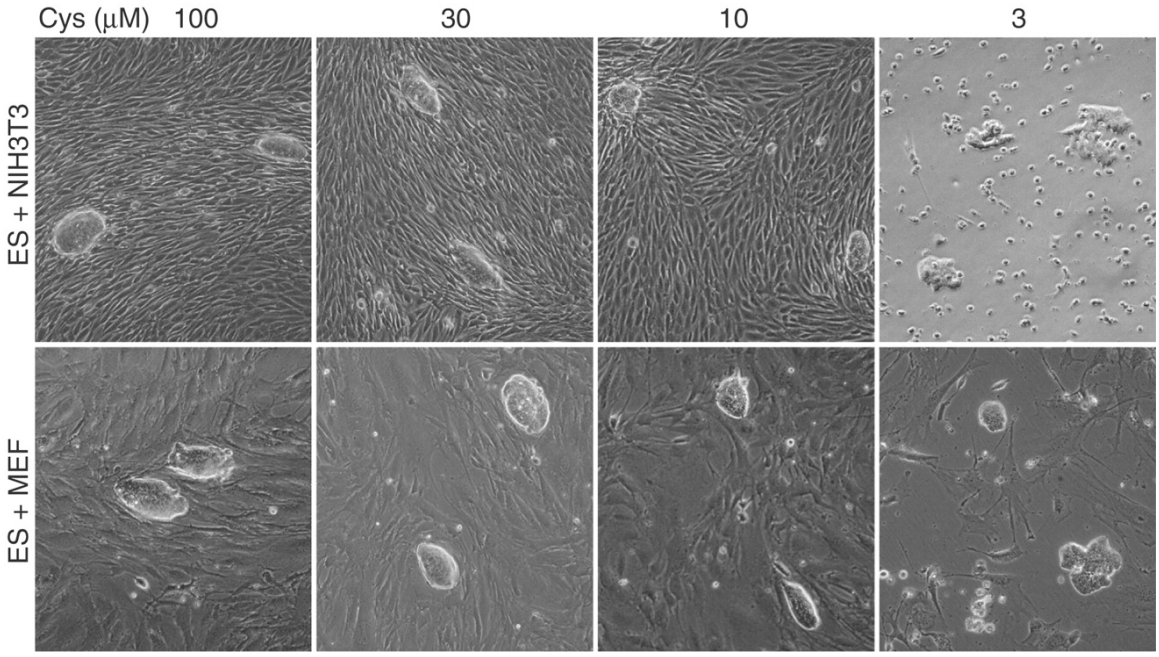

Figure 2-10 Sensitivity of fibroblast cell lines to cysteine deprivation
Cocultures of ES/MEF or ES/NIH3T3 cells were subjected for 2 days to media containing the indicated amounts of supplemented cysteine. Cysteine deprivation severely impeded fibroblast cell growth at 3 μM without affecting ES cell colony formation. Figure from (Wang et al., 2009).

It is hoped that proper choice of ThCl medium might favor the establishment of improved ES cell lines from species other than mice.

In summary, we show here that mouse ES cells exist in a unique metabolic state that closely resembles the HFB metabolism used by rapidly growing microbial organisms. An abundant supply of threonine is necessary to sustain this metabolic state, because threonine withdrawal results in decreased rates of DNA synthesis and the inability of individual ES cells to form colonies. The identification of a high-flux

pathway linking threonine catabolism to DNA synthesis helps to explain the unusually fast growth rates of mouse ES cells, and might have relevance to the derivation and maintenance of new ES cell lines from non-rodent species.

CHAPTER THREE
Results

TDH EXPRESSION IN MOUSE CELLS AND EMBRYOS

Abstract

Threonine dehydrogenase is the mitochondrial enzyme responsible for the production of glycine and acetyl-CoA from the amino acid threonine. Based on quantification of the abundance of these metabolites, we hypothesized that expression of the threonine dehydrogenase enzyme might change during the course of embryonic stem cell differentiation. Here, using multiple approaches, we show that this enzyme is highly and selectively expressed in embryonic stem cells and in the inner cell mass (ICM) of the mouse blastocyst. These findings suggest that threonine dehydrogenase might be responsible for the unique metabolic state found in these cells, and that inhibition or genetic lesion of this enzyme might result in the loss of embryonic stem cell self-renewal.

Introduction

Gene expression is the process by which genetic information is transferred from DNA to RNA and protein, and is the most basic level at which genotype gives rise to phenotype. Gene expression can be regulated through specific molecular interactions at any step from the initiation of DNA-RNA transcription to the activity of a functional protein product (Lewin, 2004). Regulation of gene expression provides the cell with exquisite control over structure and function and is the basis for cellular differentiation and morphological evolution (Carroll 2008). Quantification of the expression level of a

specific gene in different cells, tissues, or organisms provides a huge amount of information about that gene's function and biological activity. Here we report the expression pattern and subcellular localization of the metabolic enzyme threonine dehydrogenase in mouse cells and tissues.

Methods

Materials

MitoTracker Orange dye (Invitrogen) was used to localize mitochondria in ES cells. A TSA-biotin amplification kit (Perkin Elmer) was used for in situ hybridization of blastocysts. All other chemicals and reagents were obtained from Sigma-Aldrich except where specified.

Cell Culture

Feeder-independent mouse E14Tg2A (BayGenomics) ES cells were cultured on gelatinized dishes in Glasgow minimum essential medium (GMEM) supplemented with 10% FBS (Hyclone), 100 μM MEM non-essential amino acids, 1 mM sodium pyruvate, 2 mM glutamine, 200 μg/mL penicillin, 100 μg/mL streptomycin (Stemcell Technologies), 50 μM 2-mercaptoethanol, and 1000 units/mL LIF (Chemicon). Dropout medium was prepared by omitting threonine from GMEM or non-essential amino acids. Approximately 10^6 ES cells were plated per 384-well plate or 25 cm^2 flask. ES cells were passaged every 2 days, and the medium was changed on alternate days. For microscopy experiments, ES cells were grown on gelatinized glass chamber slides (Lab-Tek) and

visualized on a Zeiss AxioObserver microscope.

Quantitative RT-PCR Analysis

Total RNA was extracted with RNA STAT-60 (Tel-Test) and converted into cDNA with oligo(dT) primer using the SuperScript first-strand synthesis kit (Invitrogen). PCR was performed on an AB7900HT fast real-time PCR system (Applied Bioscience) using a TDH specific primer pair with the sequences of 5'-CCTGGAGGAGGAACAACTGACTA-3' (forward) and 5'-ACTCGAATGTGCCGTTCTTTG-3' (reverse). Results were validated by amplification of GAPDH and 18S ribosomal RNA.

Generation of TDH Antibody

Rabbit polyclonal antibodies to the mouse threonine dehydrogenase enzyme were produced using the synthetic peptides NH_2-PMILDDSNARKDWGWKHDFD-COOH and NH_2-LSDIRKPPAHVFHSGPFVYAN-COOH. Peptide design was based on protein homology, hydrophilicity, and antigenicity. 5 mg of each peptide was conjugated to KLH carrier protein (using cysteine), mixed with complete Freund's adjuvant, and injected into rabbits. Final bleeds containing TDH antibodies were taken after three additional immunizations in incomplete Freund's adjuvant. Antibodies were tested by immunoblotting protein lysates from HEK 293T cells expressing varying amounts of FLAG-tagged TDH.

In Situ Hybridization

Peri-implantation mouse embryos were subjected to in situ hybridization according to the methods described in Chazaud et al., 2006. Sense and anti-sense probes were prepared from a full length cDNA clone of the mouse TDH gene.

Immunohistochemistry

Mouse ES cells or embryos were fixed with 4% PFA in TBS for 20 minutes at room temperature and then washed 3 times for 5 minutes each with TBS. Blocking was carried out for 30 minutes (cells) or 2 hours (embryos) using 3% normal goat serum (Vector Laboratories) and 0.1% Triton X-100 in TBS. Overnight incubation with TDH antibodies diluted 1:1000 in blocking solution was performed at 4°C. After washing, cells or embryos were incubated with secondary antibody (Alexa Fluor 488 $F(ab')_2$ fragment of goat anti-rabbit IgG from Molecular Probes diluted 1:1000 in blocking solution) for 2 hours at room temperature. Cells were washed 3 times with TBS and coverslipped with Vectashield mounting medium with DAPI nuclear counterstain (Vector Laboratories). Immunostained cells and embryos were visualized on an Axiovert fluorescence microscope (Zeiss) and photographed with a Hamamatsu Orca-ER camera.

Cloning of Human TDH

Human TDH was amplified from fetal liver tissue (gift from Ann Word) cDNA and PCR products were cloned into the pGEM-T Easy Vector (Promega). Splice isoforms were identified by sequencing of vector DNA.

Results and Discussion

TDH Expression in Mouse ES Cells

In order to determine whether TDH might play a role in the HFB metabolism seen in mouse ES cells, we measured TDH mRNA levels using quantitative RT-PCR. Indeed, in total RNA isolated from ES cell cultures we detected robust expression of the TDH transcript (Ct value 18). In contrast, using the same analysis on RNA from seven tissues taken from adult mice, TDH expression was either exceedingly low or absent. In testis, where TDH was expressed higher than in any of the other tissues analyzed, the mRNA level was approximately one-thousand fold lower than in ES cells (Figure 3-1). We also analyzed the expression profile of TDH's partner enzyme, Gcat. Like TDH, Gcat was strongly expressed in mouse ES cells. However, high expression of the Gcat transcript was also found ubiquitously in adult mice. Thus, flux through the TDH pathway is likely to be regulated by the level of expression of the TDH enzyme.

Next, we measured TDH expression in pluripotent and differentiating ES cells. Feeder-independent ES cells were differentiated into embryoid body (EB) cells using LIF withdrawal, and TDH mRNA levels were measured 3, 5, and 7 days after initiation of differentiation. We found that expression of the TDH transcript declined by 75% during the first three days of differentiation, and by day 5 TDH expression was roughly one-tenth of its initial level (Figure 3-2E). To verify that active TDH enzyme is also present in ES cells, we purified mitochondrial extracts and measured TDH activity using an absorbance-based assay to monitor threonine-dependent production of NADH. As a control, we used two HEK 293T cell clones stably expressing different amounts of a

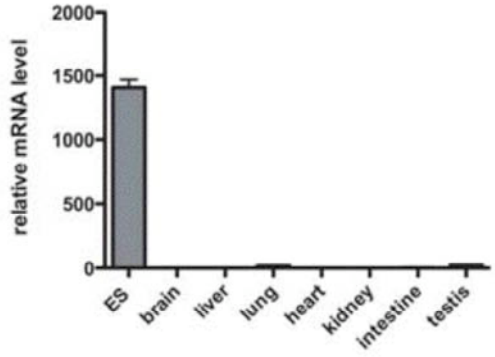

Figure 3-1 ES cell-specific expression of threonine dehydrogenase
Total RNA was isolated from cultured ES cells and from seven tissues dissected from adult mice. RNA was reverse-transcribed to make cDNA, and TDH expression was assayed by qPCR using TDH-specific primers. The TDH message level is roughly one-thousand fold higher in ES cells than in any of the adult tissues analyzed. Glyceraldehyde-3-phosphate dehydrogenase and 18S ribosomal RNA were used as internal controls. Figure from (Wang et al., 2009).

FLAG-tagged version of the TDH enzyme. Mitochondrial extracts from these cell lines contained detectable enzyme activity that matched their relative levels of TDH protein expression (analyzed by western blotting with an anti-FLAG antibody, Figure 3-2A). When assayed using mitochondrial extracts from ES cells, however, TDH activity was found to be much higher than in either of the HEK 293T stable cell lines analyzed (Figure 3-2B). Apparently, expression of ectopic TDH in transformed cell lines is not comparable to endogenous TDH expression in mouse ES cells (discussed further in Chapter 6).

In order to measure the level of endogenous TDH protein in ES cells, we generated rabbit polyclonal antibodies specific for the enzyme by injection of TDH peptide antigens. After verifying that these antibodies specifically recognized TDH using the stable cell lines expressing FLAG-tagged TDH, we blotted ES and EB cell lysates to determine TDH protein expression as a function of differentiation state. As the mRNA and enzyme expression studies indicated, TDH protein is abundantly expressed in ES cells but declines rapidly during the course of differentiation. As controls, we blotted the same lysates using antibodies against the transcription factors Oct4 and Nanog. We observed that the TDH expression pattern closely resembles that of these canonical ES cell markers (Figure 3-2D), raising the possibility that TDH transcription might be directly regulated by these factors (see below).

To directly visualize TDH in ES cell cultures, we stained ES cells grown on glass chamber slides using TDH-specific antibodies. As expected, ES cell colonies contained robust TDH protein expression that co-localized with mitochondria (Figure 3-3, top panels). As ES cells differentiated in response to LIF withdrawal, they extended processes that contained mitochondria but were negative for TDH, while the central region of the colony, which remained pluripotent, maintained appreciable TDH protein (Figure 3-3, middle). Extensively differentiated ES cells flattened out into ectoderm-like cells completely lacking TDH (Figure 3-3, bottom). Together, these studies suggest that mitochondrial TDH is expressed selectively in self-renewing mouse ES cells, and might be an important factor for specifying the pluripotent state.

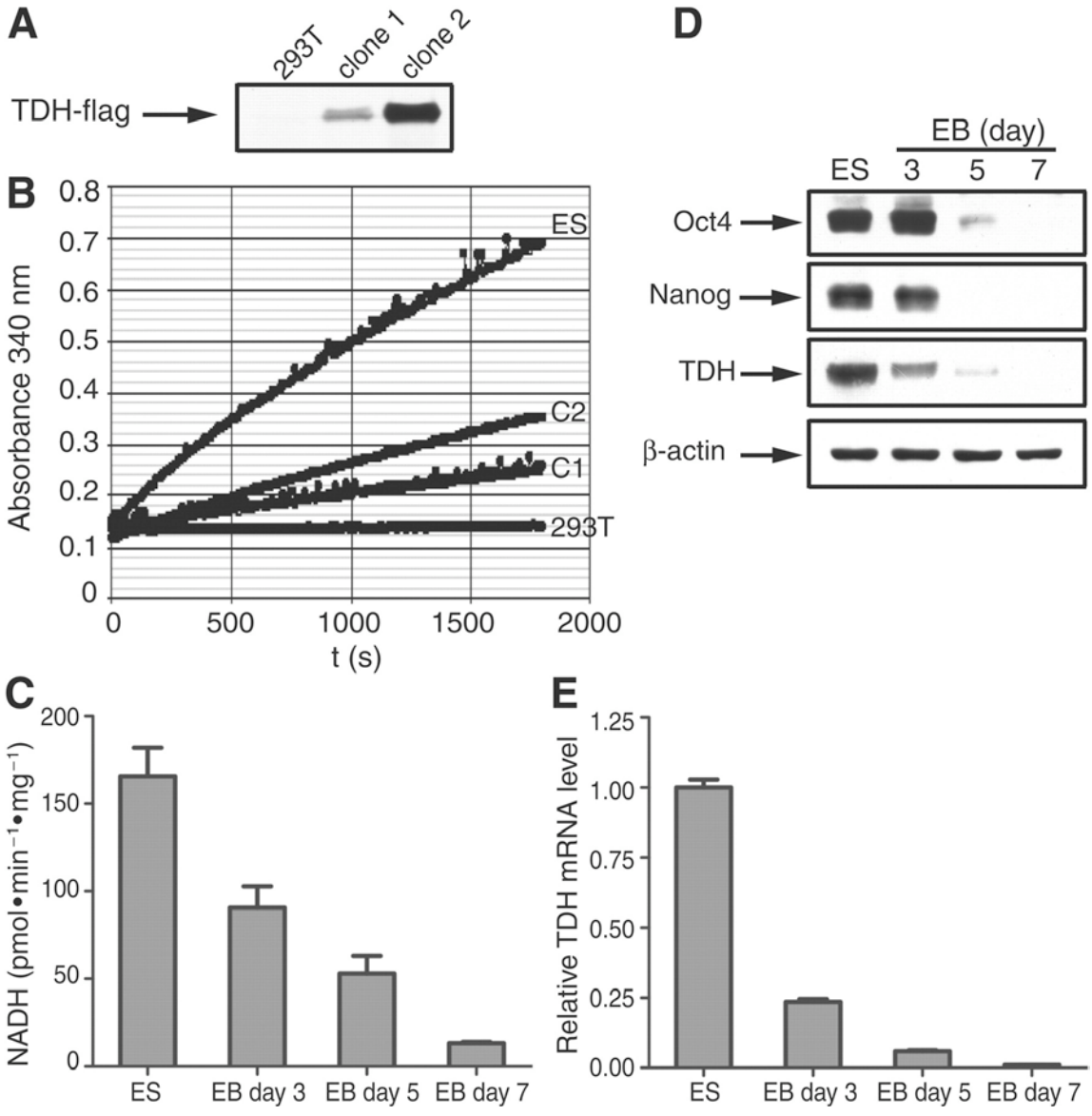

Figure 3-2 Expression of TDH enzyme, protein and mRNA in ES cells
A-B. TDH expression and activity in HEK 293T cell lines expressing a FLAG-tagged version of TDH. Enzymatic activity of FLAG-tagged TDH in HEK 293T mitochondrial extracts was detectable but much lower than in ES cell extracts. C. TDH activity as a function of differentiation. ES cells were differentiated into embryoid bodies using LIF withdrawal. D. Immunoblotting of ES and embryoid body cell lysates using Oct4, Nanog, TDH and actin specific antibodies. The TDH expression pattern closely resembles Oct4 and Nanog. E. TDH mRNA levels as assayed by qPCR for ES cells and day 3, 5, and 7 embryoid body cells. Figure from (Wang et al., 2009).

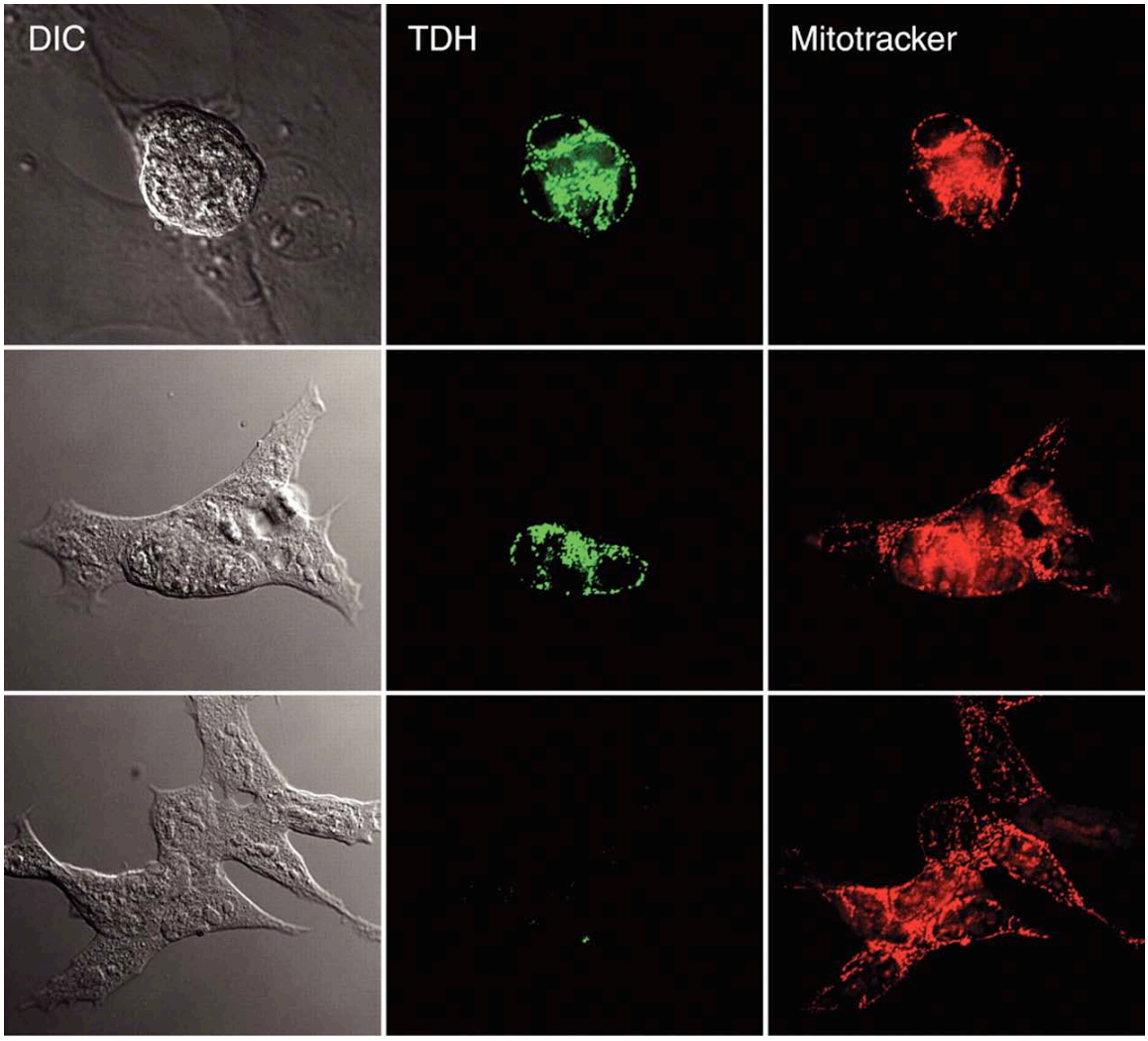

Figure 3-3 TDH expression as a function of ES cell differentiation
ES cell colonies were grown on glass chamber slides in complete media or media lacking LIF to promote differentiation. Cells were incubated with Mitotracker dye 15 minutes prior to fixation to visualize mitochondria (red). Immunocytochemistry was performed using antibodies specific for the mouse TDH enzyme. Top, an ES cell colony in which all cells stain positive for TDH, which colocalizes with mitochondria. Middle, a partially differentiated colony. The central region contains TDH staining but the differentiating processes lack TDH expression. Bottom, a fully differentiated colony devoid of TDH protein expression. Figure from (Wang et al., 2009).

TDH Expression in the Mouse Embryo

As discussed above, quantitative RT-PCR analysis did not reveal significant expression of TDH mRNA in any of the seven tissues analyzed from adult mice. Published expression arrays confirmed these results, but also showed significant TDH expression in the mouse pancreas, which was not one of the tissues analyzed in our original qPCR experiment (Bono et al., 2002). Although we were able to confirm pancreatic expression of TDH mRNA, western blotting and immunohistochemistry failed to reveal any TDH protein in pancreatic tissue (data not shown). We conclude that TDH expression is blocked in the pancreas at some post-transcriptional level. Since we have been unable to find a site of TDH enzyme expression in adult mice, it appears that TDH's role in mice might be exclusive to embryonic development.

Knowing that mouse ES cells are derived from the ICM, we analyzed TDH mRNA and protein expression in mouse blastocysts using in situ hybridization and immunohistochemistry, respectively. We detected robust TDH expression in the ICM using both methods. Indeed, ICM cells immunostained with TDH specific antibodies appeared remarkably similar morphologically to ES cell colonies grown in culture (compare Figures 3-3 and 3-4B). The finding that TDH is highly expressed in the early mouse embryo raises the possibility that TDH activity plays an important role during normal mouse embryonic development. This observation also lends credence to the idea that ES cells in culture are essentially identical to cells present in the ICM of the mouse blastocyst during embryogenesis (Ying et al., 2008).

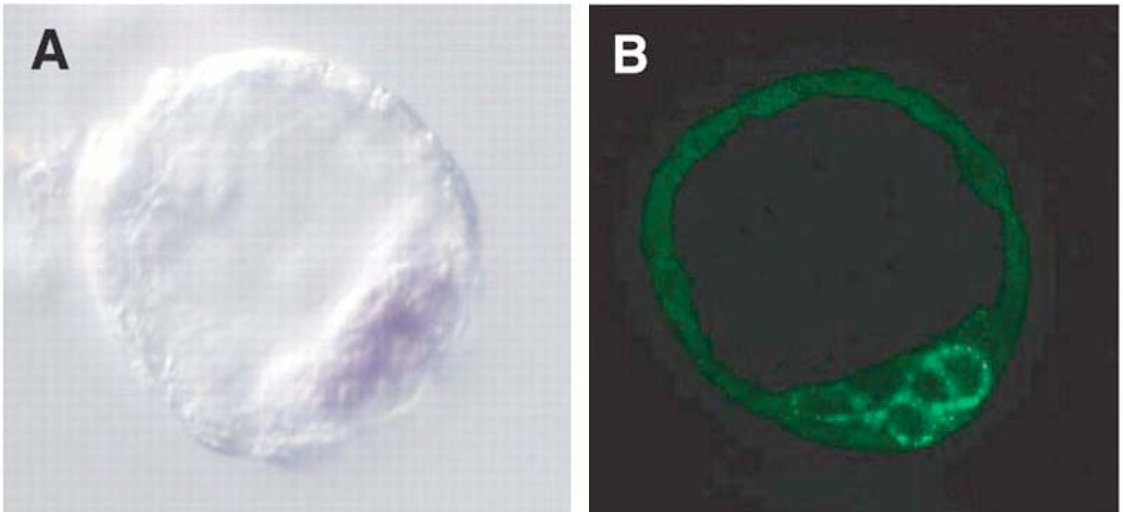

Figure 3-4 TDH mRNA and protein expression in the mouse blastocyst
A. In situ hybridization of blastocyst-stage mouse embryos localized the TDH mRNA (purple) to the ICM. Sense and anti-sense probes were prepared from a full-length cDNA clone of the mouse TDH gene. Hybridization conditions were based on the methods of (Chazaud et al., 2006). B. Antibody staining localized the TDH protein to the perinuclear region of the ICM (presumably mitochondria). Blastocysts were fixed in 4% paraformaldehyde and after fixation were incubated with TDH antiserum overnight at 4°C. Embryos were incubated with secondary antibody conjugated to Alexa488 for 2h at room temperature, and then visualized on an Axiovert fluorescence microscope (Zeiss). Figure from (Wang et al., 2009).

As noted above, the TDH expression pattern in mouse ES cells and embryos closely matches that of a handful of transcription factors known to be involved in the maintenance of the ES cell pluripotent state. In an unbiased genome-wide study, Orkin and colleagues identified target promoters of nine of these factors using chromatin immunoprecipitation (Kim et al., 2008). Strikingly, five of the nine transcription factors

implicated in ES cell pluripotency bound to the first exon of the TDH gene, a transcribed region that does not contain any amino acid coding sequence. In the Kim et al. study, the factors occupying this putative enhancer were Nanog, Dax1, Nac1, Klf4, and c-Myc. Nanog is selectively expressed in the ICM and is essential for ES cell self-renewal in culture, and forced expression of this protein alleviates the requirement for LIF (Mitsui et al., 2003, Silva et al., 2009; Chambers et al., 2003). Klf4 and c-Myc are reprogramming factors used in the generation of induced pluripotent stem cells (Takahashi and Yamanaka, 2006). Thus, it seems likely that some or all of these factors might be at least partly responsible for the robust TDH expression detected in mouse ES cells.

Hypothesizing that this enhancer element within the first exon of TDH might be important for the gene's ES cell-specific expression, we performed a BLAST search to determine the conservation of this exon's nucleotide sequence. Interestingly, we could only detect conservation of this element in mice and rats. Since mice and rats are the only species from which authentic ES cells capable of germline transmission have been derived (Buehr et al., 2008, Li et al., 2008), it is possible that TDH gene expression driven by this element plays some role in the ability to derive and maintain in culture ES cells from different organisms.

TDH is Nonfunctional in Humans

Previous work has demonstrated that the human TDH gene product is rendered nonfunctional by the presence of three inactivating mutations (Edgar, 2002). These mutations were identified to be A to G splice acceptor mutations in exons 4 and 6 and a

premature stop codon mutation within exon 6. To confirm this finding, we cloned the TDH gene from total RNA isolated from human fetal liver tissue. Indeed, PCR analysis using TDH-specific primers resulted in the identification of four distinct TDH splice isoforms, none of which corresponded to the intact, full-length cDNA (Figure 3-5). Since the truncated proteins resulting from these splice isoforms all lack the carboxy-terminal threonine-binding domain necessary for enzymatic activity, it appears that human cells are unable to produce an active TDH enzyme.

Major differences exist between mouse and human ES cells grown in culture (as discussed in Chapter 1). In addition to different cytokine and growth factor requirements, the cell division cycle of human ES cells is much slower. Human ES cells grow with a doubling time of 35 hours (Amit et al., 2000), in contrast to the 5 hour doubling time of mouse ES cells. In future experiments, forced expression of high levels of ectopic TDH could be used to test whether loss of TDH accounts for the prolonged cell division cycle of human ES cells.

Bioinformatic analysis revealed that in chimpanzees, the most closely related species to humans evolutionarily, the TDH gene is intact, containing none of the three debilitating mutations found in human TDH. Indeed, of all the metazoan genomes that have been sequenced to date, only humans lack a functional TDH gene. As such it is of interest to consider the biological implications of mutation of the TDH gene in humans. Perhaps loss of TDH in some way slows down human embryonic development. Regardless of whether inactivation of TDH provides humans with some form of selective advantage, it is shown here that the TDH enzyme is expressed copiously in mouse ES

cells but is inactive in human cells. The full functional consequences of this mutational inactivation await further study.

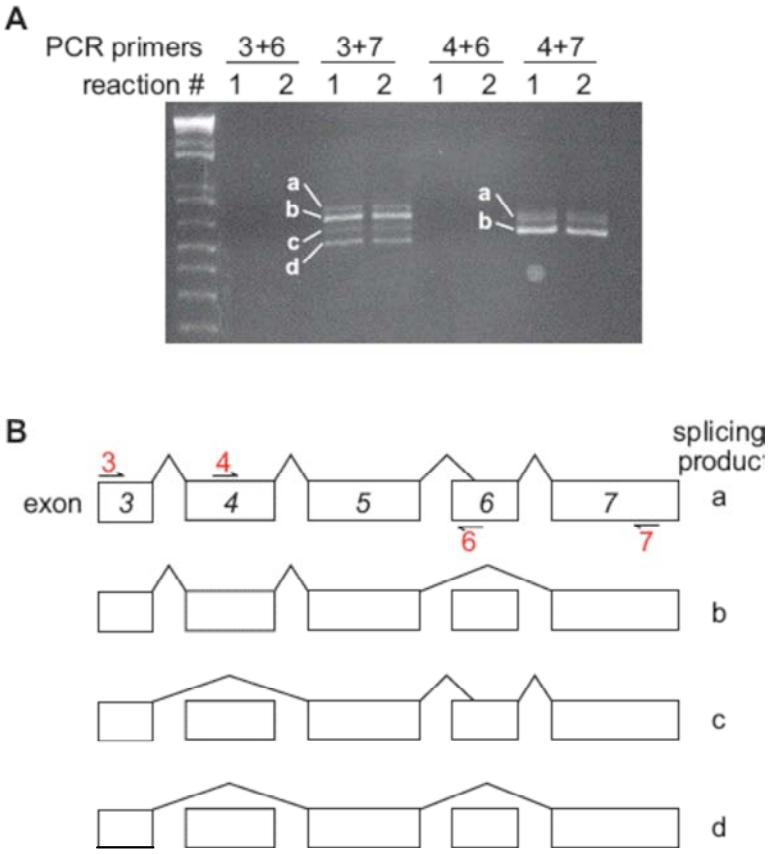

Figure 3-5 TDH is nonfunctional in humans
Total RNA was isolated from human fetal liver tissue and reverse-transcribed to produce cDNA. PCR reactions were performed using primers corresponding to exons 3, 4, 6 and 7 in the combinations indicated. Several discrete bands were obtained using the exon 7 reverse primer. Direct sequencing of PCR products identified the splice isoforms indicated in (B). Exons 4 and 6 were each skipped in two of the four isoforms. No PCR product could be obtained using the primer corresponding to the 5' end of exon 6, indicating that exon 6 was incorrectly spliced in all cases. This conclusion was verified by DNA sequencing. Figure from (Wang et al., 2009).

CHAPTER FOUR
Results

CHEMICAL INHIBITION OF MOUSE TDH

Abstract

Mouse embryonic stem (ES) cells utilize the high-flux backbone of metabolism, wherein the amino acid threonine is catabolized by threonine dehydrogenase (TDH) to yield glycine and acetyl-CoA. Here we report the results of a screen for small molecule inhibitors of TDH, an enzyme selectively expressed in ES cells. A family of quinazolinecarboxamide small molecules displayed high potency and selectivity against TDH. Moreover, ES cells incubated with these compounds failed to proliferate and eventually underwent a form of cell death characterized by increased autophagy. Importantly, addition of elevated threonine to the growth medium was able to partially rescue the cells from the TDH inhibitor-induced cell death, whereas other amino acids had no effect. We conclude that TDH-mediated threonine catabolism is necessary for ES cell self-renewal, and ES cells deficient in this pathway display autophagic features typically associated with nutrient starvation.

Introduction

Enzyme-catalyzed chemical reactions are essential for almost every aspect of cellular life. Enzyme inhibitors, which are molecules that decrease enzyme activity, enable systematic perturbation of a specific chemical reaction and are powerful tools for experimental biologists (Garrett and Grisham, 1999). Two parameters that determine the

usefulness of an enzyme inhibitor are potency, or the ability to inhibit at a relatively low concentration, and specificity, or the ability to bind and inhibit only the target enzyme of interest. Many drugs are enzyme inhibitors, and high potency and specificity offer the possibility that a drug might have low toxicity and few side effects. This chapter focuses on the identification of potent and specific inhibitors of the TDH enzyme, and their use in studying the high-flux backbone of metabolism in mouse embryonic stem cells.

Methods

Materials

Chromatographic reagents for protein purification were obtained from GE Healthcare. All other chemicals and reagents were obtained from Sigma-Aldrich except where specified.

Culture of Mouse Embryos

Eight-week old B6SJLF1 female mice were superovulated by a standard hormone regimen and mated to males of the same strain background. Fertilized one-cell eggs were cultured in microdrops of Brinster's medium for ovum culture (Brinster, 1969) under silicone oil in a 5% CO_2 humidified atmosphere for 48 hours. Pre-compacted morulae were separated into groups of 20 to 25 embryos and placed into microdrops of Brinster's medium containing 1 mM, 300 μM, 100 μM, and 30 μM concentrations of 3-hydroxynorvaline (3-HNV) with or without the addition of 4 mM threonine. Embryos were visually scored for developmental stages at 24 hours and 48 hours following the

initiation of drug administration and photographed by light microscopy.

Protein Expression and Purification

Mouse TDH was expressed as a glutathione S-transferase (GST) in *Escherichia coli* strain Rosetta. The cells were cultured at 37°C until the $A_{600\,nm}$ reached 0.6 and were then induced with 0.2 mM isopropyl β-D-thiogalactoside (Promega) for 16 hours at 20°C. The cells were suspended in 50 mM Tris-Hcl (pH 8.0) containing 50 mM NaCl, 1 mM DTT (Promega), and 1 mg/mL lysozyme, incubated on ice for 30 minutes, and sonicated (Fisher Scientific Sonic Dismembrator Model 500). After spinning in an ultracentrifuge at 30,000 rpm (Beckman rotor Ti75) for 30 minutes at 4°C, the supernatant was incubated with glutathione sepharose resin for 2 hours and, after washing, was eluted with 10 mM reduced glutathione. TDH was further purified using Superdex 200 and MonoQ chromatography (Amersham).

Enzymatic Activity Measurements

TDH activity was determined by measuring the rate of formation of NADH at 25°C. The standard assay mixture contained 100 nM purified TDH, 50 mM Tris-HCl (pH 8.0), 2 mM NAD^+, 2 mM L-threonine, 50 mM NaCl, and 1 mM DTT (Promega) in a final volume of 50 μL. The reaction was initiated by the addition of a mixture containing both substrates, and the absorbance of the reaction mixture at 340 nm was recorded continuously on a Bio-Tek Synergy HT microplate reader.

Similar absorbance assays were used to measure activity of other dehydrogenase

enzymes. Hydroxysteroid dehydrogenase activity was assayed using 30 μg/mL purified enzyme, 0.3 mM NAD^+, and 0.00005% testosterone in 50 mM Tris-HCl buffer (pH 8.0). The alcohol dehydrogenase reaction contained 30 μg/mL purified enzyme, 8 mM NAD^+, and 300 mM ethanol in 50 mM Tris-HCl (pH 8.0). The lactate dehydrogenase assay used 30 μg/mL enzyme, 200 μM NADH, and 3 mM sodium pyruvate in 0.2 M Tris-HCl (pH 7.3). Glucose-6-phosphate dehydrogenase activity was determined using a reaction mixture containing 30 μg/mL enzyme, 0.2 mM $NADP^+$, and 3 mM glucose-6-phosphate in 50 mM Tris-HCl (pH 7.8) with 3 mM $MgCl_2$.

High-Throughput Screening

Approximately 200,000 drug-like synthetic chemicals were screened using the TDH absorbance assay in 384-well UV transparent plates (Corning). The primary assay was performed as described above, with 5 μM of individual library compounds in pure dimethyl-sulfoxide (1% DMSO final concentration) added to the reaction mixture. The reaction was initiated with the addition of 5 μL per well of a mixture containing 10 mM NAD^+ and 10 mM threonine. Total reaction volume was 50 μL per well. The positive control was in column 1 of each plate, and DMSO controls were in columns 2 and 23. The reaction was allowed to proceed for 30 minutes at room temperature, at which point NADH production was measured by reading the absorbance at 340 nm. Using chemoinformatics, primary hits were clustered into families with chemically distinct core structural motifs.

For screen validation, compounds that were determined to inhibit TDH were

cherry picked from 5 mM compound stock library plates. The cherry picking of compounds was done with the use of a 384-pin array Biomek FX (Beckman Instruments) high-precision robot with a Span 8 pod. Resupply of confirmed hits was obtained from ChemDiv and ChemBridge. Purity of compounds was analyzed by LC/MS and all inhibitors were found to be >95% pure.

For cell viability assays, cells were plated in gelatinized Costar 384-well plates using an automated dispenser at 1,000 cells per well in 50 μL of media per well. 0.5 μL of compounds was added 6 hours after plating. The plates were then incubated for 24 (ES) or 48 (NIH 3T3 and HeLa cells) hours before measuring cell viability using CellTiter-Glo reagent (Promega). All solutions were dispersed robotically using a Biomek FX robot.

LC-MS/MS Analysis of ES Cell Metabolites

Feederless ES cells were grown on 60 cm^2 gelatinized cell culture dishes in the presence of 10 μM TDH inhibitor for 2 hours. Dishes were washed in cold PBS and metabolites were extracted in 1 mL of 50% aqueous methanol that was maintained at -20°C. Cells were dounced in a glass homogenizer and centrifuged at 15,000 rpm for 20 minutes to pellet cell debris, and 0.9 mL of the supernatant was transferred to a new tube and stored at -80°C until analysis. Samples were dried on a Savant Speed Vac Plus SC210A for 2 hours. Metabolites were reconstituted in 100 μL of 5 mM ammonium acetate and filtered using 0.2 μm PVDF micro-spin tubes (Grace). Samples were infused into an Applied Biosystems 3200 QTRAP triple quadrupole-linear ion trap mass

spectrometer and data was processed using Analyst software (Tu et al., 2007).

Western Blotting

ES cell proteins were extracted using a 30 minute incubation of ES cells in cold 50 mM Hepes (pH 7.4), 50 mM NaCl, 0.5% NP40, 1 mM DTT, 100 μM phenylmethylsulfonyl fluoride, and 1x protease inhibitor cocktail. Protein concentrations were determined by Bio-Rad protein assay, and 30 μg total protein was loaded in each lane of a 12% SDS-PAGE gel. Caspase 3 and LC3 antibodies were from Cell Signaling. Antibodies were diluted 1:1000 in 5% w/v nonfat dry milk (Caspase 3) or 5% w/v BSA (LC3) in TBST at 4°C with gentle shaking overnight. ES cells were nutrient-starved using Hank's Buffered Salt Solution (Invitrogen).

Transmission Electron Microscopy

ES cells were cultured on plastic coverslips for 24 hours with 10 μM TDH inhibitor or vehicle-only control (DMSO). Specimens were fixed for 60 minutes in 2.5% glutaraldehyde in 0.1 M cacodylate buffer and postfixed with 1% osmium tetroxide for 15 minutes. Cells were dehydrated in ethanol, infiltrated, and embedded in Embed-812 resin (Electron Microscopy Sciences) overnight at 70°C. Thin sections (70-90 nanometers in thickness) were cut on a Leica Ultracut E ultramicrotome and placed on 200 mesh copper grids. Sections were stained with 2% aqueous uranyl acetate and lead citrate and examined in a FEI Tecnai G2 Spirit Biotwin transmission electron microscope, operated at 120 kV. Digital images were captured with a Gatan 2Kx2K

multiport readout post column CCD.

Results and Discussion

Inhibition of TDH by the artificial substrate 3-hydroxynorvaline

As a first step toward using small molecules to determine the role of TDH in mouse ES cells, we utilized the threonine analog 3-hydroxynorvaline (3-HNV). 3-HNV, a synthetic variant of threonine containing an extra carbon atom, is oxidized by TDH to produce 2-amino-3-ketopentyrate, which is then cleaved by Gcat to yield glycine and propionyl-CoA (Figure 4-1). We hypothesized that, if glycine were the only TDH product necessary to sustain HFB metabolism, then incubation with high levels of 3-HNV might rescue ES cells from the colony formation defect observed during culture in

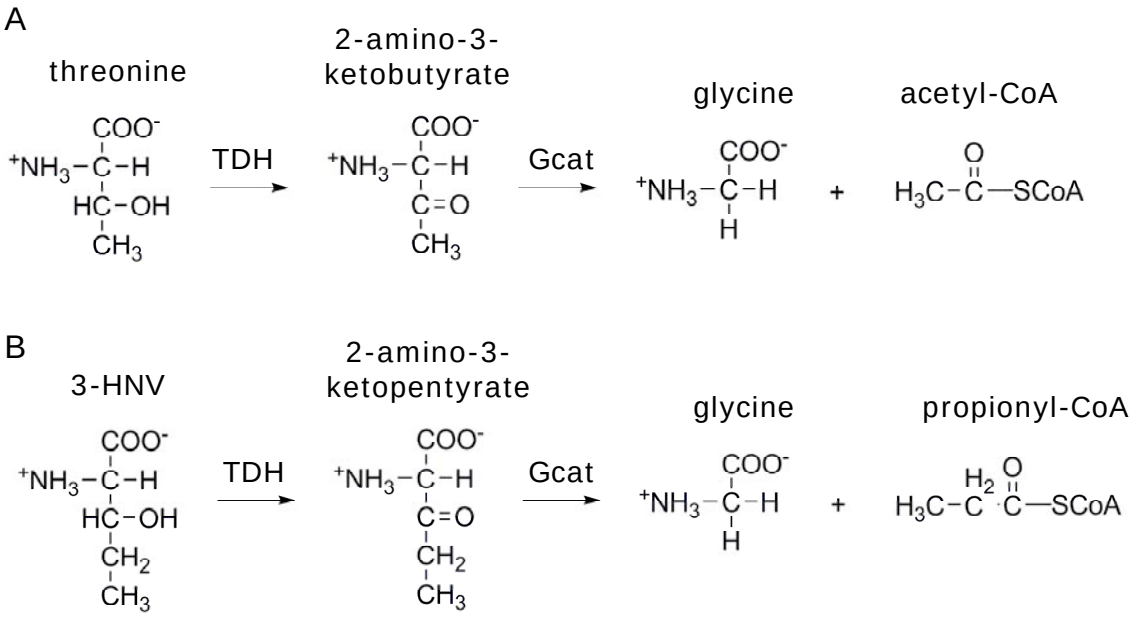

Figure 4-1 Catabolism of 3-hydroxynorvaline into glycine and propionyl-CoA
A. Normal TDH reaction operative in mitochondria of mouse ES cells results in production of glycine and acetyl-CoA. B. The threonine analog 3-HNV acts as an artificial substrate for TDH, and is oxidized to produce 2-amino-3-ketopentyrate. This short-lived intermediate is then cleaved by Gcat into glycine and propionyl-CoA.

threonine dropout medium (see Chapter 2). To test this idea, we cultured ES and fibroblast (MEF or NIH3T3) cells together in the presence of varying amounts of 3-HNV. Instead of rescuing this growth defect, we observed that the addition of 3-HNV to complete culture media was toxic to ES cells. At 0.5 mM 3-HNV, ES cell colony size was reduced by approximately fifty percent, and at 4 mM 3-HNV the ES cell colonies were completely absent (Figure 4-2A). HeLa, MEF, and NIH3T3 cells, on the other hand, grew normally even in the presence of 4 mM 3-HNV, indicating the compound was specifically inhibiting ES cell growth. We interpret this finding to mean that 3-HNV competitively inhibits the TDH enzyme, yielding only one of the two metabolites required for HFB metabolism.

In addition to being present in ES cells, TDH is also highly expressed in the ICM of the mouse blastocyst (chapter 3). Using a simple media formulation, fertilized one-cell mouse embryos can be cultured in vitro to develop into cavitated blastocysts (Brinster, 1969). To test the role of TDH in mouse embryo development, we cultured morula-stage embryos in the presence of varying amounts of 3-HNV (Figure 4-2B). Embryos exposed to 1 mM and 300 μM of 3-HNV were blocked from forming cavitated blastocysts. This developmental defect was completely rescued by incubation with 4 mM threonine, even at the highest concentration (1 mM) of 3-HNV. These studies provide evidence that, like cultured ES cell proliferation, mouse embryonic development in vitro is critically dependent on flux through the TDH pathway, with the production of both glycine and acetyl-CoA being required for normal development.

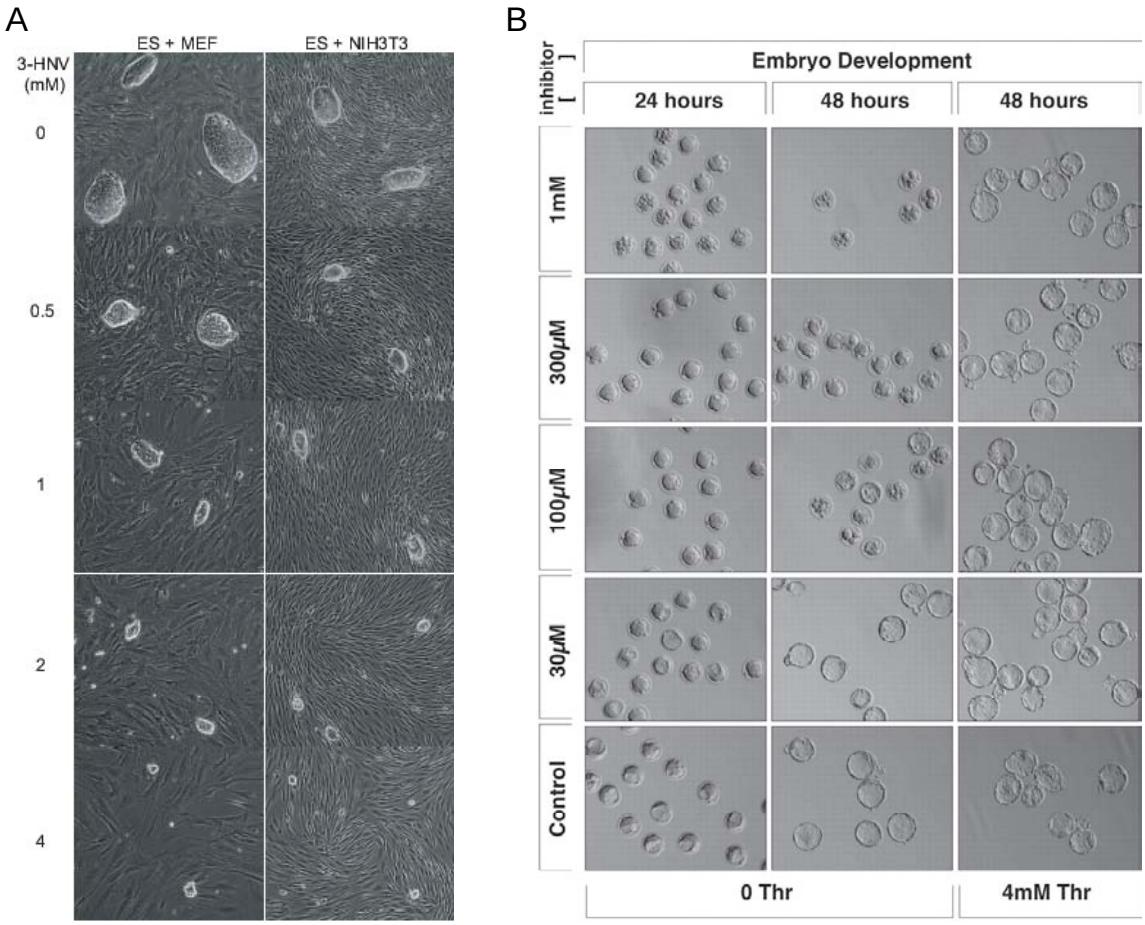

Figure 4-2 3-HNV inhibits ES cell colony formation and mouse embryo development

A. Co-cultures of ES/MEF or ES/NIH3T3 cells were subjected to media containing varying amounts of 3-HNV. ES cell colonies were markedly smaller when grown in the presence of 0.5 mM 3-HNV. In contrast, the fibroblast cell lines grew normally even at the highest concentration of 3-HNV tested (4 mM). B. Pre-compacted morula stage embryos were cultured in Brinster's medium (Brinster 1969) containing varying amounts of 3-HNV. Embryo morphology was photographed by light microscopy 24h and 48h after administration of drug. Embryos exposed to 1 mM and 300 μM 3-HNV were blocked from forming cavitated blastocysts. Addition of 4 mM threonine resulted in complete rescue of normal development even at 1 mM of 3-HNV. Figure from (Wang et al., 2009).

Purification and characterization of the mouse TDH enzyme

To initiate biochemical analysis of threonine catabolism, we expressed and purified the mouse TDH enzyme. Although the full-length protein was contained in bacterial inclusion bodies, truncating 39 amino acids from the amino terminus resulted in the production of milligram quantities of soluble, highly purified TDH protein (Figure 4-3A). This 39 amino acid stretch corresponds to a predicted mitochondrial signal sequence, which is likely to be cleaved after the protein's translocation into the mitochondrion (Attardi and Schatz, 1988). Thus, it is probable that our purified protein closely resembles the TDH enzyme active in the mitochondria of mouse ES cells.

Incubation of purified TDH with threonine and nicotinamide adenine dinucleotide (NAD^+) resulted in a dose-dependent, saturable increase in absorbance at 340 nm, indicative of formation of reduced coenzyme (NADH). This activity was dependent on the presence of both threonine and NAD^+ in the reaction mixture. To confirm that the activity was not caused by the presence of small amounts of co-purifying bacterial TDH, we further purified the recombinant mouse TDH using anion exchange and gel filtration chromatography. The threonine-dependent, NAD^+-reducing activity fractionated with the major band on the gel, which was recognized by a TDH-specific antibody (data not shown). We conclude that purified mouse TDH is capable of catalyzing the same chemical reaction as has been demonstrated for TDH orthologs from diverse metazoan and microbial species (Linstead et al., 1977, Aoyama and Motokawa, 1981, Epperly and Dekker, 1991, Ishikawa et al., 2006).

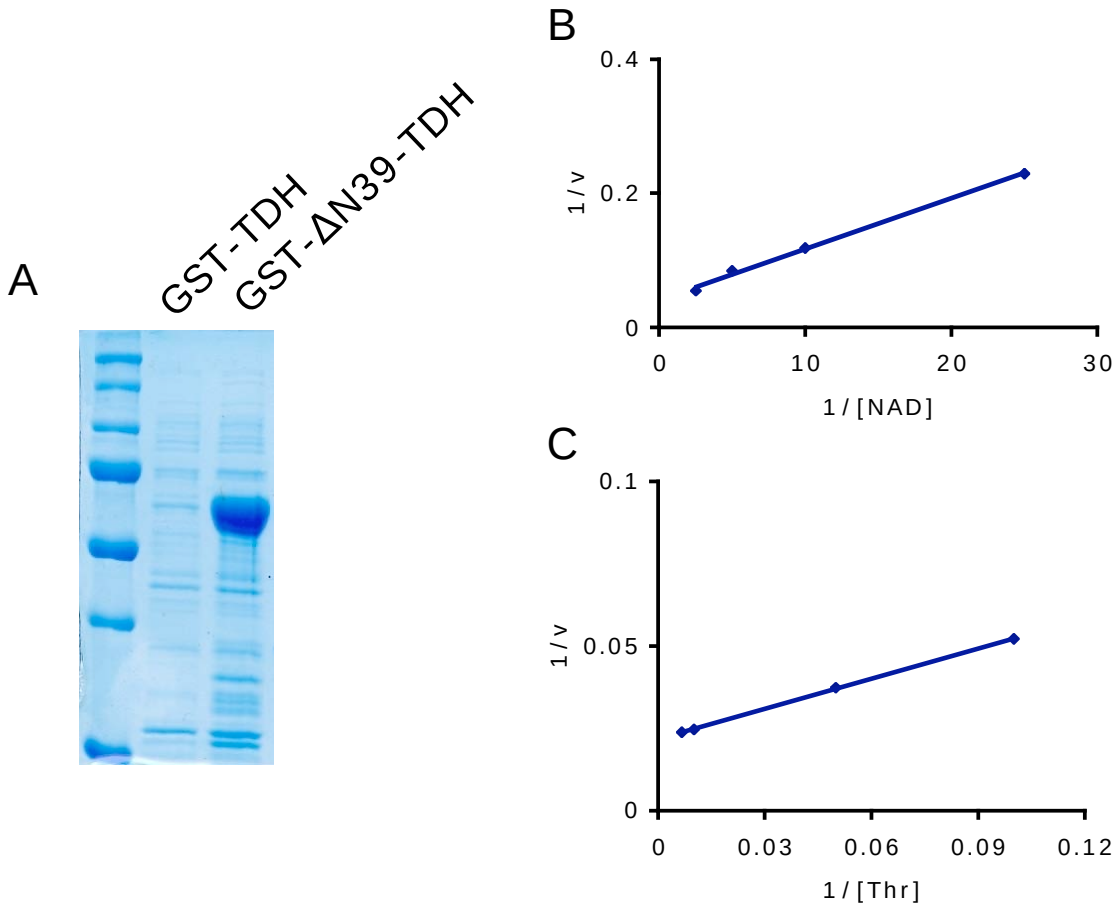

Figure 4-3 Expression and characterization of the mouse TDH enzyme
A. Recombinant TDH protein was expressed in E. coli with an amino-terminal glutathione-s-transferase (GST) tag to facilitate purification. Full length TDH was contained in inclusion bodies, but removal of a predicted mitochondrial signal sequence from the protein's amino terminus resulted in production of milligram quantities of soluble protein. B-C. Double reciprocal (Lineweaver-Burk) analysis for NAD^+ and threonine. Enzyme activity was determined by measuring increased absorbance at 340 nm following addition of substrates. The K_m for NAD^+ was 180 μM and the K_m for threonine was 14 mM. These values are in agreement with those reported for microbial TDH enzymes (Linstead et al., 1977).

To determine kinetic parameters for TDH, we constructed Lineweaver-Burk double reciprocal plots for both substrates by measuring reaction velocity as a function of threonine and NAD^+ concentrations (Figure 4-3 B and C). The Michaelis constants (K_m) for NAD^+ and threonine were 180 μM and 14 mM, respectively, and the turnover number (k_{cat}) was ~60,000 sec^{-1}. These values are in close agreement with kinetic constants reported for other TDH enzymes of eukaryotic origin (Linstead et al., 1977, Aoyama et al., 1981). The relatively weak binding affinity for threonine helps to explain why mouse ES cells are uniquely sensitive to the withdrawal of threonine from the culture medium (discussed in Chapter 2).

Identification of potent, TDH-specific small molecule inhibitors

If mouse ES cell maintenance is dependent on TDH-mediated threonine catabolism, then selective inhibition of the TDH enzyme should result in reduced proliferative capacity of ES cells. To test this hypothesis, we screened the University of Texas Southwestern chemical library for TDH inhibitors using an in vitro TDH assay. The screen was performed in 364-well plates, and assays were initiated with 5 μL of a mixture of both substrates at 10 mM and incubated for 30 minutes at room temperature (see *Materials and Methods* for details). Of the ~200,000 compounds screened, ~1,000 were able to inhibit TDH activity with a z-score greater than 3 relative to the 1% dimethyl-sulfoxide (DMSO) control (Figure 4-4). The inhibitory action of these molecules was then confirmed by repeating the same TDH absorbance assay in triplicate, and dose-dependent inhibition was determined using compound concentrations of 1, 3,

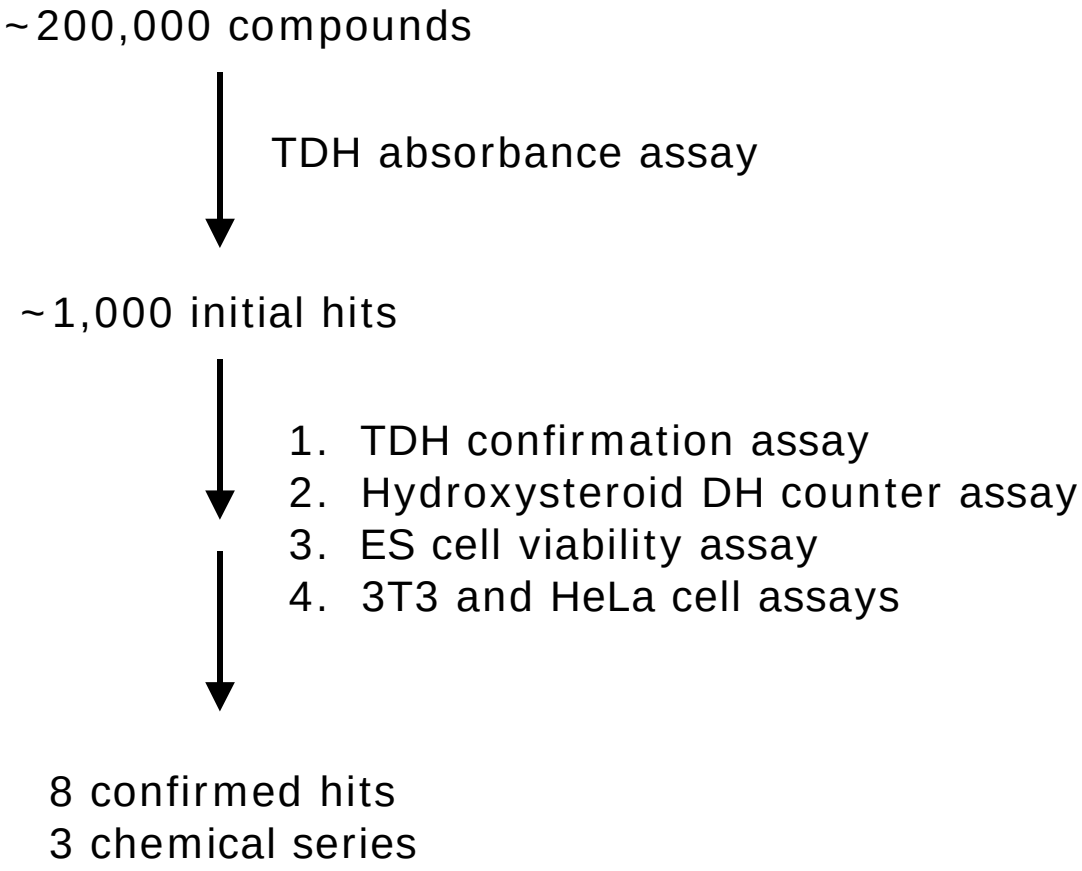

Figure 4-4 Screen for small molecule inhibitors of TDH
The UT Southwestern chemical library, containing ~200,000 small molecules with the potential for biological activity, was screened using the in vitro TDH absorbance assay in 384-well UV transparent plates. ~1,000 compounds were able to inhibit TDH activity with a z-score greater than 3 relative to the 1% DMSO control. The inhibitory action of these molecules was then confirmed by repeating the TDH absorbance assay in triplicate, and dose-dependent inhibition was determined using compound concentrations of 1, 3 and 10 μM. A similar absorbance assay using hydroxysteroid dehydrogenase with testosterone as a substrate was performed to eliminate generic dehydrogenase inhibitors. Finally, the candidate molecules were assayed for their ability to impair proliferation of ES cells relative to NIH3T3 and HeLa cells, which do not express TDH. In this case, cells were grown on 364-well tissue culture plates for 24 (ES) or 48 (NIH3T3 and HeLa) hours, at which point cell viability was measured using the CellTiter-Glo reagent (Promega). The most potent TDH inhibitors were able to impair ES cell viability with EC_{50} ~3 μM, whereas their EC_{50} on HeLa and NIH3T3 cells was ~1 mM.

and 10 μM. To identify generic dehydrogenase inhibitors, we performed a similar absorbance assay using hydroxysteroid dehydrogenase (HSDH), the enzyme most closely related to mouse TDH by primary sequence homology. Any compounds that inhibited HSDH were deemed non-specific dehydrogenase inhibitors and eliminated from further study.

The TDH inhibitors were then screened for the capacity to inhibit proliferation of mouse ES cells relative to other mammalian cell types, which do not utilize the high-flux backbone of metabolism. Mouse ES cells, 3T3 fibroblasts, and human cancer (HeLa) cells were treated with multiple concentrations of compound, and cell viability was determined using a luminescent assay to measure ATP. These experiments divided our candidate TDH inhibitors into three classes of compounds. One class was unable to impede the growth of any of the three cell types tested, perhaps due to an inability of the compounds to enter cells or mitochondria. The second class killed the three cell types indiscriminately. Toxic compounds with off-target activity were hypothesized to constitute this category. The third class of compounds severely inhibited the proliferation of ES cells but not fibroblasts or cancer cells at 10 μM compound concentration. Because of their specificity against ES cells relative to other cell types, these molecules were selected as candidates that might impair ES cell proliferation by selectively inhibiting the TDH enzyme. Using chemoinformatics, we clustered these hits into families with chemically distinct core structural motifs.

Based on its potency in both the enzyme and cell-based assays, a cluster of six closely related quinazolinecarboxamide (Qc) compounds was chosen for further study

(Figure 4-5A). We noted that this chemical series, as well as several other clusters of TDH inhibitors, all contained thiourea moieties, which have use as enantioselective reductive catalysts in organic synthesis (Li et al., 2010). To further test for specificity against TDH, we examined whether these compounds were able to inhibit alcohol dehydrogenase, lactate dehydrogenase, or glucose-6-phosphate dehydrogenase. None of the six Qc small molecules showed any inhibitory activity against the other dehydrogenase enzymes at a concentration of 10 μM (data not shown). In addition, we measured EC_{50} values against ES, HeLa, and NIH 3T3 cells. Whereas the TDH inhibitors killed ES cells with an EC_{50} of ~3 μM, the EC_{50} against the other cell types, which do not express TDH, was ~1 mM (data not shown). Thus, the Qc compounds have a 300-fold toxicity difference for ES cells versus other cell types, strongly arguing that these small molecules are killing ES cells through specific inhibition of the TDH enzyme.

To determine half maximal inhibitory concentrations (IC_{50}'s) of the Qc compounds against TDH, we titrated the inhibitors from 10 nM to 10 μM and measured TDH activity (Figure 4-5B). The IC_{50} for all of the Qc molecules tested was ~0.5 μM. To establish the mechanism of TDH inhibition, we constructed Lineweaver-Burk plots for both substrates in the presence and absence of inhibitor (Figure 4-6 A and B). We determined that both K_m and V_{max} are altered upon addition of inhibitor, a pattern known as mixed noncompetitive inhibition. The standard explanation for this mode of inhibition is that the inhibitor binds at a site distinct from the active site, but influences the binding of substrates at the active site through an allosteric mechanism (Garrett and Grisham, 1999). We also tested the reversibility of the Qc inhibitors by incubating purified TDH

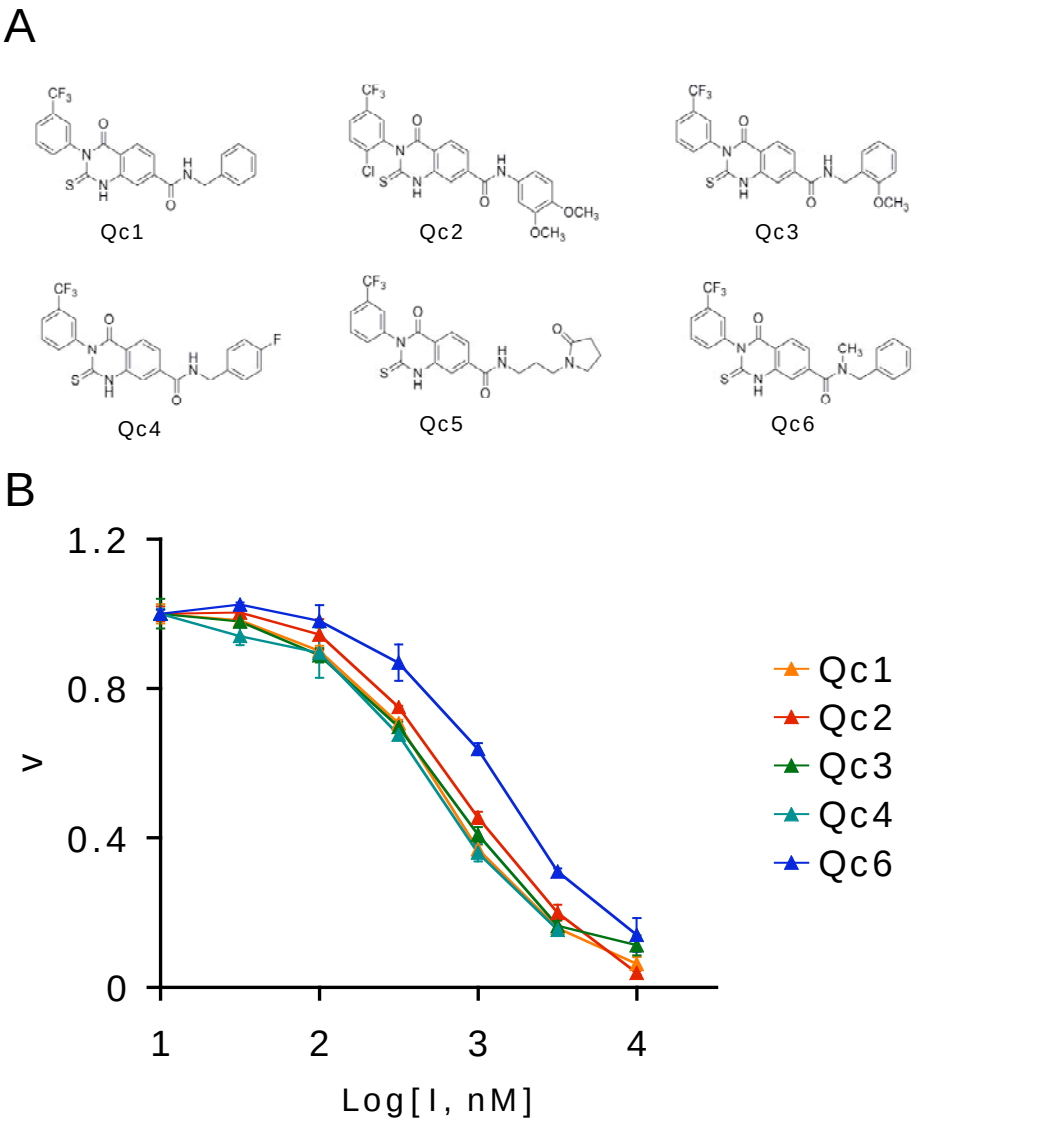

Figure 4-5 Chemical structures and potency of TDH inhibitors
A. Structures of the six best hits from the TDH inhibitor screen. The compounds contained a quinazolinecarboxamide (Qc) scaffold with various peripheral modifications. The inhibitors all contained thiourea moieties, which are useful chemical catalysts. B. IC_{50} values were determined by titrating the compounds from 10 nM to 10 µM and measuring TDH activity. The IC_{50} for Qc1-Qc4 was ~0.5 µM.

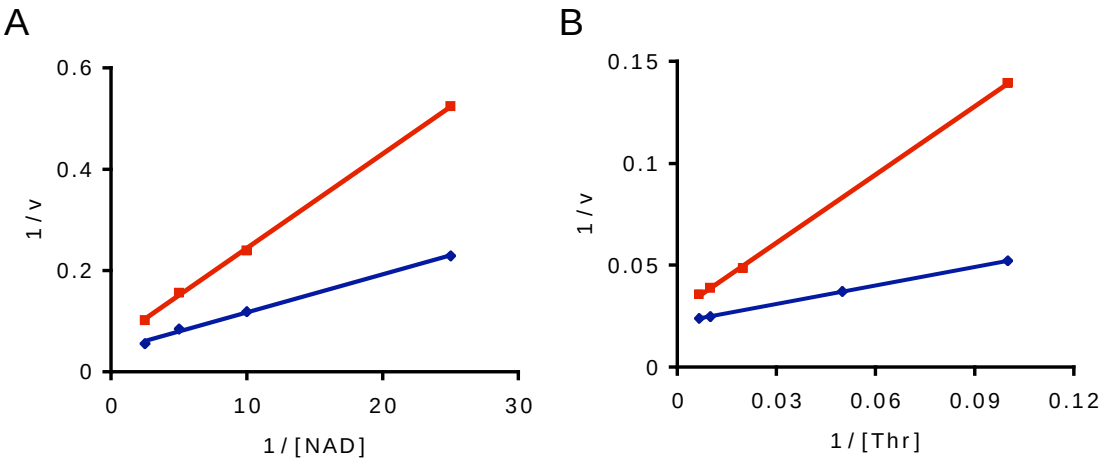

Figure 4-6 TDH inhibition is mixed noncompetitive for both NAD^+ and threonine Lineweaver-Burk analysis of enzyme inhibition. TDH activity was assayed in the absence and presence of inhibitor at the NAD^+ and threonine concentrations shown. Blue curves depict data obtained in the absence of inhibitor, and red curves depict data obtained in the presence of inhibitor. Both V_{max} (y-intercept) and K_m (x-intercept) are altered in the presence of inhibitor, a pattern known as mixed noncompetitive inhibition. The standard interpretation for this mode of inhibition is that the inhibitor binds at a site distinct from the enzyme's active site, but influences binding of substrates at the active site through an allosteric mechanism.

enzyme with varying concentrations of inhibitor for 30 minutes at room temperature and then dialyzing the mixture in four liters of buffer overnight in the cold room. After dialysis, TDH activity was comparable to the DMSO control at all concentrations of inhibitor tested (up to 10 μM, or 20-fold greater than the IC_{50}, data not shown). We conclude that TDH inhibition by the Qc compounds is fully reversible. Since none of the functional groups present on these molecules are predicted to covalently modify proteins, this result was expected.

To more closely examine the effects of TDH inhibition on ES cell growth, we incubated ES cell colonies grown in glass chamber slides with the Qc compounds and monitored colony morphology using phase contrast microscopy (Figure 4-7). Initially, colonies treated with TDH inhibitors appeared normal but failed to proliferate, whereas those treated with vehicle (DMSO) rapidly grew in size. After 24 hours of TDH inhibition, groups of dead cells became apparent at the surface of colonies, and longer incubation resulted in the majority of cells appearing as collections of opaque cells with indistinct boundaries.

Previous work has demonstrated that colony formation is blocked when ES cells are treated with the threonine analog 3-hydroxynorvaline (3-HNV, see above). There are two major distinctions between 3-HNV and the Qc molecules identified here. First, 3-HNV is an artificial substrate for TDH, and as such millimolar concentrations of 3-HNV are required to effectively compete with threonine for access to the TDH active site. Being mixed noncompetitive inhibitors, the Qc molecules are ~1,000-fold more potent, with EC_{50} values of ~3 μM on ES cells. Second, as an amino acid, there is the possibility that some small percentage of 3-HNV is incorporated into newly synthesized proteins. This concern is not applicable to the Qc compounds.

With the purified TDH enzyme, we observed that elevated threonine could stimulate enzymatic activity in the presence of a fixed concentration of inhibitor (Figure 4-8A). Since the K_m for threonine is 14 mM, relatively high amounts of substrate are required to saturate the enzyme. We reasoned that if the Qc compounds were blocking ES cell proliferation through inhibition of TDH, then adding high amounts of threonine to

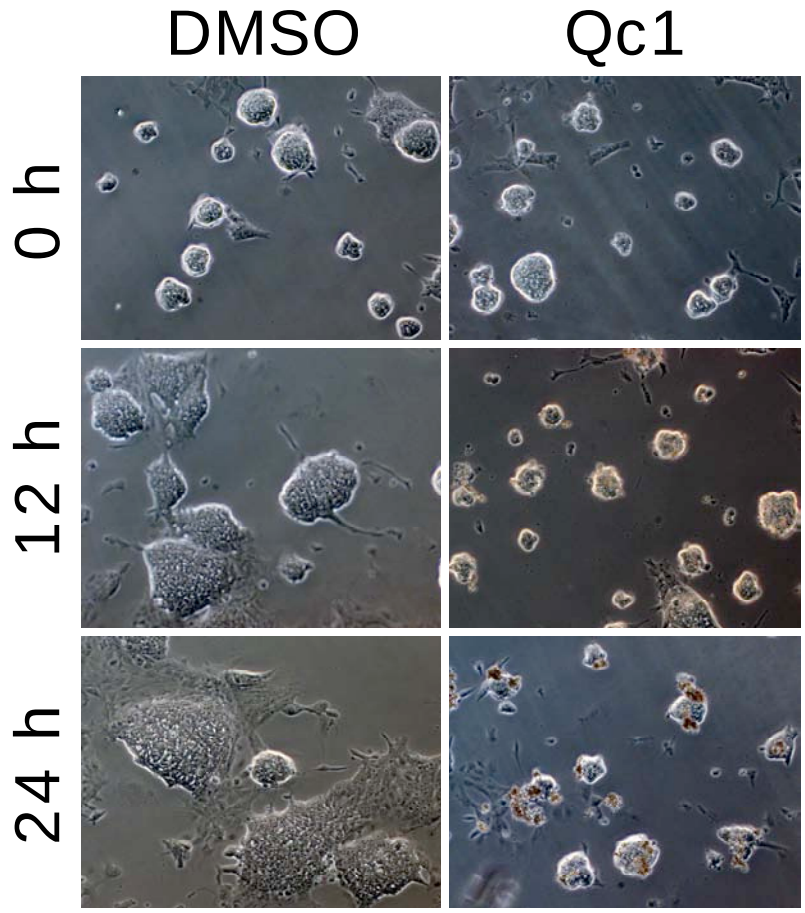

Figure 4-7 Effect of TDH inhibition on ES cell colony morphology
Feederless ES cells (E14 strain) were cultured on glass chamber slides and imaged using phase contrast microscopy. When treated with vehicle (DMSO) alone, ES cell colonies rapidly grew in size. Upon exposure to 10 μM of the TDH inhibitor, the colonies initially failed to proliferate, with their size remaining unchanged for the first 12 hours. After 24 hours, clusters of densely packed cells became apparent at the surface of the colonies, indicative of cell death.

the culture medium might confer a protective benefit. Indeed, addition of 12 mM threonine to the ES cell medium provided a modest, but significant, rescue of Qc-mediated toxicity, whereas cells cultured in the presence of excess valine, an unrelated amino acid, provided no such benefit (Figure 4-8B). The fact that exogenous threonine can partially rescue ES cell growth rates provides further evidence that the Qc small molecules are blocking ES cell proliferation through selective inhibition of the TDH enzyme.

As a first attempt at probing the structure-activity relationship (SAR) of the Qc compounds, we searched the University of Texas Southwestern chemical library for molecules whose structures were closely related to the TDH inhibitors identified in the high-throughput screen. Using cluster analysis, we were able to identify six compounds (Qc7-12) with structures similar to the TDH inhibitors that displayed selective killing of ES cells (Qc1-6, shown in Figure 4-9C). To test the activity of these related compounds, we carried out TDH enzymatic assays and ES cell viability assays. Four of the related compounds (Qc9-12) did not inhibit TDH activity at a concentration of 10 μM, nor did they impede ES cell growth at a concentration of 50 μM (Figure 4-9A). Two of the structural analogs, Qc7 and Qc8, showed weak inhibitory activity in vitro, and also inhibited ES cell proliferation at high concentrations of compound. The TDH inhibitors identified through chemical screening inhibit enzyme activity with an IC_{50} of ~0.5 μM, and kill ES cells with an EC_{50} of ~3 μM. Thus, there is a positive correlation between TDH inhibition and ES cell toxicity for the various structurally related small molecules (Figure 4-9B). This positive correlation is consistent with the hypothesis that the Qc

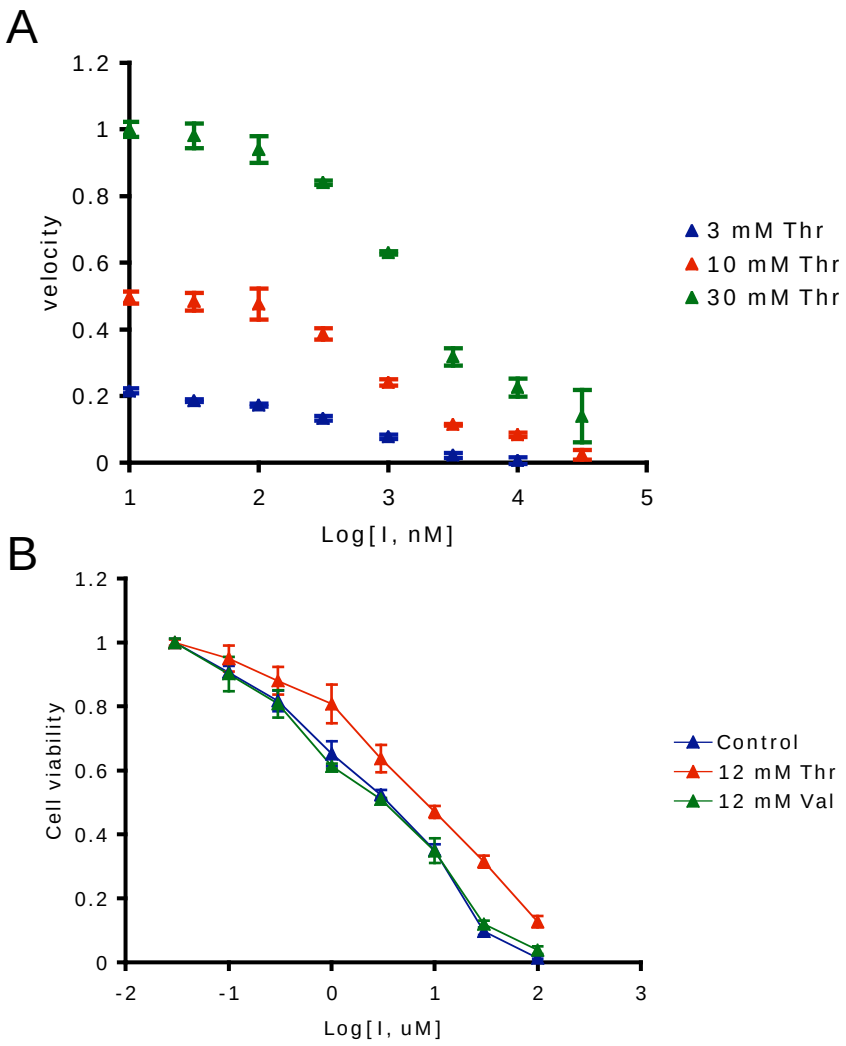

Figure 4-8 Rescue of TDH inhibitor-mediated cytotoxicity by elevated threonine
A. Threonine rescue of in vitro TDH activity. Using a fixed concentration of inhibitor, addition of elevated threonine to the reaction mixture resulted in the recovery of enzyme activity. Since TDH binds threonine relatively weakly (K_m = 14 mM), high concentrations of threonine are required to saturate the enzyme. B. Threonine rescue of TDH inhibitor-mediated cell death. ES cells were cultured in the presence of multiple concentrations of Qc4 with and without the addition of 12 mM threonine to the normal culture media. Increased threonine resulted in a statistically significant increase in cell viability, whereas an unrelated amino acid (12 mM valine) provided no such protective benefit.

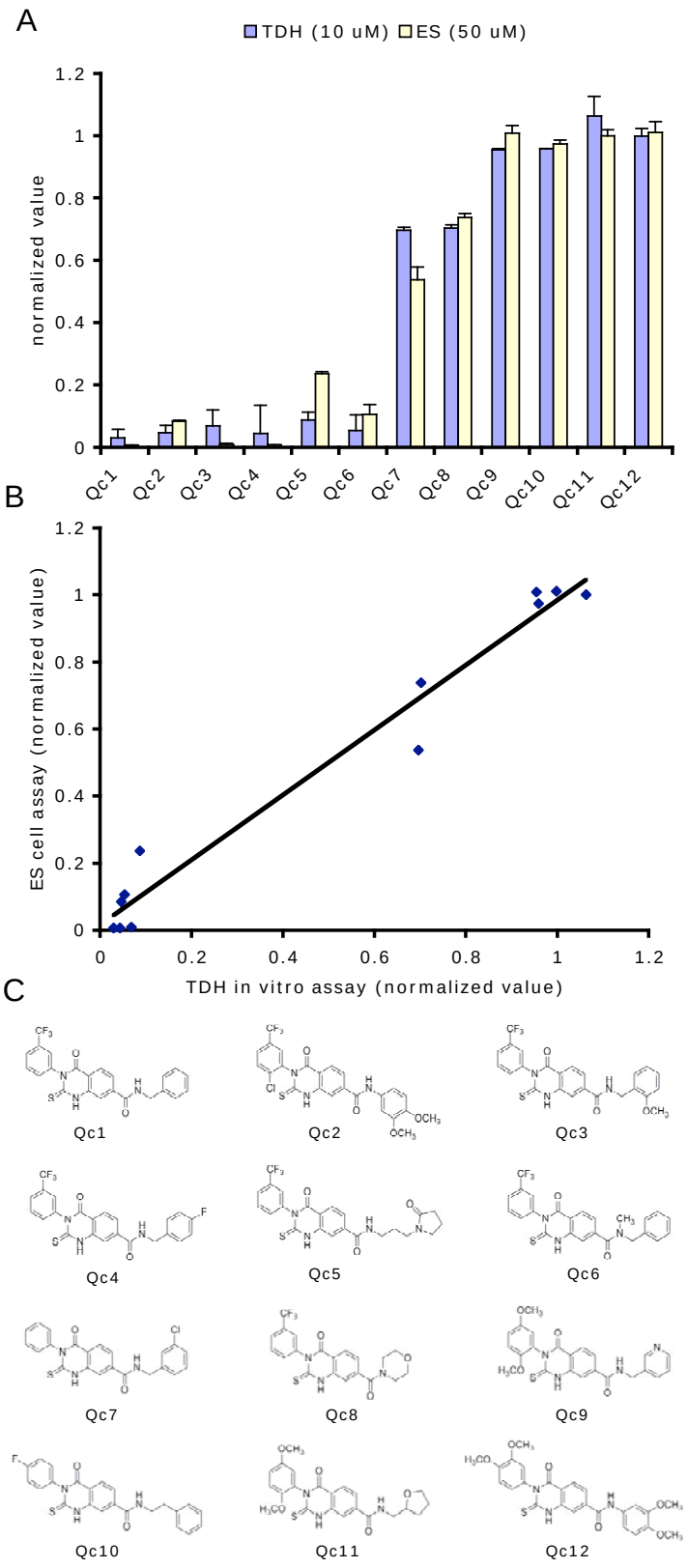
A
TDH (10 uM)
ES (50 uM)
normalized value
1.2
1
0.8
0.6
0.4
0.2
0
Qc1
Qc2
Qc3
Qc4
Qc5
Qc6
Qc7
Qc8
Qc9
Qc10
Qc11
Qc12
B
ES cell assay (normalized value)
TDH in vitro assay (normalized value)
C
Qc1
Qc2
Qc3
Qc4
Qc5
Qc6
Qc7
Qc8
Qc9
Qc10
Qc11
Qc12

Figure 4-9 Correlation between TDH inhibition and ES cell cytotoxicity for twelve quinazolinecarboxamide compounds
A. Twelve structurally related Qc compounds were assayed for their ability to inhibit TDH in vitro (10 μM compound) and impair proliferation of ES cells (50 μM compound). The normalized values for both assays are plotted in histogram form. Qc1-Qc6 are the TDH inhibitors identified through the small molecule screen, and Qc7-Qc12 are structurally related compounds in the UT Southwestern chemical library that were not identified in the screen (structures shown in C). Qc1-Qc6 are potent TDH inhibitors that kill ES cells with EC_{50} ~ 3 μM. Qc7 and Qc8 are weak TDH inhibitors with EC_{50} > 50 μM. Qc9-Qc12 did not inhibit TDH in vitro and displayed no toxicity when added to the ES cell growth medium. B. Same as in A with data plotted as an XY scatter plot. C. Chemical structures of the twelve Qc compounds.

compound-mediated ES cell death results from TDH inhibition.

Realizing that the TDH enzyme's role in ES cells was initially identified through changes in metabolite levels as a function of differentiation, we measured the effects of TDH inhibition on metabolite abundance. ES cells were cultured on gelatinized 60 cm^2 dishes for 2 hours in the presence of TDH inhibitor, and metabolites were extracted in 50% aqueous methanol and subjected to LC-MS/MS analysis. Inhibition of TDH might be predicted to result in increased levels of substrate (threonine) and decreased levels of product (acetyl-CoA). Indeed, addition of TDH inhibitor to the ES cell cultures resulted in a 2-fold increase in threonine (Figure 4-10B) and a 4-fold decrease in acetyl-CoA (Figure 4-10A). The levels of most other metabolites analyzed by this method remained unchanged under conditions of TDH inhibition. This finding, combined with the other results presented in this chapter, supports the conclusion that flux through the TDH pathway plays a major role in shaping mouse ES cell metabolism, and that TDH enzymatic activity is required for ES cells to enter into a high-flux metabolic state compatible with pluripotency and self-renewal.

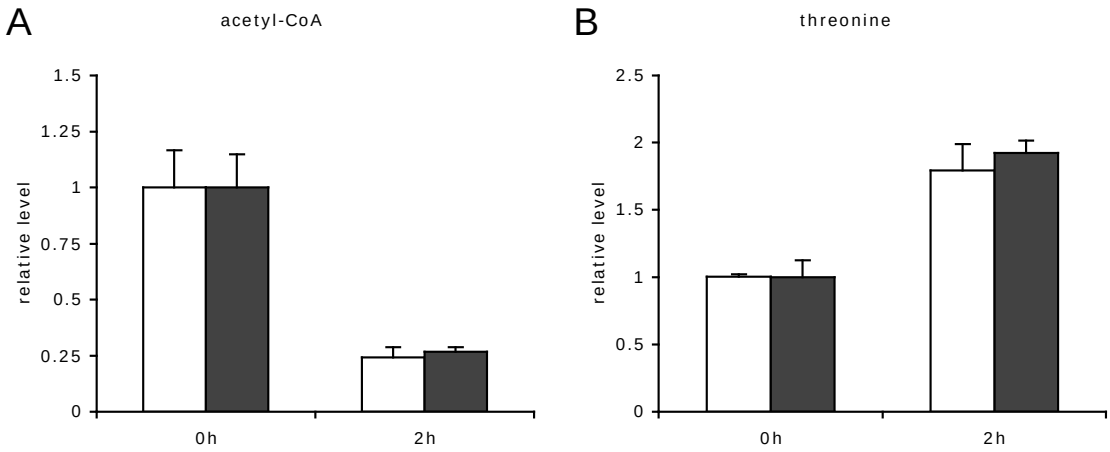

Figure 4-10 Accumulation of threonine and depletion of acetyl-CoA in ES cells treated with TDH inhibitors

Feederless ES cells were treated with 10 μM of TDH inhibitor for 2 hours before extraction of metabolites in 50% aqueous methanol and subjection to LC-MS/MS analysis. Acetyl-CoA levels decreased ~4-hold and threonine levels increased ~2-fold as a consequence of TDH inhibitor treatment, indicating that flux through the TDH pathway is a major source of acetyl-CoA in ES cells. Most other metabolite levels analyzed by this method did not change under conditions of TDH inhibition.

TDH inhibition induces autophagy in ES cells

We next focused our attention on the mechanism of ES cell death resulting from TDH inhibition, hypothesizing that ES cells treated with TDH inhibitors might be dying by apoptosis. Apoptosis, or programmed cell death, is characterized by blebbing, nuclear fragmentation, and the shearing of chromosomal DNA, and is executed by cysteine proteases called caspases. Caspase 3, a critical executioner of apoptosis, is activated by proteolytic processing of its inactive zymogen during apoptotic cell death originating from both extrinsic and intrinsic pathways (Nicholson et al., 1995). Activation of Caspase 3 results in the proteolytic cleavage of many key apoptotic proteins such as the nuclear enzyme poly (ADP-ribose) polymerase (Fernandes-Alnemri et al., 1994). To assay for apoptosis in ES cells treated with TDH inhibitors, we immunoblotted cell lysates with antibodies recognizing both the uncleaved and cleaved forms of Caspase 3. This analysis revealed a strong 35 kDa band representing the full-length Caspase 3 zymogen present in all samples tested. However, after 24 hours of TDH inhibition, when widespread cell death was clearly visible, we could not detect any activated (cleaved) Caspase 3 (Figure 4-11A). In control experiments, lysates from ES cells treated with staurosporine, a molecule known to induce apoptosis, contained Caspase 3 cleavage products that became apparent four hours after treatment (Figure 4-11B). We conclude that TDH inhibitor-mediated cell death does not result from increased apoptosis.

An alternative, and less understood, death pathway is characterized by increased cellular autophagy. Autophagy (self-eating) is the process by which bulk cytoplasmic proteins and organelles reach lysosomes for degradation (Mizushima et al., 2010).

Although associated with cell death, elevated autophagy likely provides a protective benefit to cells by salvaging nutrients from dispensable cytoplasmic contents so that vital processes can be maintained (Reggiori and Klionsky, 2002, Levine and Yuan, 2005). During autophagy, a protein called light chain 3 (LC3) is conjugated to phosphatidylethanolamine and associates with autophagosomes, and this lipidation can serve as a marker for autophagy (Kabeya et al., 2000). To assay for autophagy, we cultured ES cells for 24 hours in the presence of TDH inhibitor and immunoblotted cell lysates with an anti-LC3 antibody (Figure 4-11C). Initially, a substantial fraction of the total LC3 protein was in the LC3-I (cytoplasmic) form. After 16 hours of TDH inhibition, most LC3 was converted to the LC3-II (lipid-modified) form, indicative of increased autophagic activity. This pattern was similar to that of ES cells grown under conditions of nutrient starvation (Figure 4-11D), as well as to ES cells cultured in growth medium lacking threonine (data not shown). We conclude that blocking metabolic flux through the TDH pathway, either through small molecule inhibition or threonine deprivation, results in a form of cell death associated with increased autophagy.

As a complementary approach, we examined the morphology of ES cells treated with the TDH inhibitors using transmission electron microscopy (TEM). Autophagy was first described using TEM (Novikoff and Essner, 1962), and TEM is still one of the most sensitive methods to detect the presence of autophagic compartments in mammalian cells (Eskelinen 2008). To directly visualize autophagy, we cultured feederless mouse ES cells on gelatinized coverslips in the presence of 10 μM TDH inhibitor. Cells were fixed in glutaraldehyde and postfixed in osmium tetroxide, dehydrated with ethanol, and

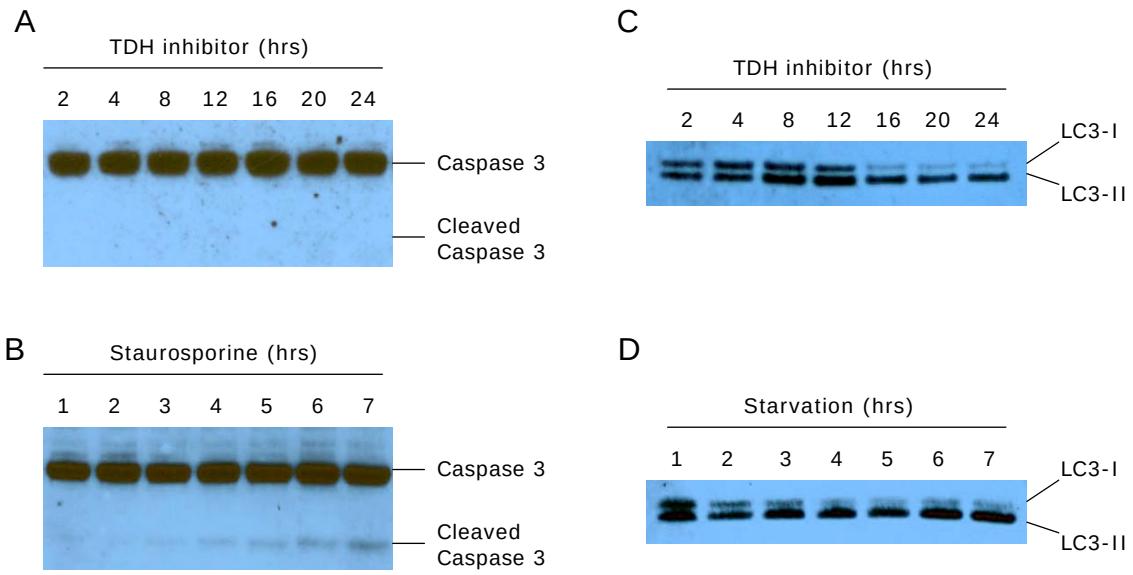

Figure 4-11 TDH inhibition results in elevated autophagy but not apoptosis
A. Protein lysates from ES cells treated with 10 μM TDH inhibitor were extracted in 0.5% NP40, separated using SDS-PAGE, and immuoblotted using an antibody specific for Caspase 3. Despite visible cell death, no cleaved Caspase 3 could be detected after 24 hours of TDH inhibitor treatment. B. Control western blot showing cleaved Caspase 3 in response to treatment with 1 μM staurosporine. C. ES cell lysates were immunoblotted with an antibody to LC3. After 16 hours of TDH inhibitor treatment, most of the LC3 protein was in the LC3-II (lipidated) form, indicative of increased autophagic activity. D. Control western blot showing increased autophagy in response to nutrient starvation. ES cells were cultured in HBSS and harvested at the times indicated.

embedded in resin polymerized by heat. Control ES cells treated with DMSO appeared as small, densely packed cells with prominent nuclei. A few mitochondria were visible in these cells but otherwise the cytoplasm was relatively clear (Figure 4-12A). In contrast, distinct autophagic structures were visible in ES cells treated with TDH inhibitor (Figure

4-12B). Less mature autophagosomes present in these cells appeared to contain whole organelles, while more mature autophagosomes contained partially degraded (electron dense) cytoplasmic contents. Electron dense lysosomes were also present. Thus, two independent methods bear out that specific inhibition of the TDH enzyme in ES cells results in increased cellular autophagy.

The classic inducer of autophagy is nutrient starvation (Reggiori and Klionsky, 2002). Apparently, insufficient production of mitochondrial acetyl-CoA and glycine in ES cells results in a cellular state resembling starvation. In HFB metabolism, glycine generated via threonine catabolism is used to fuel one-carbon metabolism for purine biosynthesis, whereas most mitochondrial acetyl-CoA enters the TCA cycle for ATP production (Dale, 1978). Thus, TDH inhibition might be predicted to result in a shortage of nucleotides for DNA replication as well as a decline in energy production. It appears that ES cells attempt to degrade nonessential cellular components to overcome these deficiencies. Under conditions of severe TDH inhibition, however, ES cells are unable to maintain their high proliferative rate and undergo a form of cell death containing features of autophagy.

In summary, we show here that ES cells treated with specific TDH inhibitors fail to proliferate and instead increase rates of autophagy in response to an altered metabolic state. In the next chapter we use a genetic approach to determine the biological role of TDH in the developing and adult mouse.

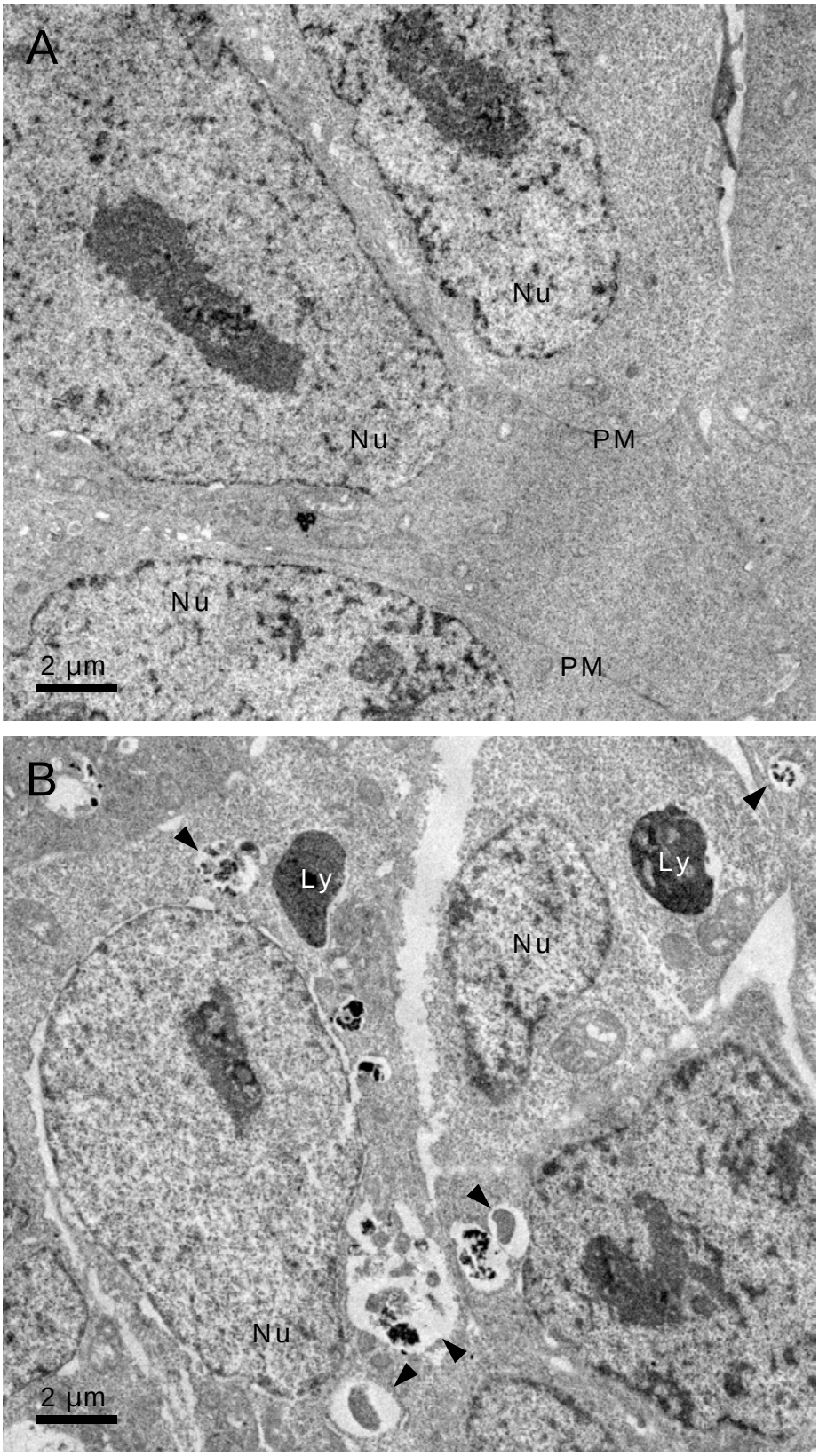
A
Nu
Nu
PM
Nu
2 µm
PM
B
Ly
Ly
Nu
Nu
2 µm

Figure 4-12 Electron microscopy of ES cells treated with TDH inhibitor
Mouse ES cells were cultured on plastic coverslips for 24 hours with or without TDH inhibitor. Cells were fixed with 2.5% glutaraldehyde in 0.1 M cacodylate buffer and embedded in Embed-812 Resin. Thin sections (70-90 nanometers in thickness) were stained with 2% aqueous uranyl acetate and lead citrate and examined by transmission electron microscopy. A. Control ES cells treated with DMSO only. B. ES cells cultured in the presence of 10 μM TDH inhibitor. Arrowheads indicate autophagic compartments. Nu, nucleus, PM, plasma membrane, Ly, dense lysosomes.

CHAPTER FIVE
Results

TARGETED DELETION OF TDH IN MICE

Abstract

Mouse TDH is strongly expressed in the ICM cells of the blastocyst and in cultured ES cells, where it is required for their self-renewal. To determine the biological function of TDH in the context of the whole animal, we generated mice conditionally lacking the TDH gene using Cre-Lox technology. Although we anticipated a severe embryological defect in these animals, TDH-null animals lacked any obvious developmental phenotype. This unexpected finding means that TDH activity, while necessary for the proliferation of ES cells in culture, appears to be nonessential for the proliferation of ICM cells in developing mouse embryos. The distinct environmental conditions encountered by proliferating pluripotent stem cells in vitro and in vivo may account for this apparent discrepancy.

Introduction

Precise modifications can be introduced into the mouse genome using gene targeting, allowing the study of the biological function of any gene of interest (Thomas and Capecchi, 1987). Two technological breakthroughs enabled gene targeting in mice. The first was the establishment of cultured ES cell lines capable of contributing to the mouse germline (discussed in chapter 1). The second was the ability to modify a single genomic locus in mammalian cells through the process of homologous DNA

recombination. Using these techniques, ES cells can be genetically altered in culture and then injected into mouse blastocysts such that the alterations are propagated to offspring through the germline. More recently, conditional gene targeting has made possible the deletion of a gene either at a specific time during the life of the animal or in a specific tissue or cell type.

Methods

Materials

All restriction enzymes were from New England BioLabs. Meox-Cre mice were a kind gift from Michelle Tallquist. All other chemicals and reagents were obtained from Sigma-Aldrich except where specified.

Targeting Vector Construction

Targeting vectors were generated in pGKneoF2L2DTA, a plasmid containing a DTA selection cassette and a neomycin cassette flanked by nested loxP and FRT sites. The short arm of homology, a 0.9 kB *Not*I fragment contained in the first intron of the *TDH* gene, was inserted upstream of the 5' loxP site in the same orientation as the neomycin cassette. The knockout arm was 1.0 kB in length, included the entire second exon and regions of introns one and two, and was inserted between the first loxP site and the first FRT site using *Xma*I. The long arm of homology, a 6.2 kB sequence spanning exons 3-8, was cloned between the second loxP site and DTA using *Sal*I and *EcoR*V. All PCR products incorporated into targeting vectors were generated using *Pfu* (Stratagene)

and were verified by sequencing.

Targeting vector plasmid DNA was isolated using a Qiagen Plasmid Midi Kit. 300 μg of purified plasmid DNA was linearized using the restriction enzyme *Pvu*I. 1 μL of reaction was analyzed by agarose gel electrophoresis to verify complete digestion. DNA was extracted using phenol chloroform/isoamyl alcohol and precipitated with cold ethanol and ammonium acetate. DNA was washed 3 times with cold 70% ethanol, dried, and resuspended in 50 μL of sterile, nuclease-free water. 2 μL of DNA was used to measure concentration and analyze purity, and the stock was diluted to 2 μg/μL and stored at -20°C.

Electroporation and Screening of ES Cells

100 μg of linearized targeting construct DNA was electroporated into 1 x 10^7 wild type ES cells from the 129/SvEvTac (SM-1) mouse strain. After selection in G418, three 96-well plates of colonies were picked from the electroporation in triplicate. Two stock plates from each set were frozen, and genomic DNA was isolated from the third plate as follows. Colonies were washed twice with 100 μL PBS, frozen at -80°C for three hours, and then lysed overnight at 55°C in a shaking incubator in 50 μL of 10 mM Tris-HCl pH 7.5, 10 mM EDTA, 10 mM NaCl, 0.5% SDS, and 1 mg/mL Proteinase K (Invitrogen). The following day, DNA was precipitated by adding 100 μL of cold ethanol with 50 mM NaCl per well, and plates were centrifuged in a 96-well plate holder for 5 minutes at 2500 rpm. Precipitated DNA was washed 3 times with 70% ethanol, dried, and suspended in 100 μL sterile water. Colonies were screened for integration at the TDH locus by PCR

using GoTaq DNA Polymerase (Promega) with the primers 5'-TGCATCGGATTGTCTGAGTAG-3' (forward) and 5'-GATAGAGCCAGTAAGACTCC-3' (reverse) such that correct targeting resulted in a 1.5 kB PCR product. DNA was re-screened by a second round of PCR using different primers, and correct targeting was confirmed by sequencing of targeted DNA.

Generation of Mouse Lines

Correctly targeted ES cells were injected into wild type C57BL/6J blastocysts to generate chimeras. 10-12 ES cells were injected into each blastocyst, and 10-15 injected blastocysts were transferred into the uterine lumens of pseudopregnant (day 2.5) recipients. The highest ES cell contributions were ~90% based on pup coat color. F0 chimeric male mice were bred with wild-type C57Bl/6 females, and agouti offspring were screened for the presence of the floxed TDH allele using a PCR reaction with two primers with the sequences 5'-AGCGCGGCCGCTCCCCTCCTTATGA-3' (forward) and 5'-GCCCTCCTCATCCTCATAGG-3' (reverse). F1 mice containing one floxed TDH allele were then mated to Meox-Cre mice to produce F2 heterozygotes with one excised TDH allele. These were genotyped using a 4-primer PCR reaction using primers with the sequences 5'-GGTAGTCTCTTATCTGGTGC-3' (forward), 5'-AGGGCTTGCAATCTCGACTA-3' (reverse), 5'-TGCATCGGATTGTCTGAGTAG-3' (forward), and 5'- GCCCTCCTCATCCTCATAGG -3' (reverse). Using these primers, PCR of the wild-type allele produces a 1.1 kB band, the floxed (loxP-flanked) allele is 0.3 kB, and the Cre-excised TDH allele results in a PCR product of 1.3 kB. F2 heterozygote mice were then crossed to produce homozygote

knockout mice.

Results and Discussion

Anticipating that TDH-null mice might have a strong embryological phenotype, we generated a conditional null allele to investigate the role of TDH at specific stages of development and in adults. Targeting of TDH was performed by introducing loxP sites flanking exon 2 through homologous recombination (Figure 5-1). This mutation deletes the translational start codon, the mitochondrial signal sequence, and several amino acids predicted to be required for NAD^+ binding (Edgar, 2002). In addition, the deletion of exon 2 produces a shift in the translational reading frame. Germline transmission of targeted ES cells was detected by PCR, and confirmed at the genomic level by sequencing of amplified genomic DNA.

$TDH^{neo\text{-}loxP}$ mice were bred to Meox-Cre transgenic mice, which express Cre recombinase from the Mox2 locus (Tallquist and Soriano, 1999). In Meox-Cre embryos, Cre activity is first detectable in the epiblast at day E5. At E6 and E7, Cre recombinase is expressed in primitive ectoderm but is absent in trophectoderm and primitive endoderm, which will form the yolk sac (Figure 1-1). Because Cre is also expressed in germ cells, Meox-Cre mice can also be used as a germline deleter line (Tallquist and Soriano, 1999). Therefore, in combination with TDH conditional knockout mice, Meox-Cre mice can be used to separate the biological functions of TDH before and after day E5.

Breeding of $TDH^{neo\text{-}loxP}$ mice to Meox-Cre mice allowed for the generation of $TDH^{+/epi}$ mice, in which one TDH allele has been deleted beginning at the epiblast stage

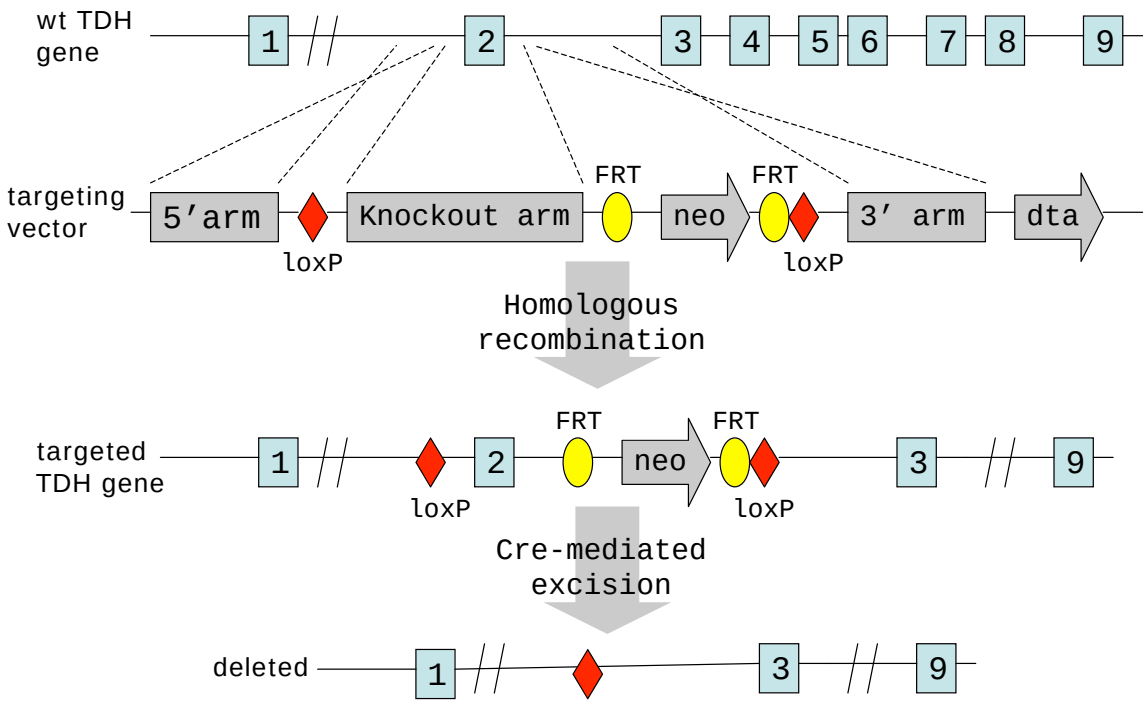

Figure 5-1 Strategy used to generate conditional TDH knockout mice
Exon structure of the mouse TDH gene is shown. The three arms were amplified from mouse strain 129 cDNA using high fidelity PCR and cloned into the PGKneoF2L2DTA targeting vector (Montgomery et al., 2008). Neomycin-resistant ES cells were produced by electroporation of linearized vector DNA and screened for correct targeting using PCR. Cre-mediated excision leaves one loxP site in place of exon 2 and shifts the transcript's reading frame.

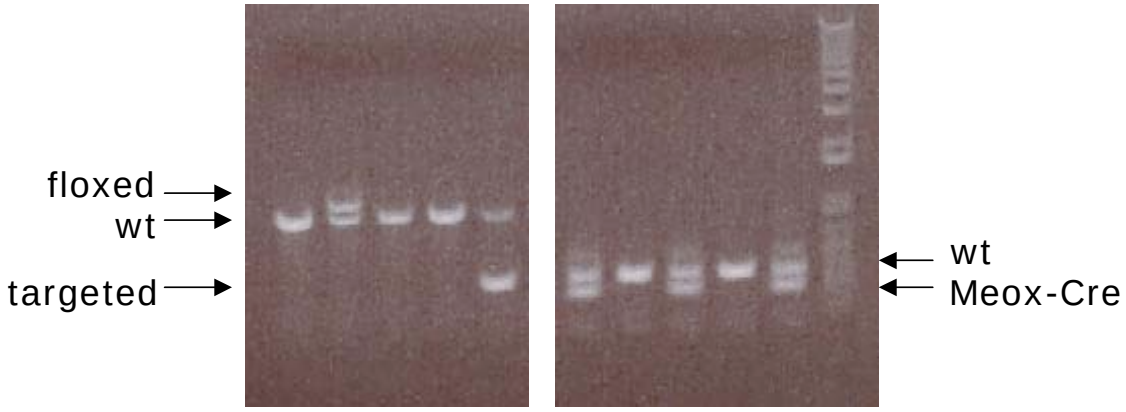

Figure 5-2 Genotyping of targeted mice
Shown is an ethidium bromide-stained agarose gel of a typical series of PCR reactions using tail snip DNA as a template. The left panel shows the results of reactions using primers specific for TDH, and the right panel shows the results of reactions using primers specific for Meox-Cre. For the TDH genotyping, the 1.1 kB band corresponds to the wild-type TDH allele, the 0.3 kB band represents the loxP-flanked allele, and the 1.3 kB band is the Cre-excised TDH allele. The Meox-Cre PCR results in a wild-type product of 0.4 kB and a mutant product of 0.3 kB. Generic Cre primers can also be used to genotype these mice. See *Materials and Methods* for primer sequences.

of development. Mice were genotyped using PCR reactions that could distinguish between the wild-type, targeted, and excised TDH alleles (Figure 5-2). Since Cre recombinase is expressed in the germline of Meox-Cre animals, subsequent breeding of $TDH^{+/epi}$ and $TDH^{neo\text{-}loxP}$ mice resulted in the generation of $TDH^{epi/-}$ mice. These animals contain one TDH allele deleted at the epiblast stage, whereas the other allele is deleted in the zygote owing to germline Cre expression. $TDH^{epi/-}$ mice were born at Mendelian ratios and lacked an obvious phenotype. Initially, we speculated that TDH might be required for formation of the ICM, which does not contain Cre expression in these animals. Therefore, we generated complete (conventional) knockout animals by intercrossing $TDH^{+/epi}$ mice to obtain $TDH^{-/-}$ mice. To our surprise, these animals also appeared phenotypically normal.

We are still in the initial stages of characterizing the $TDH^{-/-}$ mice, and are currently breeding these animals to test for sterility. In addition, we will attempt to derive new ES cell lines from these animals to genetically test whether TDH is necessary for the maintenance of cultured ES cells (discussed in chapter 6). Although it appears that TDH activity is not essential for embryonic development in mice, we anticipate that the TDH enzyme may be critically important in a subset of cells or during a specific biological process. As such, careful analysis of $TDH^{-/-}$ mice might reveal new roles for HFB metabolism in the context of normal mouse physiology.

CHAPTER SIX
Conclusions and Future Directions

Studies involving TDH knockout mice

Generation of TDH-null ES cells

In this study we have shown using specific enzyme inhibitors that TDH enzymatic activity is necessary for the self-renewal of mouse ES cells grown in culture (chapter 4). Since TDH is highly expressed in the mouse blastocyst ICM (chapter 3), it was surprising that mice completely lacking the TDH enzyme do not display any obvious developmental phenotype (chapter 5). Thus, it appears that TDH activity is necessary to maintain rapidly proliferating ES cells in culture but not necessary in the context of the developing mouse embryo, perhaps due to different environmental conditions.

To genetically verify that TDH is required in cultured mouse ES cells, we will attempt to derive new ES cell lines from the TDH-null mice. Based on the effects of TDH inhibition in ES cells, we expect that these lines should have defects in self-renewal and perhaps increased levels of autophagy. Since some mouse strains are more permissive to ES cell derivation than others (discussed in chapter 1), we must consider the genetic background of the TDH knockout mice. At present our TDH null mice are a mix of the 129 and C57BL/6 strains. This line was generated by injecting ES cells from the 129/SvEv strain into wild type C57BL/6 blastocysts, resulting in chimeric animals that were approximately 90% 129 strain. However, excision of the floxed TDH allele required the breeding of these mice to Meox-Cre animals that were of the C57BL/6

strain, which is refractory to efficient ES cell derivation.

To attempt to generate TDH-null ES cells from a strain fully permissive to ES cell derivation, we are currently backcrossing the TDH knockouts to the inbred 129/SvEv strain from Taconic to generate a 129 congenic strain. To accelerate this process we are using a method called speed congenics (or marker-assisted breeding, Markel et al., 1997). Traditional backcrossing methods typically require ten backcross generations, or approximately thirty months, to create a 99.9% congenic strain. Using hundreds of DNA microsatellite markers that are polymorphic between inbred mouse strains, speed congenics can be used to shorten the backcrossing to five generations. Since our initial TDH knockouts are approximately 50% 129 strain, it should be possible using this approach to reach 99% congenicity within three generations (approximately nine months), and thus a strain background that is suitable for efficient ES cell derivation.

In vitro development of TDH-null embryos

In cultured mouse embryos, administration of the threonine analog 3-HNV blocks the conversion of morula-stage embryos into cavitated blastocysts (Figure 4-2). If 3-HNV is indeed acting through the TDH enzyme in this assay, then it appears that TDH activity is necessary for mouse embryo development in vitro, but is nonessential for in vivo development. This would suggest that the embryo's environment in the uterus, in particular the nutrient conditions, might be radically different than our experimental culture conditions for in vitro blastocyst development. Mouse breeding is currently underway to determine whether the TDH-null mice are fertile. If these mice breed

normally, then we will isolate mouse embryos devoid of TDH to test directly whether TDH is required for blastocyst development in vitro.

Requirement of TDH for embryonic diapause

Embryonic diapause, also called delayed implantation, is a reproductive strategy in which the late blastocyst arrests its normal development and is maintained in a quiescent state. Mammals that use diapause include rodents, bears, mustelids, and marsupials. It is thought that the function of embryonic diapause is to time the birth of offspring to match favorable environmental conditions (Hondo and Stewart, 2005).

The idea has been proposed that an association may exist between the capacity of a rodent species to carry out embryonic diapause and the permissivity of the species to ES cell derivation (Nichols and Smith, 2009). It is possible that the ability of ICM cells to exit dormancy and resume rapid proliferation might have some relevance to ES cell derivation. Gene deletion studies have revealed that LIF/STAT3 signaling is necessary for diapause to occur in mice (Nichols, et al., 2001), indicating a connection between diapause and the conditions normally used to grow ES cells in culture.

Given its copious expression in ICM cells and its requirement for rapid proliferation in cultured ES cells, it is possible that TDH plays a critical role in embryonic diapause. To address this hypothesis, we can test whether TDH knockout mice are able to carry out this process. A method commonly used to induce diapause is to ovariectomize pregnant mice four days after fertilization. Following three days of delayed implantation, dormant blastocysts can be activated by injection of estradiol

(Hamatani et al., 2004). If TDH is required for embryonic diapause, then TDH-null mice should not be able to give birth to live pups after entering diapause. This result would suggest a close association between TDH, diapause, and the difficulty of obtaining authentic ES cell lines from non-rodent species.

TDH inhibitors as anti-parasitic agents

In this study, small molecule TDH inhibitors have been identified and used to show that mouse ES cell self-renewal has a strict requirement for metabolic flux through the TDH pathway. However, in addition to their value as scientific reagents, these inhibitors might also have medical relevance. We and others have shown that the human TDH gene is inactive as a result of three debilitating mutations (Edgar, 2002; chapter 3 above). On the other hand, microbial organisms such as bacteria and yeast have been shown to utilize HFB metabolism to maintain growth rates under nutrient-limiting conditions (Almaas et al., 2004; Hartman, 2007). The TDH enzyme is also found in disease-causing species such as trypanosomes and parasitic worms. If parasitic organisms can be identified that rely on TDH-mediated threonine catabolism for viability or reproduction, then TDH inhibitors might prove useful for the treatment of human disease.

As a first step toward reaching this objective, we have cloned and expressed the TDH enzymes from the nematode C. elegans (ceTDH) and the trypanosome T. brucei (tbTDH). Nematodes, or roundworms, are a diverse phylum containing approximately 28,000 species, of which over 16,000 are parasitic (Hugot et al., 2001). Parasitic

nematodes include hookworms, pinworms, and whipworms, all of which prey on humans, in addition to parasites that infect plants and are responsible for major crop losses, such as root-knot nematodes. Trypanosomes are protists that cause African trypanosomiasis (or sleeping sickness) in humans and livestock. T. brucei is transmitted by the tsetse fly and exists in bloodstream and procyclic forms. Trypanosomiasis is fatal if left untreated, and, because existing therapies are costly and have severe side effects, there is an urgent need for new drugs to combat this disease (Barrett et al., 2003).

TDH inhibitors have several properties that suggest their potential usefulness as anti-parasitic agents. Therapeutic drugs should have high potency and be effective when administered at low concentrations. The small molecules identified by chemical screening inhibit mouse TDH with an IC_{50} of 0.5 μM, and this potency could likely be improved by using medicinal chemistry to systematically modify the inhibitors' functional groups (structure-activity relationships). Anti-parasitic drugs should also be safe to humans and produce side effects that are few and tolerable. Since humans do not express an active TDH enzyme, a specific TDH inhibitor might achieve this goal. Indeed, the inhibitors identified in this study were toxic to human HeLa cells only at very high (millimolar) concentrations, and were about 300-fold more potent in their activity toward mouse ES cells. Finally, the biological target of an effective anti-parasitic drug must be essential to the viability or reproduction of the parasitic organism.

Gene silencing using RNA interference (RNAi) can be performed in both C. elegans and T. brucei to test the biological role of TDH in these organisms. Indeed, RNAi experiments to examine the function of TDH in T. brucei are currently underway.

Published data suggests that TDH might be critical in T. brucei because threonine catabolism in this organism apparently occurs exclusively via the TDH pathway (Linstead et al., 1977). Since trypanosomes lack a functional TCA cycle, acetyl-CoA generated from TDH-mediated threonine catabolism is likely used as a substrate for lipid biosynthesis.

To test the activity of the mouse TDH inhibitors on TDH enzymes from these parasitic organisms, we expressed and purified tbTDH and ceTDH. The tbTDH protein was expressed at high levels in E. coli, and the purified enzyme contained activity comparable to mouse TDH. Although ceTDH was expressed at much lower levels and found to be unstable when stored at 4°C, the purified ceTDH enzyme also contained robust NAD^+-reducing activity in the presence of threonine (data not shown). The primary sequence homology among the mouse, worm, and trypanosome TDH enzymes is high, with 51% amino acid identity for the mouse and worm enzymes and 42% identity for the mouse and trypanosome enzymes. Thus it was surprising when only one of the six Qc compounds was able to inhibit ceTDH at a concentration of 10 μM, and none of the six were able inhibit tbTDH (data not shown). The likely explanation for the failure of the mouse TDH inhibitors to inhibit orthologous TDH enzymes is that, since these compounds are mixed noncompetitive inhibitors, they bind outside of the enzyme's active site, which may not be strictly conserved between mice, worms, and trypanosomes.

To identify small molecules capable of inhibiting the TDH enzymes originating from parasitic organisms, it will be necessary to perform a new chemical screen using the enzyme from the species of interest. Since tbTDH is robustly expressed in E. coli, the

identification of inhibitors specific for tbTDH by high-throughput screening should be feasible. However, before undertaking this screen, one should first verify that TDH has an essential role in this parasite. The RNAi knockdown experiment that is currently underway should reveal whether a screen for tbTDH inhibitors might prove fruitful for the identification of new drugs for the treatment of trypanosomiasis.

Concluding remarks

This study provides evidence for the strict requirement of TDH enzymatic activity for the process of mouse embryonic stem cell self-renewal in culture. Through analysis of metabolite abundance as a function of ES cell differentiation, we were able to identify the TDH gene as being robustly and specifically expressed in ES cells and in the ICM of the mouse blastocyst. This TDH enzyme activity is necessary for ES cell proliferation, because blocking this metabolic pathway either through threonine deprivation or enzyme inhibition results in increased autophagy and cell death.

During the course of this work, several reagents have been developed that should prove valuable for furthering our understanding of the TDH metabolic pathway. First, antibodies specific for TDH have been generated and used to study TDH localization in mouse ES cells and embryos. Using these antibodies, it was determined that the TDH enzyme is copiously expressed in pluripotent ES cells and in ICM cells of the early mouse embryo. Although we have yet to find a site of TDH protein expression in adult mice, it is possible that TDH is expressed in rare cell types or during specific biological processes. For example, TDH might be expressed in adult stem cell niches, or during

conditions of tissue regeneration. In future studies, these antibodies could be used to identify these sites of expression, providing useful information about TDH's normal biological function.

Second, our study of TDH at the biochemical level has led to the development of highly potent and specific small molecule inhibitors of the mouse TDH enzyme. These compounds have been found to selectively impede ES cell proliferation through alterations in metabolic flux. These results indicate that ES cells are uniquely dependent on the HFB of metabolism. In the future it may be possible to use medicinal chemistry to further improve the potency of these inhibitors. In addition, high-throughput screens similar to the screen reported here could be performed to identify inhibitors specific to TDH enzymes from parasitic organisms, and these molecules may turn out to have medicinal or agricultural utility.

Finally, TDH conditional knockout mice have been generated to study the role of TDH at the organismal level. Since these mice appear to lack the early development lethality we expected based on the requirement for TDH in ES cell culture, several experiments are underway to probe the biological role of TDH in mice. For example, we have plans to generate TDH-null ES cells from these knockout animals, and to test the role of TDH in embryonic diapause and in vitro blastocyst development, as described above. If specific biological settings that are dependent on TDH can be identified, then Cre transgenic lines can be used for the detailed study of these TDH-dependent processes.

One longstanding mystery in the ES cell field is why ES cells capable of germline

transmission have thus far only been obtained from mice and rats. Since ES cells enable the production of knockout animals via gene targeting, authentic ES cells from additional species would prove immensely useful both scientifically and commercially. It has been shown that TDH is necessary for mouse ES cell proliferation in culture. It is possible that ICM cells from other mammalian species do not express TDH, or that TDH expression is rapidly shut off when these cells are plated in culture. Thus, TDH expression may be a critical factor that enables the derivation of germline-transmitting ES cells. Supporting this hypothesis is the observation that several key transcription factors regulating pluripotency bind to TDH's first exon (Kim et al., 2008), which is only conserved in mice and rats. If lack of TDH expression does in fact play a role in the failure to derive ES cells from non-rodent species, then ectopic expression of TDH might support the derivation of new ES cell lines.

In addition to enabling the production of non-rodent ES cells, it is hoped that forced expression of TDH might be used to stimulate growth rates of cell lines not normally expressing the enzyme. Besides providing proof-of-principle that TDH is in fact used to drive rapid cell division in ES cells, stimulation of growth rates via TDH expression would be a useful scientific tool, particularly for experiments relying on the culture of slowly dividing cells. Thus far, TDH gain-of-function studies have proven technically challenging. Since TDH is a metabolic enzyme, relatively high levels are required to appreciably alter the metabolic flux within a cell, and it appears to be difficult to engineer cell lines to express exogenous TDH at a level comparable to mouse ES cells.

There are several possible explanations for this difficulty. One possibility is that

high expression of TDH overwhelms the mitochondrial import machinery, resulting in degradation of the protein. Alternatively, there might be some unknown post-translational modification that targets TDH for degradation in differentiated cell types, but is inactive in mouse ES cells. In support of this possibility is the observation that TDH mRNA is expressed at a high level in mouse pancreas, whereas TDH protein is undetectable. Finally, most gain-of-function experiments in mammalian cells involve the expression of transcription factors or signaling proteins, which require very low levels of protein to support their biological activity. As a result, new technical methods might need to be developed in order to express TDH at a level high enough to drive rapid cell division.

One final unexplained observation concerns the mutational inactivation of the human TDH gene. It is puzzling that two of the three debilitating mutations are AG to GG splice acceptor site mutations, suggesting that there was strong selection pressure for these specific changes. Could there be an unidentified mechanism that results in the repair of these mutations in specific cell types to produce a functional TDH enzyme? No evidence for such a process exists. It is also strange that humans appear to be the only metazoan species with an inactive TDH; the genome of the chimpanzee, our closest living relative, contains an intact TDH gene. When the Neanderthal genome sequence is completed, it will be interesting to see if these mutations were present in the Neanderthal TDH gene. It will also be interesting to explore what selective advantage, if any, is conferred on humans by mutational inactivation of the TDH gene.

BIBLIOGRAPHY

Alberts, B., Johnson, A., Lewis, J., Raff, M., Roberts, K., and Walter, P. (2002). Molecular biology of the cell. (New York: Garland).

Almaas, E., Kovács, B., Vicsek, T., Oltvai, Z. N., and Barabási, A. L. (2004). Global organization of metabolic fluxes in the bacterium Escherichia coli. Nature *427*, 839-843.

Amit, M., Carpenter, M. K., Inokuma, M. S., Chiu, C. P., Harris, C. P., Waknitz, M. A., Itskovitz-Eldor, J., and Thomson, J. A. (2000). Clonally derived human embryonic stem cell lines maintain pluripotency and proliferative potential for prolonged periods of culture. Dev Biol *227*, 271-278.

Aoyama, Y., and Motokawa, Y. (1981). L-threonine dehydrogenase of chicken liver. Purification, characterization, and physiological significance. J Biol Chem *256*, 12367-12373.

Attardi, G., and Schatz, G. (1988). Biogenesis of mitochondria. A Rev Cell Biol *4*, 289-331.

Barrett, M. P., Burchmore, R. J., Stich, A., Lazzari, J. O., Frasch, A. C., Cazzulo, J. J., and Krishna, S. (2003). The trypanosomiases. Lancet *362*, 1469-1480.

Batlle-Morera, L., Smith, A., and Nichols, J. (2008). Parameters influencing derivation of embryonic stem cells from murine embryos. Genesis *46*, 758-767.

Benkovic, S. J. (1984). The transformylase enzymes in de novo purine biosynthesis. Trends in Biochemical Sciences *9*, 320-322.

Bono, H., Kasukawa, T., Hayashizaki, Y., an Okazaki, Y. (2002). READ: RIKEN Expression Array Database. Nucleic Acids Res *30*, 211-213.

Bowyer, A., Mikolajek, H., Stuart, J. W., Wood, S. P., Jamil, F., Rashid, N., Akhtar, M., and Cooper, J. B. (2009). Structure and function of the l-threonine dehydrogenase (TkTDH) from the hyperthermophilic archaeon Thermococcus kodakaraensis. J Struct Biol *168*, 294-304.

Bradley, A., Evans, M., Kaufman, M. H., and Robertson, E. (1984). Formation of germ-line chimaeras from embryo-derived teratocarcinoma cell lines. Nature *309*, 255-256.

Brinster, R. L. (1969). The mammalian oviduct. (Chicago: University of Chicago Press).

Brinster, R. L. (1974). The effect of cells transferred into the mouse blastocyst on subsequent development. J Exp Med *140*, 1049-1056.

Buehr, M., and Smith, A. (2003). Genesis of embryonic stem cells. Phil Trans R Sc B *358*, 1397-1402.

Buehr, M., Meek, S., Blair, K., Yang, J., Ure, J., Silva, J., McLay, R., Hall, J., Ying, Q. L., and Smith, A. (2008). Capture of authentic embryonic stem cells from rat blastocysts. Cell *135*, 1287-1298.

Carroll, S. B. (2008). Evo-devo and an expanding evolutionary synthesis: a genetic theory of morphological evolution. Cell *134*, 25-36.

Chambers, I., Colby, D., Robertson, M., Nichols, J., Lee, S., Tweedie, S., and Smith, A. (2003). Functional expression cloning of Nanog, a pluripotency sustaining factor in embryonic stem cells. Cell *113*, 643-655.

Chambers, I., Silva, J., Colby, D., Nichols, J., Nijmeijer, B., Robertson, M., Vrana, J., Jones, K., Grotewold, L., and Smith, A. (2007). Nanog safeguards pluripotency and mediates germline development. Nature *450*, 1230-1234.

Chazaud, C., Yamanaka, Y., Pawson, T., and Rossant, J. (2006). Early lineage segregation between epiblast and primitive endoderm in mouse blastocysts through the Grb2-MAPK pathway. Dev Cell *10*, 615-624.

Codogno, P., and Meijer, A. J. (2005). Autophagy and signaling: their role in cell survival and cell death. Cell Death Differ *12 Suppl 2*, 1509-1518.

Daheron, L., Opitz, S. L., Zaehres, H., Lensch, M. W., Andrews, P. W., Itskovitz-Eldor, J., and Daley, G. Q. (2004). LIF/STAT3 signaling fails to maintain self-renewal of human embryonic stem cells. Stem Cells *22*, 770-778.

Dale, R. A. (1978). Catabolism of threonine in mammals by coupling l-threonine 3-dehydrogenase with 2-amino-3-oxobutyrate-CoA ligase. Biochim Biophys Acta *544*, 496-503.

Devlin, T. M. (2002). Textbook of biochemistry with clinical correlations. (New York: Wiley-Liss).

Edgar, A. J. (2002). The human l-threonine 3-dehydrogenase gene is an expressed pseudogene. BMC Genet *3*, 18.

Edgar, A. J. (2005). Mice have a transcribed l-threonine aldolase/GLY1 gene, but the human GLY1 gene is a non-processes pseudogene. BMC Genomics *6*, 32.

Epperly, B. R., and Dekker, E. E. (1991). L-threonine dehydrogenase from Escherichia coli. Identification of an active site cysteine residue and metal ion studies. J Biol Chem *266*, 6086-6092.

Eskelinen, E. L. (2008). To be or not to be? Examples of incorrect identification of autophagic compartments in conventional transmission electron microscopy of mammalian cells. Autophagy *4*, 257-260.

Evans, M. J., and Kaufman, M. H. (1981). Establishment in culture of pluripotential cells from mouse embryos. Nature *292*, 154-156.

Evans, M. J. (2007). Embryonic stem cells: the mouse source – vehicle for mammalian genetics and beyond. Nobel Lecture.

Fernandes-Alnemri, T., Litwack, G., and Alnemri, E. S. (1994). CPP32, a novel human apoptotic protein with homology to Caenorhabditis elegans cell death protein Ced-3 and mammalian interleukin-1 beta-converting enzyme. J Biol Chem *269*, 30761-30764.

Gardner, R. L. (1998). Contributions of blastocyst micromanipulation to the study of mammalian development. BioEssays *20*, 168-180.

Garrett, R. H., and Grisham, C. M. (1999). Biochemistry. (Pacific Grove: Brooks/Cole).

Graf, T., and Enver, T. (2009). Forcing cells to change lineages. Nature *462*, 587-594.

Guo, G., Yang, J., Nichols, J., Hall, J. S., Eyres, I., Mansfield, W., and Smith, A. (2009). Klf4 reverts developmentally programmed restriction of ground state pluripotency. Development *136*, 1063-1069.

Hamatani, T., Daikoku, T., Wang, H., Matsumoto, H., Carter, M. G., Ko, M. S., and Dey, S. K. (2004). Global gene expression analysis identifies molecular pathways distinguishing blastocyst dormancy and activation. Proc Natl Acad Sci USA *101*, 10326-10331.

Hanna, J., Saha, K., Pando, B., van Zon, J., Lengner, C. J., Creyghton, M. P., van Oudenaarden, A., and Jaenisch, R. (2009). Direct cell reprogramming is a stochastic process amenable to acceleration. Nature *462*, 595-601.

Hartman, J. L. (2007). Buffering of deoxyribonucleotide pool homeostastis by threonine metabolism. Proc Natl Acad Sci USA *104*, 11700-11705.

He, H., Dang, Y., Dai, F., Guo, Z., Wu, J., She, X., Pei, Y., Chen, Y., Ling, W., Wu, C., Zhao, S., Liu, J. O., and Yu, L. (2003). Post-translational modifications of three members

of the human MAP1LC3 family and detection of a novel type of modification for MAP1LC3B. J Biol Chem *278*, 29278-29287.

Higashi, N., Tanimoto, K., Nishioka, M., Ishikawa, K., and Taya, M. (2008). Investigating a catalytic mechanism of hyperthermophilic L-threonine dehydrogenase from Pyrococcus horikoshii. J Biochem *144*, 77-85.

Hoch, R. V., and Soriano, P. (2005). Context-specific requirements for Fgfr1 signaling through Frs2 and Frs3 during mouse development. Development *133*, 663-673.

Hondo, E., and Stewart, C. L. (2005). Profiling gene expression in growth-arrested mouse embryos in diapause. Genome Biol *6*, 202.

Hugot, J. P., Baujard, P., and Morand, S. (2001). Biodiversity in helminths and nematodes as a field of study: an overview. Nematology *3*, 199-208.

Ichimura, Y., Kirisako, T., Takao, T., Satomi, Y., Shimonishi, Y., Ishihara, N., Mizushima, N., Tanida, I., Kominami, E., Ohsumi, M., Noda, T., and Ohsumi, Y. (2000). A ubiquitin-like system mediates protein lipidation. Nature *408*, 488-492.

Ishikawa, K., Higashi, N., Nakamura, T., Matsuura, T., and Nakagawa, A. (2006). The first crystal structure of l-threonine dehydrogenase. J Mol Biol *366*, 857-867.

Ivanova, N., Dobrin, R., Lu, R., Kotenko, I., Levorse, J., DeCoste, C., Schafer, X., Lun, Y., Lemischka, I. R. (2006). Dissecting self-renewal in stem cells with RNA interference. Nature *442*, 533-538.

Kabeya, Y., Mizushima, N., Ueno, T., Yamamoto, A., Kirisako, T., Noda, T., Kominami, E., Ohsumi, Y., and Yoshimori, T. (2000). LC3, a mammalian homologue of yeast Apg8p, is localized in autophagosome membranes after processing. EMBO J *19*, 5720-5728.

Kabeya, Y., Mizushima, N., Yamamoto, A., Oshitani-Okamoto, S., Ohsumi, Y., and Yoshimori, T. (2004). LC3, GABARAP and GATE16 localize to autophagosomal membrane depending on form-II formation. J Cell Sci *117*, 2805-2812.

Kahan, B. W., and Ephrussi, B. (1970). Developmental potentialities of clonal in vitro cultures of mouse testicular teratoma. J Natl Cancer Inst *44*, 1015-1036.

Kawase, E., Suemori, H., Takahashi, N., Okazaki, K., Hashimoto, K., and Nakatsuji, N. (1994). Strain difference in establishment of mouse embryonic stem (ES) cell lines. Int J Dev Biol *38*, 385-390.

Kim, J., Chu, J., Shen, X., Wang, J., Orkin, S. H. (2008). An extended transcriptional network for pluripotency of embryonic stem cells. Cell *132*, 1049-1061.

Kleinsmith, L. J., and Pierce, G. B. (1964). Multipotentiality of single embryonal carcinoma cells. Cancer Res *24*, 1544-1551.

Kroemer, G., and Levine, B. (2008). Autophagic cell death: the story of a misnomer. Nat Rev Mol Cell Biol *9*, 1004-1010.

Kunath, T., Saba-El-Leil, M. K., Almousailleakh, M., Wray, J., Meloche, S., and Smith, A. (2007). FGF stimulation of the Erk1/2 signalling cascade triggers transition of pluripotent embryonic stem cells from self-renewal to lineage commitment. Development *134*, 2895-2902.

Lang, T., Schaeffeler, E., Bernreuther, D., Bredschneider, M., Wolf, D. H., Thumm, M. (1998). Aut2p and Aut7p, two novel microtubule-associated proteins are essential for delivery of autophagic vesicles to the vacuole. EMBO J *17*, 3597-3607.

Ledermann, B., and Burki, K. (1991). Establishment of a germ-line competent C57BL/6 embryonic stem cell line. Exp Cell Res *197*, 254-258.

Levine, B., and Yuan, J. (2005). Autophagy in cell death: an innocent convict? J Clin Invest *115*, 2679-2688.

Lewin, B. (2004). Genes VIII. (Upper Saddle River: Pearson Prentice Hall).

Li, D. R., He, A., and Falck, J. R. (2010). Enantioselective, organocatalytic reduction of ketones using bifunctional thiourea-amine catalysts. Org Lett *12*, 1756-1759.

Li, P., Tong, C., Mehrian-Shai, R., Jia, L., Wu, N., Yan, Y., Maxson, R. E., Schulze, E. N., Song, H., Hsieh, C. L., Pera, M. F., and Ying, Q.L. (2008). Germline competent embryonic stem cells derived from rat blastocysts. Cell *135*, 1299-1310.

Linstead, D. J., Klein, R. A., and Cross, G. A. M. (1977). Threonine catabolism in Trypanosoma brucei. J General Microbiology *101*, 243-251.

Lu, R., Markowetz, F., Unwin, R. D., Leek, J. T., Airoldi, E. M., MacArthur, B. D., Lachmann, A., Rozov, R., Ma'ayan, A., Boyer, L. A., Troyanskaya, O. G., Whetton, A. D., and Lemischka, I. R. (2009). Systems-level dynamic analyses of fate change in murine embryonic stem cells. Nature *462*, 358-362.

Ludwig, T. E., Levenstein, M. E., Jones, J. M., Berggren, W. T., Mitchen, E. R., Frane, J. L., Crandall, L. J., Daigh, C. A., Conard, K. R., Piekarczyk, M. S., Llanas, R. A., and

Thomson, J. A. (2006). Derivation of human embryonic stem cells in defined conditions. Nat Biotechnol *24*, 185-187.

Ma, Y. G., Rosfjord, E., Huebert, C., Wilder, P., Tiesman, J., Kelly, D., and Rizzino, A. (1992). Transcriptional regulation of the murine k-FGF gene in embryonic cell lines. Dev Biol *154*, 45-54.

MacArthur, B. D., Ma'ayan, A., and Lemischka, I. R. (2009). Systems biology of stem cell fate and cellular reprogramming. Nat Rev Mol Cell Biol *10*, 672-681.

Mann, S. S., and Hammarback, J. A. (1994). Molecular characterization of light chain 3. A microtubule binding subunit of MAP1A and MAP1B. J Biol Chem *269*, 11492-11497.

Markel, P., Shu, P., Ebeling, C., Carlson, G. A., Nagle, D. L., Smutko, J. S., and Moore, K. J. (1997). Theoretical and empirical issues for marker-assisted breeding of congenic mouse strains. Nat Genet *17*, 280-284.

Martin, G. R. (1981). Isolation of a pluripotent cell line from early mouse embryos cultured in medium conditioned by teratocarcinoma stem cells. Proc Natl Acad Sci USA *78*, 7634-7638.

Matsuda, T., Nakamura, T., Nakao, K., Arai, T., Katsuki, M., Heike, T., and Yokota, T. (1999). STAT3 activation is sufficient to maintain an undifferentiated state of mouse embryonic stem cells. EMBO J *18*, 4261-4269.

McGilvray, D., and Morris, J. G. (1969). Utilization of l-threonine by a species of Arthrobacter. Biochem J *112*, 657-671.

Mitsui, K., Tokuzawa, Y., Itoh, H., Segawa, K., Murakami, M., Takahashi, K., Maruyama, M., Maeda, M., and Yamanaka, S. (2003). The homeoprotein Nanog is required for maintenance of pluripotency in mouse epiblast and ES cells. Cell *113*, 631-642.

Mizushima, N., Yoshimori, T., and Levine, B. (2010). Methods in mammalian autophagy research. Cell *140*, 313-326.

Montgomery, R. L., Potthoff, M. J., Haberland, M., Qi, X., Matsuzaki, S., Humphries, K. M., Richardson, J. A., Bassel-Duby, R., Olson, E. N. (2008). Maintenance of cardiac energy metabolism by histone deacetylase 3 in mice. J Clin Invest *118*, 3588-3597.

Navarro, P., and Avner, P. (2009). When X-inactivation meets pluripotency: an intimate rendezvous. FEBS Letters *583*, 1721-1727.

Nichols, J., Evans, E. P., and Smith, A. G. (1990). Establishment of germ-line-competent embryonic stem (ES) cells using differentiation inhibiting activity. Development *110*, 1341-1348.

Nichols, J., Zevnik, B., Anastassiadis, K., Niwa, H., Klewe-Nebenius, D., Chambers, I., Schöler, H., and Smith, A. (1998). Formation of pluripotent stem cells in the mammalian embryo depends on the POU transcription factor Oct4. Cell *95*, 379-391.

Nichols, J., Chambers, I., Taga, T., and Smith, A. (2001). Physiological rationale for responsiveness of mouse embryonic stem cells to gp130 cytokines. Development *128*, 2333-2339.

Nichols, J., Silva, J., Roode, M., and Smith, A. (2009). Suppression of Erk signaling promotes ground state pluripotency in the mouse embryo. Development *136*, 3215-3222.

Nichols, J., and Smith, A. (2009). Naïve and primed pluripotent states. Cell Stem Cell *4*, 487-492.

Nicholson, D. W., Ali, A., Thornberry, N. A., Vaillancourt, J. P., Ding, C. K., Gallant, M., Gareau, Y., Griffin, P. R., Labelle, M., Lazebnik, Y. A., et al. (1995). Identification and inhibition of the ICE/CED-3 protease necessary for mammalian apoptosis. Nature *376*, 37-43.

Niwa, H., Burdon, T., Chambers, I., and Smith, A. (1998). Self-renewal of pluripotent embryonic stem cells is mediated via activation of STAT3. Genes Dev *12*, 2048-2060.

Niwa, H., Miyazaki, J., and Smith, A. G. (2000). Quantitative expression of Oct-3/4 defines differentiation, dedifferentiation or self-renewal of ES cells. Nat Genet *24*, 372-376.

Niwa, H., Ogawa, K., Shimosato, D, and Adachi, K. (2009). A parallel circuit of LIF signaling pathways maintains pluripotency of mouse ES cells. Nature *460*, 118-122.

Novikoff A. B. and Essner, E. (1962). Cytolysosomes and mitochondrial degradation. J Cell Biol *15*, 140-146.

Okita, K., Ichisaka, T., and Yamanaka, S. (2007). Generation of germline-competent induced pluripotent stem cells. Nature *448*, 313-317.

Palmieri, S. L., Peter, W., Hess, H., Schöler, H. R. (1994). Oct-4 transcription factor is differentially expressed in the mouse embryo during establishment of the first two extraembryonic cell lineages involved in implantation. Dev Biol *166*, 259-267.

Phear, E. A., and Greenberg, D. M. (1957). The methylation of deoxyuridine. J Am Chem Soc *79*, 3737-3741.

Reggiori, F., and Klionsky, D. J. (2002). Autophagy in the eukaryotic cell. Eukaryot Cell *1*, 11-21.

Rossant, J. (2007). The magic brew. Nature *448*, 260-262.

Sato, N., Meijer, L., Skaltsounis, L., Greengard, P., and Brivanlou, A. H. (2004). Maintenance of pluripotency in human and mouse embryonic stem cells through activation of Wnt signaling by a pharmacological GSK-3 specific inhibitor. Nature Med *10*, 55-63.

Schmidt, A., Sivaraman, J., Li, Y., Larocque, R., Barbosa, J. A., Smith, C., Matte, A., Schrag, J. D., Cygler, M. (2001). Three-dimensional structure of 2-amino-3-ketobutyrate CoA ligase from Escherichia coli complexed with a PLP-substrate intermediate: inferred reaction mechanism. Biochemistry *40*, 5151-5160.

Silva, J., Barrandon, O., Nichols, J., Kawaguchi, J., Theunissen, T. W., and Smith A. (2008) Promotion of reprogramming to ground state pluripotency by signal inhibition. PLoS Biol *6*, 2237-2247.

Silva, J., Nichols, J., Theunissen, T. W., Guo, G., van Oosten, A. L., Barrandon, O., Wray, J,. Yamanaka, S., Chambers, I., Smith, A. (2009). Nanog is the gateway to the pluripotent ground state. Cell *138*, 722-737.

Silva, J., and Smith, A. (2008). Capturing pluripotency. Cell *132*, 532-536.

Singh, A. M., and Dalton, S. (2009). The cell cycle and Myc intersect with mechanisms that regulate pluripotency and reprogramming. Cell Stem Cell *5*, 141-149.

Smith, A. G., Heath, J. K., Donaldson, D. D., Wong, G. G., Moreau, J., Stahl, M., and Rogers, D. (1988). Inhibition of pluripotential embryonic stem cell differentiation by purified polypeptides. Nature *336*, 688-690.

Smith, A. G. (2001). Embryo-derived stem cells: of mice and men. A Rev Cell Dev Biol *17*, 435-462.

Srere, P. A. (1987). Complexes of sequential metabolic enzymes. Ann Rev Biochem *56*, 89-124.

Sridharan, R., Tchieu, J., Mason, M. J., Yachechko, R., Kuoy, E., Horvath, S., Zhou, Q., Plath, K. (2009). Role of the murine reprogramming factors in the induction of pluripotency. Cell *136*, 364-377.

Stavridis, M. P., Lunn, J. S., Collins, B. J., Storey, K. G. (2007). A discrete period of FGF-induced Erk1/2 signalling is required for vertebrate neural specification. Development *134*, 2889-2894.

Takahashi K., and Yamanaka, S. (2006). Induction of pluripotent stem cells from mouse embryonic and adult fibroblast cultures by defined factors. Cell *126*, 663-676.

Tanida, I., Ueno, T., and Kominami, E. (2004). Human light chain 3/MAP1LC3B is cleaved at its carboxyl-terminal Met121 to expose Gly120 for lipidation and targeting to autophagosomal membranes. J Biol Chem *279*, 47704-47710.

Tallquist, M. D., and Soriano, P. (2000). Epiblast-restricted Cre expression in MORE mice: a tool to distinguish embryonic vs. extra-embryonic gene function. Genesis *26*, 113-115.

Tesar, P. J., Chenoweth, J. G., Brook, F. A., Davies, T. J., Evans, E. P., Mack, D. L., Gardner, R. L., and McKay, R. D. (2007). New cell lines from mouse epiblast share defining features with human embryonic stem cells. Nature *448*, 196-199.

Thomas, K. R., and Capecchi, M. R. (1987). Site-directed mutagenesis by gene targeting in mouse embryo-derived stem cells. Cell *51*, 503-512.

Thomson, J. A., Kalishman, J., Golos, T. G., Durning, M., Harris, C. P., Becker, R. A., and Hearn, J. P. (1995). Isolation of a primate embryonic stem cell line. Proc Natl Acad Sci USA *92*, 7844-7848.

Thomson, J. A., Kalishman, J., Golos, T. G., Durning, M., Harris, C. P., and Hearn, J. P. (1996). Pluripotent cell lines derived from common marmoset (Callithrix jacchus) blastocysts. Biol Reprod *55*, 254-259.

Thomson, J. A., Itskovitz-Eldor, J., Shapiro, S. S., Waknitz, M. A., Swiergiel, J. J., Marshall, V. S., and Jones, J. M. (1998). Embryonic stem cell lines derived from human blastocysts. Science *282*, 1145-1147.

Tu, B. P., Mohler, R. E., Liu, J. C., Dombek, K. M., Young, E. T., Synovec, R. E., and McKnight, S. L. (2007). Cyclic changes in metabolic state during the life of a yeast cell. Proc Natl Acad Sci USA *104*, 16886-16891.

Wang, J., Alexander, P., Wu, L., Hammer, R., Cleaver, O., and McKnight, S. L. (2009). Dependence of mouse embryonic stem cells on threonine catabolism. Science *325*, 435-439.

Warren, L., and Buchanan, J. M. (1957). Biosynthesis of the purines. XIX. 2-Amino-N-ribosylacetamide 5'-phosphate (glycinamide ribotide) transformylase. J Biol Chem *229*, 613-626.

Watts, R. W. (1983). Some regulatory and integrative aspects of purine nucleotide biosynthesis and its control: an overview. Adv Enzyme Regul *21*, 33-51.

Weissbach, H., Peterkofsky, A., Redfield, B. G., and Dickerman, H. (1963). Studies on the terminal reaction in the biosynthesis of methionine. J Biol Chem *238*, 3318-3324.

Wernig, M., Meissner, A., Foreman, R., Brambrink, T., Ku, M., Hochedlinger, K., Bernstein, B. E., and Jaenisch, R. (2007). In vitro reprogramming of fibroblasts into a pluripotent ES-cell-like state. Nature *448*, 318-324.

Williams, R. L., Hilton, D. J., Pease, S., Willson, T. A., Stewart, C. L., Gearing, D. P., Wagner, E. F., Metcalf, D., Nicola, N. A., and Gough, N. M. (1988). Myeloid leukaemia inhibitory factor maintains the developmental potential of embryonic stem cells. Nature *336*, 684-687.

Wilson, P. A., and Hemmati-Brivanlou, A. (1995). Induction of epidermis and inhibition of neural fate by Bmp-4. Nature *376*, 331-333.

Wu, J., Dang, Y., Su, W., Liu, C., Ma, H., Shan, Y., Pei, Y., Wan, B., Guo, J., and Yu, L. (2006). Molecular cloning and characterization of rat LC3A and LC3B--two novel markers of autophagosome. Biochem Biophys Res Commun *339*, 437-442.

Wynegaarden, J. B. (1976). Regulation of purine biosynthesis and turnover. Adv Enzyme Regul *14*, 25-42.

Xu, C., Rosler, E., Jiang, J., Lebkowski, J. S., Gold, J. D., O'Sullivan, C., Delavan-Boorsma, K., Mok, M., Bronstein, A., and Carpenter, M. K. (2005). Basic fibroblast growth factor supports undifferentiated human embryonic stem cell growth without conditioned medium. Stem Cells *23*, 315-323.

Ying, Q. L., Nichols, J., Chambers, I., and Smith, A. (2003). BMP induction of Id proteins suppresses differentiation and sustains embryonic stem cell self-renewal in collaboration with STAT3. Cell *115*, 282-292.

Ying, Q. L., Stavridis, M., Griffiths, D., Li, M., and Smith, A. (2003). Conversion of embryonic stem cells into neuroectodermal precursors in adherent monoculture. Nat Biotechnol *21*, 183-186.

Ying Q. L., Wray, J., Nichols, J., Batlle-Morera, L., Doble, B., Woodgett, J., Cohen, P., and Smith, A. (2008). The ground state of embryonic stem cell self-renewal. Nature *453*, 519-523.

Yu, J., and Thomson, J. A. (2008). Pluripotent stem cell lines. Genes Dev *22*, 1987-1997.